RSC Advances

REVIEW

View Article Online
View Journal | View Issue

Cite this: *RSC Adv.*, 2025, **15**, 39235

5-Amino- and 6-amino-uracils in the synthesis of various heterocycles as therapeutic agents: a review

Ashraf A. Aly,* Esraa M. Osman, Sara M. Mostafa, Tarek M. Bedair, Mohamed Abd-Elmonem, Kamal Usef Sadek and Asmaa H. Mohamed

5-Amino- and 6-amino-uracil derivatives are used as precursors in the synthesis of various heterocyclic compounds, which have attracted great interest because of their potent biological activities and therapeutic uses. Multicomponent reactions (MCRs) are a quite significant green technique as they directly correlate with fewer byproducts as well as lower time and energy consumption. These benefits of MCRs expand their potential in the preparation of a variety of new catalytic systems for the synthesis of essential organic compounds in environmentally friendly reaction circumstances. Herein, we focus on some MCR sequences that evolved during the last decade, especially from 2014 to 2024, for the synthesis of target heterocycles starting from either 5-amino- or 6-amino-uracil derivatives. In addition, we discuss the mechanism by which the selected catalyst helps in the selectivity of the target molecules. Furthermore, the biological activity of the synthesized materials as therapeutic agents was reviewed.

Received 17th July 2025
Accepted 18th September 2025

DOI: 10.1039/d5ra05123a

rsc.li/rsc-advances

1 Introduction

Uracil is a naturally occurring pyrimidine-based compound, which is considered one among the four nucleobases in RNA.[1–3] The chemical characteristics of uracil and its derivatives, such as 5-aminouracils and 6-aminouracils (Fig. 1), vary because these molecules have the ability to function as both electrophiles and nucleophiles.[4] Numerous bioactive chemical compounds can be synthesized using 5-aminouracils and/or 6-aminouracils as precursors.[5–8] Because of their synthetic accessibility and a variety of biological actions, uracil derivatives are regarded as preferred structures in drug discovery.[9–14] Particularly, 5- and 6-aminouracils and their derivatives have revealed various biological properties such as antioxidant,[15] antimicrobial,[16,17] anticancer,[18–20] anti-Alzheimer[21] and antiviral activity.[9,22] Pyrido-, pyrrolo- and pyrimido-pyrimidines, phenazine, chromenes and xanthines of 5- and 6-aminouracils and their derivatives have been reported to be biologically active compounds.[23–38]

1.1. Synthesis of 5-amino- and 6-amino-uracil derivatives

Aminouracil-based compounds are effective ligands in chemical reactions and readily form metal complexes.[39–41] In the presence of Cu(II) and molecular oxygen, 5-aminouracil (**1**) underwent oxidation to form 5,5,6-trihydroxy-pyrimidine-2,4(1*H*,3*H*)-dione.[42] During the wet chemical production of silver nanoparticles (AgNPs), 5-aminouracils were employed as a capping and reducing agent.[43,44] Furthermore, 6-aminouracil (**2**) can be functionalized as it was sulfenylated through visible-light or electrochemical reactions[45] in addition to thioarylation,[46] thiocyanation,[47] nitrosation[48] and formylation.[49,50] Despite the wide range of reactions involving amino uracil derivatives, chemists have shown great interest in green synthesis techniques,[51,52] metal nanocatalysts,[53,54] and catalyst free methods.[55,56]

Several approaches explaining the synthetic routes of 5-aminouracil (**1**) have been previously reported in the literature. The first methods dealt with the amination process of 5-halouracils using aqueous ammonia treatment, whereas the second method includes the reduction process of 5-nitrouracil[57–59] with various reducing agents such as Sn/HCl,[24,60] Zn/HCl,[23] Zn ammonia solution, Fe_2SO_4, sodium thiolate (NaSH), or Al amalgam.[23,61,62] Additionally, a sealed tube was used to heat the appropriate 5-bromo/nitro-methyl(aryl)-uracil with excess NH_3 to obtain 5-amino-1-methyluracil and 5-amino-1-phenyluracil.[24]

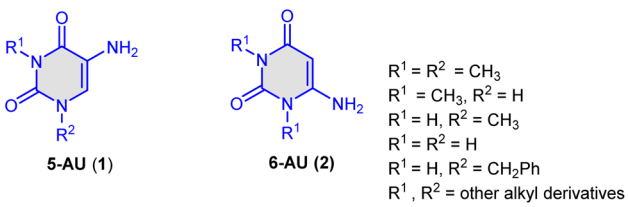

Fig. 1 Structures of 5-amino- and 6-amino-uracil derivatives **1** and **2**.

Chemistry Department, Faculty of Science, Minia University, 61519-El-Minia, Egypt. E-mail: ashrafaly63@yahoo.com; ashraf.shehata@mu.edu.eg; esraamah33@gmail.com; sara.ahmed@mu.edu.eg; dr.tarek.bedair.2@mu.edu.eg; m_chemistry4you@yahoo.com; kusadek@yahoo.com; asmaa.hamouda@mu.edu.eg

The preparation of 5-aminouridines has also been demonstrated to be used in the biosynthesis of nucleic acids, which was accomplished by reacting either 5-bromouridine with ammonia[23,60–62] or by reducing 5-nitrouridine.[63]

1.2. Some biological aspects of 5-amino- and 6-amino-uracil derivatives

Fig. 2 illustrates the most biologically active aminouracil compounds such as 5,5′-(1,4-diamino-but-2-ene-2,3-diyl)-bis(6-amino-1-(2-aminoethyl)pyrimidine-2,4-dione) (**I**, Fig. 2), which is known as an antimicrobial agent.[16] The synthesized compound **I** revealed an inhibitory effect towards various bacterial strains. The inhibitory effect of the synthesized acyclic nucleoside **I** was more pronounced against Gram-positive bacteria (*B. cereus*, *B. subtilis*, and *S. aureus*) than against those of Gram-negative bacteria in comparison to the reference drug. The most susceptible bacterial species to the synthesized compound **I** was *B. cereus*, where the recorded MIC and MLC values were 32 and 64 μg mL^{-1}, respectively, compared with 64 and 128 μg mL^{-1} for gentamicin, respectively.[16]

Moreover, 1-(2,4-dioxo-1,2,3,4-tetrahydropyrimidin-5-yl)-3-(3-methoxyphenyl)thiourea (**II**, Fig. 2) is known as an anticancer agent.[64] Synthesis of compound **II** was achieved *via* the reaction of 5-aminouracil (**1**) with 3-methoxyphenyl isothiocyanate in refluxing methanol. Using the MTT assay and doxorubicin as the reference drug, compound **II** was tested for its antiproliferative activity against four human cancer cell lines: Panc-1 (pancreatic cancer cell line), MCF-7 (breast cancer cell line), HT-29 (colon cancer cell line), and A-549 (epithelial cancer cell line). The synthesized compound **II** had the main backbone assigned as the thio of uracil, which was tested with an IC_{50} value of 125 ± 11 nM.[64]

Both 1-aryl-5-(arylamino)pyrimidine-2,4(1*H*,3*H*)-diones (**III**, Fig. 2)[21] and 6-amino-5-((2-hydroxy-benzyl)amino)-1,3-dimethyl-pyrimidine-2,4(1*H*,3*H*)-diones (**IV**, Fig. 2) were reported as antiviral and anti-Alzheimer agents, respectively.[22]

The synthesis of series **III** was achieved by the reaction of 2,4-bis(trimethylsilyloxy)-5-phenylaminouracil with benzyl bromides in refluxing 1,2-dichloroethane.[21] The compounds were then subjected to screening across a broad range of viruses in order to evaluate their biological potential. Two of the compounds R^1 = 3,5-Me, R^2 = H, X = – and 3,5-Me, R^2 = H, X = CH_2 revealed promising inhibitory activity against HIV. A 50% protective effect was observed at concentrations of 11.9 and 9.5 μM, respectively, in the CEM-SS cell culture. It is noteworthy that both former compounds possess the same benzyl fragment, that is, a 3,5-dimethylphenylmethyl residue at the *N*−1 position of the uracil ring. It was found that the presence of the methyl substituents in the *m*-position of the benzyl fragment favorably affects the inhibitory properties of these compounds.[21] In addition to the anti-HIV activity noted, several of the compounds also exhibited activity against the Epstein–Barr virus in the AKATA cell culture. The most active compound was 1-(3-phenoxybenzyl)-5-(phenylamino)uracil, with an IC_{50} value of 2.3 μM, and no toxicity was observed at a concentration of 100 μM. The second active compound was 1-(2-methylbenzyl)-5-(phenylamino)uracil, with an IC_{50} value of 12 μM.[21]

For series **IV** (Fig. 2), the synthesis was established by reductive amination, with moderate to good yields (30–84% yields). 5-(Arylidene)-6-aminouracils were *in situ* prepared *via* a condensation reaction between 5,6-diamino-1,3-dimethyluracil and substituted salicylaldehydes using an excess of sodium borohydride. The inhibitory abilities of uracil attached to benzylic amines were examined against

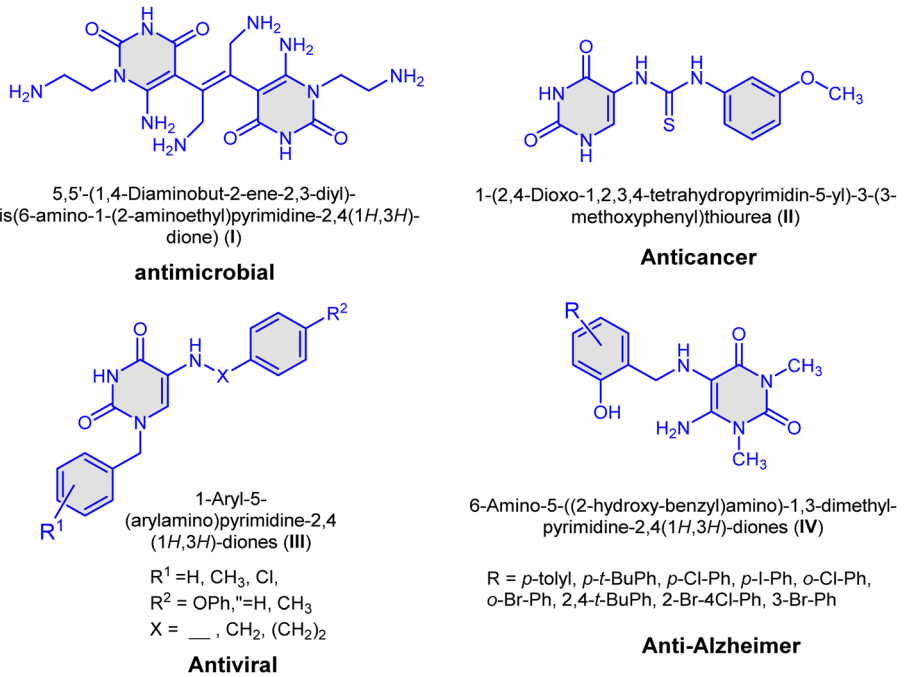

Fig. 2 Examples of some biologically active aminouracil-based compounds I–IV.

acetylcholinesterase (AChE) and human carbonic anhydrase I and II (hCA I and II) isoenzymes, which were linked to some global disorders, such as Alzheimer's disease (AD), epilepsy, diabetes and glaucoma. The compounds displayed inhibition profiles with Ki values ranging from 2.28 ± 0.41 nM to 5.25 ± 0.75 nM for AChE, 36.10 ± 5.22–110.31 ± 54.81 nM for hCA I and 16.33 ± 4.91–72.03 ± 28.86 for hCA II.[22]

2 Discussion

In this review, we discuss the synthesis of heterocycles using 5-amino- and 6-amino-uracils over the past 10 years, especially from 2014 to 2024. We also provide more insight into the multi-component reaction in one-pot process pertaining to the synthesis of target compounds. Some reaction mechanisms are also covered. We also address the biological significance of target heterocycles as therapeutic agents.

2.1. Heterocycles from 5-aminouracil

5-Aminouracil and its building blocks behave as anticancer, antibacterial, and antiviral drugs.[19,20,65–68] In 2016,[68] a review article dealt with the synthesis and reactions of 5-aminouracil (**1**) and its derivatives. The review also dealt with a brief survey of biological activities, such as the chemotherapeutic and pharmacological activities of the announced uracil **1**.

2.1.1. Synthesis of pyrazolo-pyrimidine derivatives. The reaction of 5-aminouracil (**1**) with ethyl cyanoacetate (**3**) under neat conditions under microwave (MW) irradiation for 5 min afforded 2-cyano-*N*-(2,4-dioxo-1,2,3,4-tetrahydropyrimidin-5-yl) acetamide (**4**) in 90% yield. Subsequently, the addition of benzaldehyde to ethanol using piperidine as the catalyst afforded the corresponding arylidine **5** in 88% yield (Scheme 1). Finally, the arylidine was led to react with hydrazine hydrate in ethanol (EtOH) under MW at 130 °C to produce 3-amino-*N*-(2,4-

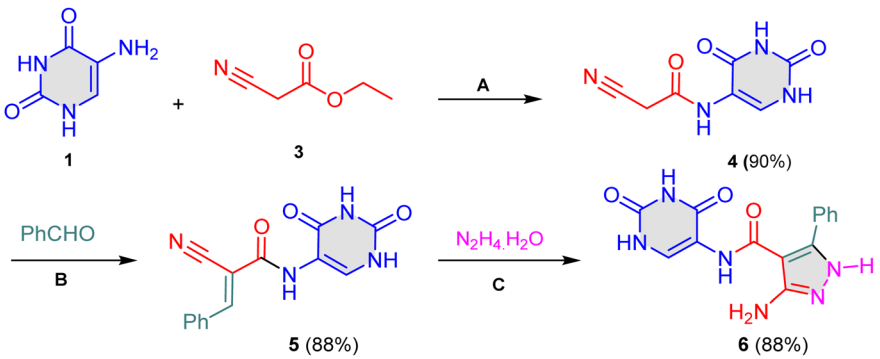

Scheme 1 Synthesis of aminopyrazole **6**. Reagents and conditions: A = neat, MW, 180 °C, 5 min. B = PhCHO, Pip, EtOH, MW. C = EtOH, MW, 130 °C, 10 min.

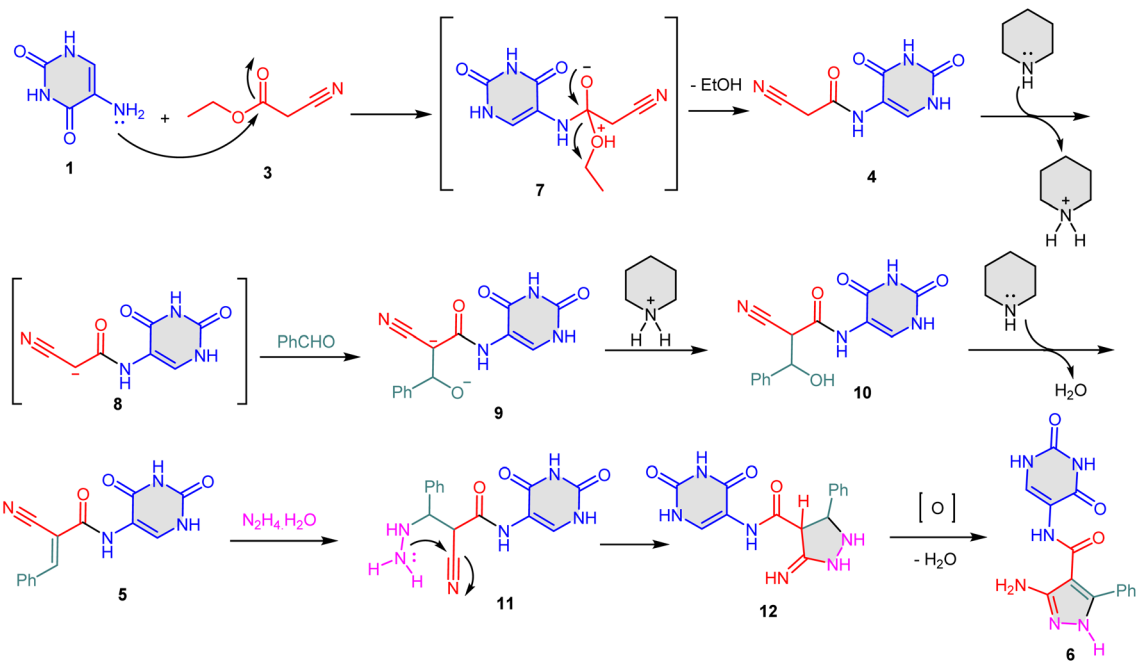

Scheme 2 Proposed mechanism for the formation of aminopyrazole **6**.

dioxo-1,2,3,4-tetrahydropyrimidin-5-yl)-5-phenyl-1*H*-pyrazole-4-carboxamide (**6**) in 88% yield (Scheme 1).[69]

The mechanism described for the formation of **6** is shown in Scheme 2. First, the lone pair of nitrogen of 5-aminouracil (**1**) attacked the carbonyl group of ethyl cyanoacetate (**3**) to give intermediate **7** (Scheme 2). Subsequently, cyanoacetamide **4** was produced when intermediate **7** lost an ethanol molecule. Piperidine then abstracted a hydrogen proton from **7** to form the enol form **8**. Next, the active methylene of intermediate **8** was added to the carbonyl of benzaldehyde to produce intermediate **9**. The ***E*** isomer of compound **5** was then obtained when a water molecule was eliminated from adduct **10** and a piperidine molecule was recycled (Scheme 2). Finally, Michael's addition of hydrazine hydrate to the β-carbon of compound **5** afforded intermediate **11**. Finally, an intramolecular cyclization of intermediate **11** would give intermediate **12**, which underwent an autoxidation to give (pyrimidin-5-yl)-5-phenyl-1*H*-pyrazole-4-carboxamide **6** (Scheme 2).[69]

Another work reported the synthesis of compounds **15a–d** *via* the reaction of compound **4** with diazonium salt derivatives **13** to give the corresponding hydrazones **14a–d**. Heating the hydrazones **14a–d** in pyridine gave the final of pyrazolo[5,1-*c*][1,2,4]triazine-3-carboxamides **15a–d** (Scheme 3).[66] Compounds **15a–d** were screened against Gram-positive and Gram-negative bacteria as well as four spore-forming fungal strains (Table 1). Compound **15c** showed high activity against all strains because it exhibited activity against *Bacillus subtilis* (G+)Bs (IC_{50} = 23.2 ± 0.23 mm) compared with Ampicillin (IC_{50} = 32.4 ± 0.3 mm). Moreover, compound **15c** revealed IC_{50} = 16.3 ± 0.15 against Ampicillin (IC_{50} = 23.8 ± 0.2) for *Streptococcus pneumoniae* (G+)Sp. However, compound **15a** showed high activity against *Geotrichum candidum* (Gc) with IC_{50} = 19.9 ± 0.3 compared with Amphotericin B (IC_{50} = 25.4 ± 0.1). Table 1 illustrates the activities of compounds **15a–d** against antibacterial Gram (+ve), Gram (−ve) and fungal microorganisms. Methoxy substituent **15c** exhibited the most active compound as a promising antimicrobial and anti-fungal agent.

2.1.2. Synthesis of thiazolo-pyrimidines. Aly *et al.*[64] reported the synthetic route of uracil-thios **17a–f** by refluxing 5-aminouracil (**1**) with different isothiocyanates (**16**) in methanol

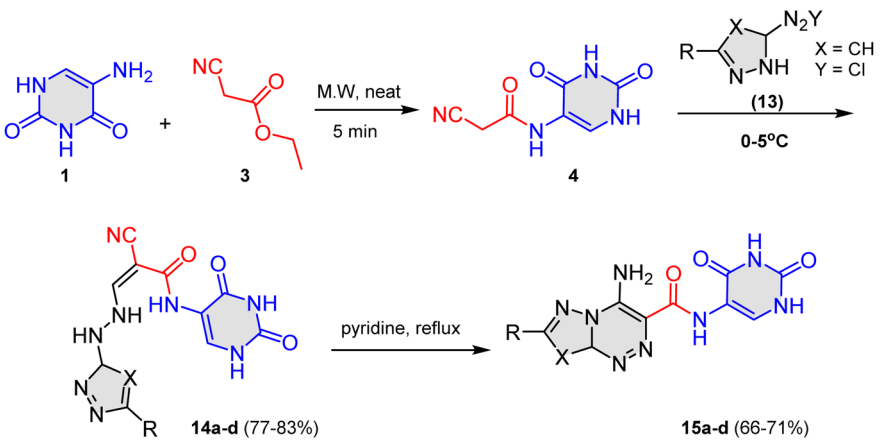

14 and **15a-d**; **a**: R = 4-MeC_6H_4; **b**: R = 4-$MeOC_6H_4$; **c**: R = 4-FC_6H_4; **d**: R = 4-BrC_6H_4

Scheme 3 Synthesis of pyrazolo[5,1-*c*][1,2,4]triazine-3-carboxamides **15a–d**.

Table 1 Antimicrobial and antifungal screening of compounds **15a–d**[a]

Compd	*Bacillus subtilis* (G+) Bs	*Streptococcus pneumoniae* (G+) Sp	*Escherichia coli* (G−) Ec	*Pseudomonas aeruginosa* (G−) Pa	*Aspergillus flavus* (fungus) Af	*Syncephalastrum racemosum* (Sr)	*Geotrichum candidum* (Gc)
15a	21.3 ± 0.12	15.2 ± 0.23	11.3 ± 0.12	10.6 ± 0.09	13.5 ± 0.13	15.5 ± 0.11	19.8 ± 0.19
15b	17.2 ± 0.26	10.2 ± 0.29	10.02 ± 0.11	8.9 ± 0.12	11.4 ± 0.14	13.6 ± 0.13	17.6 ± 0.21
15c	23.2 ± 0.23	16.3 ± 0.15	11.6 ± 0.09	10.9 ± 0.15	14.2 ± 0.09	18.5 ± 0.06	15.7 ± 0.25
15d	15.2 ± 0.33	12.3 ± 0.12	9.8 ± 0.08	9.8 ± 0.17	11.3 ± 0.08	11.2 ± 0.08	12.4 ± 0.19
Amphotericin B	—	—			23.7 ± 0.1	28.7 ± 0.2	25.4 ± 0.1
Ampicillin	32.4 ± 0.3	23.8 ± 0.2	—	—	—	—	—
Gentamicin	—	—	19.9 ± 0.3	17.3 ± 0.1	—	—	—

[a] Screening organisms, Mold: *A. flavus* (RCMB 02568, Af); *Syncephalastrum racemosum* (RCMB, 016 001, Sr) and *Geotrichum candidum* (RCMB, 052 006 Gc); two Gram-positive bacteria: *S. pneumoniae* (RCMB 010010, Sp) and *B. subtilis* (RCMB 010069, Bs); two Gram-negative bacteria: *E. coli* (RCMB 010052, Ec) and *P. aeruginosa* (RCMB 004, Pa); inhibition zone (IZ): high activity >15 (mm); moderate activity 11–14 (mm); slight activity 8–10 (mm) and non-sensitive 0–7 (mm).

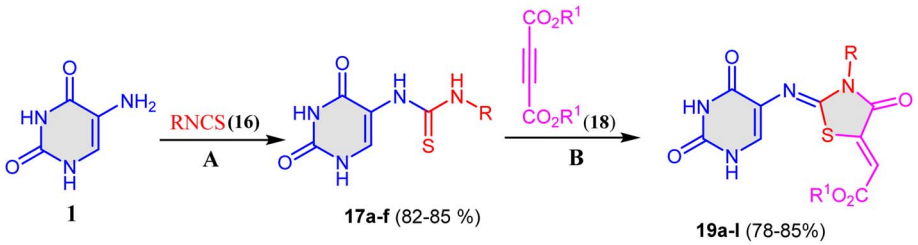

17a-f: **a**: R = Ph; **b**: R = 4-MePh; **c**: R = 3-OMePh; **d**: R = benzyl: **e**: R = CH_3; **f**: R = allyl

19a-f: **a**: R = Ph, R^1= Et; **b**: R = 4-MePh, R^1= Et; **c**: R = 3-OMePh, R^1= Et; **d**: R = benzyl, R^1= Et; **e**: R = Me, R^1= Et; **f**: R = allyl, R^1= Et; **g**: R = Ph, R^1= Me; **h**: R = 4-MePh, R^1= Me; **i**: R = 3-OMePh, R^1= Me; **j**: R = benzyl, R^1= Me; **k**: R = R^1= Me; **l**: R = allyl, R^1= Me

Scheme 4 Synthesis of uracil–thiazoles hybrid molecules **19a–l**. Reagents and conditions: **A** = MeOH, reflux, Et_3N, 10–12 h. **B**; EtOH, reflux, 6–12 h.

Table 2 Antiproliferative properties of compounds **17a–f** and **19a–l**

			Antiproliferative activity $IC_{50} \pm$ SEM (nM)				
Compd		Cell viability%	A-549	MCF-7	Panc-1	HT-29	Average
17a	R = Ph	86	8.90 ± 0.80	8.50 ± 0.80	8.80 ± 0.80	9.10 ± 0.80	8.80
17b	R = 4-MePh	87	3.70 ± 0.30	3.60 ± 0.30	4.10 ± 0.30	3.90 ± 0.30	3.80
17c	R = 3-OMePh	89	1.80 ± 0.20	1.40 ± 0.10	2.10 ± 0.20	2.10 ± 0.20	1.85
17d	R = benzyl	91	4.10 ± 0.40	3.90 ± 0.40	4.30 ± 0.40	4.30 ± 0.40	4.15
17e	R = Me	89	9.70 ± 0.80	9.60 ± 0.80	9.80 ± 0.80	10.80 ± 0.90	10.0
17f	R = allyl	89	3.80 ± 0.30	3.70 ± 0.30	3.90 ± 0.30	4.10 ± 0.30	3.90
19a	R = Ph, R^1 = Et	91	3.50 ± 0.30	3.10 ± 0.30	3.30 ± 0.30	3.90 ± 0.30	3.45
19b	R = 4-MePh, R^1 = Et	92	1.20 ± 0.10	1.10 ± 0.10	1.40 ± 0.10	1.40 ± 0.10	1.30
19c	R = 3-MeOPh, R^1 = Et	96	1.50 ± 0.10	1.60 ± 0.10	1.90 ± 0.20	1.80 ± 0.10	1.70
19d	R = benzyl, R^1 = Et	86	4.90 ± 0.50	4.70 ± 0.40	5.50 ± 0.50	5.50 ± 0.50	5.15
19e	R = Me, R^1 = Et	86	7.20 ± 0.60	6.70 ± 0.70	7.30 ± 0.70	7.20 ± 0.70	7.10
19f	R = allyl, R^1 = Et	89	8.20 ± 0.70	7.90 ± 0.70	8.80 ± 0.70	8.90 ± 0.70	8.50
19g	R = Ph, R^1 = Me	87	2.70 ± 0.20	2.20 ± 0.20	2.90 ± 0.20	2.20 ± 0.20	2.50
19h	R = 4-MePh, R^1 = Me	92	1.40 ± 0.10	1.70 ± 0.10	1.80 ± 0.10	1.70 ± 0.10	1.65
19i	R = 3-MeOPh, R^1 = Me	89	1.30 ± 0.10	1.00 ± 0.08	1.50 ± 0.10	1.60 ± 0.10	1.35
19j	R = benzyl, R^1 = Me	89	1.10 ± 0.10	0.90 ± 0.10	1.20 ± 0.10	1.20 ± 0.10	1.10
19k	R = R^1 = Me	89	5.70 ± 0.60	5.10 ± 0.50	5.90 ± 0.50	6.20 ± 0.60	5.70
19l	R = allyl, R^1 = Me	86	6.00 ± 0.60	6.50 ± 0.60	6.40 ± 0.60	6.60 ± 0.60	6.40
Doxorubicin		—	**1.20 ± 0.10**	**0.90 ± 0.10**	**1.40 ± 0.10**	**1.00 ± 0.10**	**1.10**

(MeOH) and triethylamine (Et_3N) (Scheme 4). Thereafter, thio derivatives **17a–f** were reacted with acetylene dicarboxylate derivatives **18a**, **b** in EtOH to produce thiazolidin-4-ones **19a–l** in good yields (78–85%). The IC_{50} values for the synthesized compounds ranged from 1.1 μM to 10 μM, indicating an antiproliferative action (Table 2). Compounds **17c**, **17b**, **19c**, **19h**, **19i**, and **19j** were the most effective derivatives, with IC_{50} values ranging from 1.1 μM to 1.8 μM. Compound **19j** displayed the most potent activity, with an IC_{50} value of 1.1 μM, in comparison to the reference doxorubicin (IC_{50} = 1.1 μM) and was even more potent than doxorubicin against A-549 and Panc-1 cancer cell lines. The six most potent antiproliferative derivatives (**17c**, **19b**, **19c**, **19h**, **19i**, and **19j**) were further investigated against EGFR as potential targets for their antiproliferative activity (Table 3). Compound **19b** displayed potent inhibitory activity against EGFR and $BRAFV^{600E}$ with IC_{50} values of 91 ± 0.7 and 93 ± 0.8 μM, respectively, indicating that this compound could act as a dual inhibitor of EGFR and $BRAFV^{600E}$ with significant antiproliferative activities.[64]

Table 3 IC_{50} of compounds **17c**, **19b**, **19c**, **19h**, **19i**, and **19j** against EGFR and $BRAFV^{600E}$

	EGFR inhibition	$BRAF^{V600E}$ inhibition
Compd	$IC_{50} \pm$ SEM (nM)	$IC_{50} \pm$ SEM (nM)
17c	125 ± 11	148 ± 12
19b	91 ± 0.7	93 ± 0.8
19c	115 ± 10	107 ± 10
19h	112 ± 10	137 ± 12
19i	96 ± 0.7	122 ± 12
19j	87 ± 0.5	115 ± 12
Erlotinib	**80 ±0.5**	**60 ±0.5**

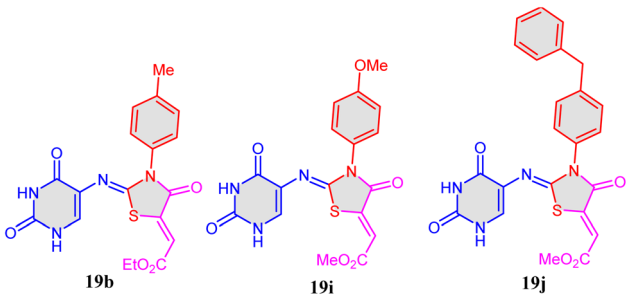

Fig. 3 Structure of antiproliferative uracil–thiazolidin-4-one derivatives **19b**, **19i** and **19i**.

2.1.2.1 Structure activity relationship. The data in Tables 2 and 3 show the findings of the antiproliferative assay, in which compound **19j** (R = benzyl, R^1 = Me; thiazolidin-4-one) was found to be the most potent antiproliferative and demonstrated the highest inhibitory activity against EGFR with an IC_{50} value of 87 ± 05 nM, which is very close to that of the reference erlotinib (IC_{50} = 80 ± 05 nM). Compounds **19b** (R = 4-CH_3-Ph, R^1 = Et; thiazolidin-4-one) and **19i** (R = 3-OCH_3-Ph, R^1 = Me; thiazolidin-4-one) rank second and third in activity, with IC_{50} values of 91 ± 07 nM and 97 ± 07 nM, respectively. Based on the results of this assay, compounds **19b**, **19i**, and **19j** (Fig. 3)

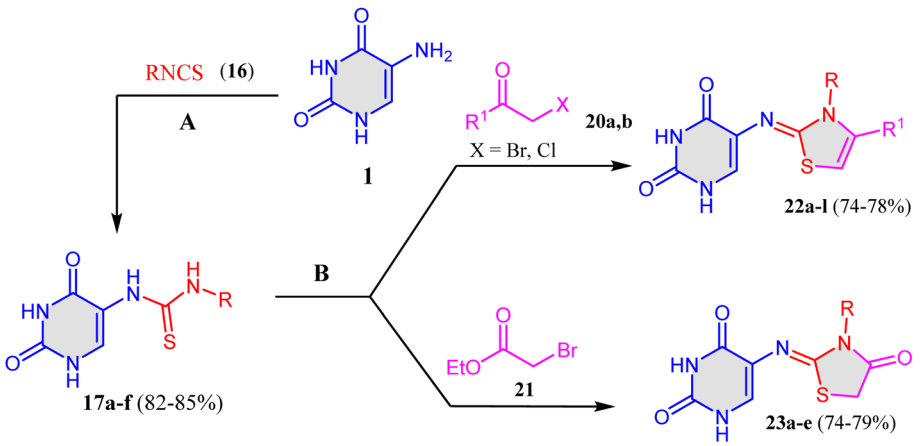

17a: R = Ph; **b**: R = 4-MePh; **c**: R = 3-OMePh; **d**: R = benzyl: **e**: R = CH_3; **f**: R = allyl
22a: R = R^1=Ph; **b**: R = 4-MePh, R^1= Ph; **c**: R = 3-OMePh, R^1= Ph; **d**: R = benzyl, R^1= Ph; **e**: R = Me, R^1= Ph; **f**: R = allyl, R^1= Ph; **g**: R = Ph, R^1= Me; **h**: R = 4-MePh, R^1= Me; **i**: R = 3-OMePh, R^1= Me; **j**: R = benzyl, R^1= Me; **k**: R = R^1= Me; **l**: R = allyl, R^1= Me
23a: R = R^1=Ph; **b**: R = 4-MePh, R^1= Ph; **c**: R = 3-OMePh, R^1= Ph; **d**: R = benzyl, R^1= Ph; **e**: R = Me, R^1= Ph

Scheme 5 Synthesis of uracil–thiazole **22a–l** and **23a–e** building blocks. Reagents and conditions: **A** = MeOH, reflux, 10–12 h. **B**; EtOH, Et_3N, reflux.

Table 4 IC_{50} values of compounds **22a–l** and **23a–e** against four cancer cell lines

		Antiproliferative activity IC_{50} ± SEM (mM)				
Compd	Cell viability%	A-549	MCF-7	Panc-1	HT-29	Average (GI_{50})
22a	90	1.20 ± 0.20	1.10 ± 0.10	1.40 ± 0.20	1.30 ± 0.20	1.25
22b	89	2.70 ± 0.30	2.60 ± 0.30	3.10 ± 0.30	2.90 ± 0.30	2.80
22c	91	0.80 ± 0.10	0.90 ± 0.10	1.00 ± 0.10	0.90 ± 0.10	0.90
22d	91	2.00 ± 0.20	1.90 ± 0.20	2.30 ± 0.20	2.20 ± 0.20	2.10
22e	87	2.90 ± 0.30	2.80 ± 0.30	3.30 ± 0.30	3.20 ± 0.30	3.05
22f	89	1.80 ± 0.20	1.60 ± 0.10	2.10 ± 0.20	2.10 ± 0.20	1.90
22g	91	2.30 ± 0.20	2.10 ± 0.20	2.50 ± 0.20	2.40 ± 0.20	2.30
22h	92	3.30 ± 0.30	3.10 ± 0.30	3.50 ± 0.30	3.60 ± 0.30	3.40
22i	89	1.10 ± 0.10	1.00 ± 0.10	1.30 ± 0.10	1.20 ± 0.10	1.15
22j	87	6.20 ± 0.60	6.00 ± 0.60	6.50 ± 0.60	6.40 ± 0.60	6.30
22k	90	4.80 ± 0.50	4.70 ± 0.40	4.90 ± 0.50	4.90 ± 0.50	4.80
22l	87	5.50 ± 0.60	5.30 ± 0.50	5.80 ± 0.60	5.70 ± 0.60	5.60
23a	92	2.40 ± 0.20	2.30 ± 0.20	2.80 ± 0.20	2.70 ± 0.20	2.55
23b	90	1.50 ± 0.10	1.60 ± 0.10	1.80 ± 0.20	1.80 ± 0.20	1.70
23c	91	1.40 ± 0.10	1.30 ± 0.10	1.60 ± 0.10	1.50 ± 0.10	1.45
23d	87	7.70 ± 0.70	7.50 ± 0.70	7.80 ± 0.80	7.90 ± 0.80	7.70
23e	89	7.00 ± 0.60	6.80 ± 0.70	7.30 ± 0.70	7.20 ± 0.70	7.10
Doxorubicin	—	1.20 ± 0.10	0.90 ± 0.10	1.40 ± 0.10	1.00 ± 0.10	1.10

showed promising antiproliferative activities and have the potential to act as EGFR inhibitors.

Compound **19b** (R = 4-CH_3-Ph, R^1 = Et; thiazolidin-4-one) was the most potent derivative as $BRAF^{V600E}$ inhibitor with an IC_{50} value of 93 ± 08 nM, indicating that this compound could behave as a dual inhibitor of EGFR and $BRAFV^{600E}$ with promising antiproliferative properties. It can be concluded that the presence of ethyl ester together with an *N*-aromatic system attached to an electron donating methyl group, as in **19b**, would increase the antiproliferative activity in the series of **19a–l**.

Correspondingly, Aly *et al.*[70] reacted thioureas derived from 5-aminouracil **17a–f** with α-halo-acetophenones **20a,b**, and ethyl bromoacetate (**21**) in EtOH using Et_3N as a base catalyst to obtain uracil–thiazolidene derivatives **22a–l** and uracil–thiazoliden-4-one hybrids **23a–e**, respectively (Scheme 5).[70] The cell viability of compounds was evaluated using the normal human mammary gland epithelial (MCF-10A) cell line. None of the compounds under investigation showed cytotoxic effects, with cell viability higher than 87% when investigated at 50 μM (Table 4). When tested against four human cancer cell lines (A-549, MCF-7, Panc-1, and HT-29), the antiproliferative properties of **22a–l** and **23a–e** demonstrated significant effects when compared to doxorubicin (IC_{50} = 1.1 μM). It was found that the most effective derivatives were compounds **22a**, **22c**, **22f**, **22i**, and **23b**, with IC_{50} values ranging from 0.9 mM to 1.7 mM against the four cancer cell lines.

2.1.2.2 Structure activity relationship. From the data provided in (Table 4), it was illustrated that the most potent derivatives were compounds **22a**, **22c**, **22f**, **22i**, and **23b** (Fig. 4). Compound **22c** (R = 3-MeO-Ph, R^1 = Ph) was the most effective molecule among the tested products compared to doxorubicin (GI_{50} = 1.10 mM). Compound **22i** (R = 3-MeO-Ph, R^1 = CH_3) has a GI_{50} value of 1.15 mM, which is equivalent to the potency of doxorubicin. With the exception of the methyl group at position four of the thiazolidine ring, compound **22i** resembles the same structural backbone as compound **22c**. This suggests that, like compound **22c**, the phenyl group has a better effect on antiproliferative action than the methyl group. Compounds **22a** (R = R^1 = Ph) and **22b** (R = 4-Me-Ph, R^1 = Me) demonstrated significant antiproliferative activity, with GI_{50} values of 1.25 mM and 2.80 mM, respectively, being 1.4-fold and 3-fold less potent than **22c**, respectively. These results demonstrated that the phenyl moiety's substitution pattern in the thiazolidine ring's third position is necessary for its antiproliferative properties. Compounds **22e** (R = Me, R^1 = Ph) and **22f** (R = allyl, R^1 = Ph) were less effective than **22a** (R = R^1 = Ph), with GI_{50} values of 3.05 mM and 1.90 mM, respectively. Compounds **22c** (R = 3-MeO-Ph) and **22d** (R = CH_2-Ph) demonstrated great activity, with GI_{50} values of 1.70 mM and 1.45 mM, respectively.

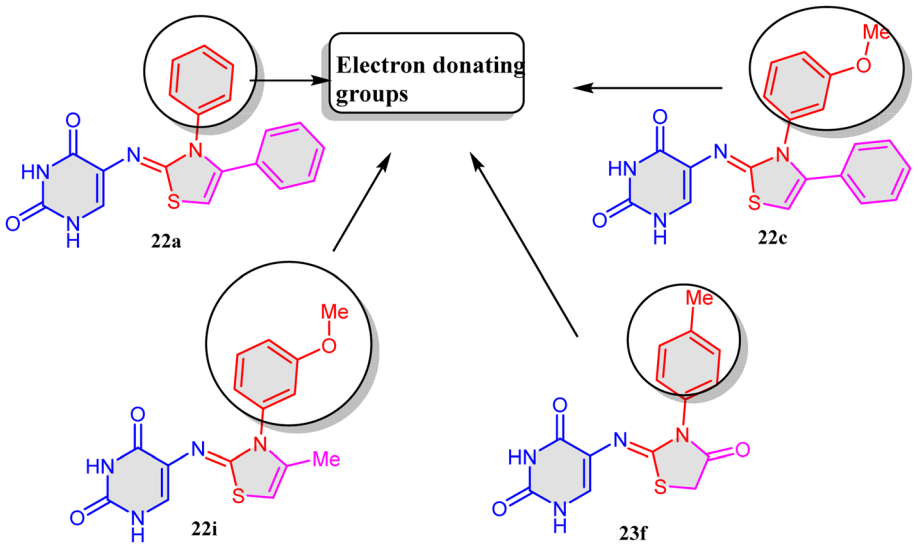

Fig. 4 Structure of antiproliferative uracil–thiazole derivatives.

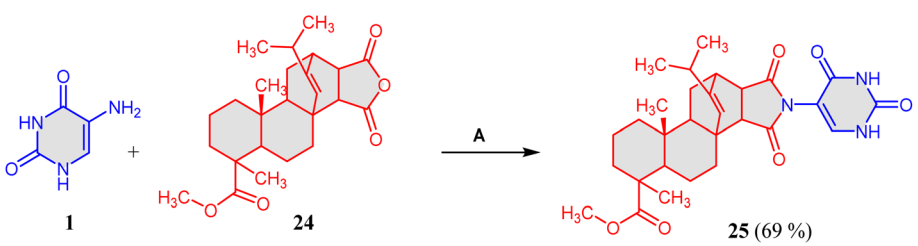

Scheme 6 Ultrasound irradiation synthesis of compound **25**. Reagents and conditions: A = DMSO, ultrasound, 120 °C, 30 min.

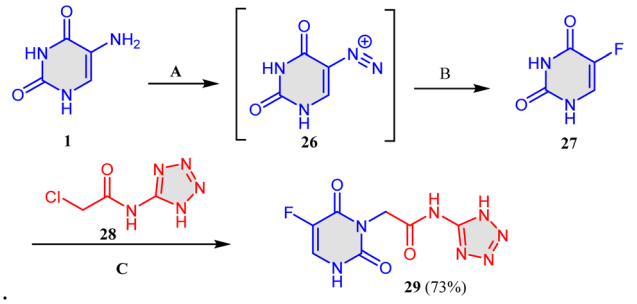

Scheme 7 Synthesis of tetrazole-uracil hybrid **29**. Reagents and conditions: A = $NaNO_2$, AcOH. B; HF, pyridine. C = solvent free, 90 °C, 1 h.

However, compounds **22e** (R = CH_3) and **22f** (R = allyl) were the least potent derivatives, with GI_{50} values of 7.70 mM and 7.10 mM, respectively.

2.1.3. Synthesis of diverse hybrid-pyrimidine compounds. It has reported on the synthesis of maleopimarimide **25** in 69% yield *via* the condensation reaction between 5-aminouracil (**1**) and compound **24** in DMSO under ultrasonic (US) irradiation at 120 °C for 30 min (Scheme 6).[71]

Nowdehi *et al.*[71] developed an efficient synthetic route for tetrazine-uracil hybrid **29** (Scheme 7). First, 5-aminouracil (**1**) was treated with sodium nitrite in acetic acid (AcOH) to produce diazonium salt **26**, which reacted with hydrogen fluoride (HF) in pyridine to produce 5-flourouracil (**27**). Eventually, 2-(5-fluoro-2,6-dioxo-3,6-dihydropyrimidin-1(2*H*)-yl)-*N*-(1*H*-tetrazol-5-yl)acetamide (**29**) was obtained from the reaction of **27** with 2-chloro-*N*-(1*H*-tetrazol-5-yl)acetamide (**28**) (Scheme 7). Compound **29** displayed enhanced inhibition of AGS cancer cell (a human gastric adenocarcinoma cell line derived from stomach tissues) proliferation compared to 5-fluorouracil, with an IC_{50} value of 15.67 μg mL^{-1} *vs.* 36.42 μg mL^{-1} and 45.90 μg mL^{-1} for synthesized and reported 5-FU values, respectively.

2.2. Heterocycles from 6-aminouracil

6-Aminouracil is a privileged scaffold and one of the main starting materials for synthesizing complex compounds because it plays dual roles as an electrophile and a nucleophile.[5] The most notable nucleophilic activity is found at position-3, and it is easy to prepare polycyclic compounds with biological targets like pyrido-, pyrrolo-, and pyrimido-pyrimidines as well as fused annulated compounds with other materials.[72,73] A wide range of pharmacological and biological effects have been demonstrated by these compounds, such as antimicrobial[74–76] and anticancer,[77–79] and they are employed as anticoagulant,[80,81] antifungal,[82,83] antiviral,[84,85] antitumor,[86,87] antioxidant,[72,88] and anti-inflammatory agents,[89] as well as HIV protease inhibitors[90–93] and tyrosine kinase inhibitors.[94]

6-Aminouracil (**2**) is an essential component of numerous synthetic[5,95–98] and natural compounds[94,95] with medicinal properties. Also, 6-aminouracil(s) has/have broad biological activities such as antiviral,[99,100] antidiarrheal,[101] anti-microbial,[102] anti-allergic,[103] anticancer,[78] adenosine receptor antagonist antifungal,[104] insecticidal,[105] and acaricidal activities.[106] They are found in pyrido, pyrrolo, pyrimido, fused spiro oxindole, and arylmethane structures.[107] For example, 6-amino-5-((4-hydroxy-2-oxo-2*H*-benzo[*h*]chromen-3-yl)(4-(trifluoromethyl)phenyl)methyl)-1,3-dimethylpyrimidine-2,4-dione (**V**, Fig. 5) and 5-(3-bromophenyl)-1*H*-indeno[2′,1′:5,6]pyrido[2,3-*d*]pyrimidine-2,4,6-trione (**VI**, Fig. 5) were known as antimicrobial and antidiarrhea, respectively.[101,102] Moreover, Fuentes-Rios *et al.*[108] utilized 1,3-dimethyl-4,5-diaminouracil to form an imine group, which effectively protected the carbonyl group in sugars. It is interesting to mention that compound **V** could be generally prepared *via* the one-pot reaction of 4-hydroxy-2*H*-benzo[*h*]chromen-2-one with 4-triflormethyl benzaldehyde and 6-amino-1,3-dimethylpyrimidine-2,4(1*H*,3H)-dione in refluxing AcOH.[102] Compound **V** exhibited significant activity against *Staphylococcus aureus* MTCC 96 with IC_{50} = 9.37 μg mL^{-1}, and very good activity against *Staphylococcus aureus* MLS 16 MTCC 2940 with IC_{50} = 2.34 μg mL^{-1}, comparable to the reference Ciprofloxacin (IC_{50} = 0.58 μg mL^{-1}).[102]

Similarly, compound **VI** can be generally prepared by the one-pot condensation of 3-bromobenzaldehyde, 1,3-indandione and 6-aminouracil (**2**) in water in the presence of graphene oxide.[109] It was reported that compound **VI** suppresses cyclic nucleotide synthesis in the presence of STa (with an IC_{50} value of 3.4 ± 1.6 μM at 100 nM STa) and is active *in vivo* in an intestinal loop animal model of acute diarrhea.[101]

2.2.1. Synthesis of bis-(6-aminouracils). Using the green approach, Lotfifar *et al.*[53] were able to successfully synthesize

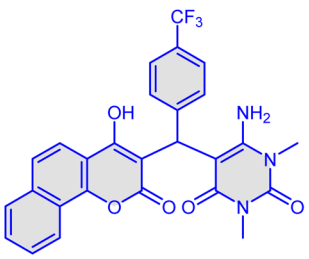

6-Amino-5-((4-hydroxy-2-oxo-2*H*-benzo[*h*]chromen-3-yl)(4-(trifluoromethyl)phenyl)methyl)-1,3-dimethylpyrimidine-2,4(1*H*,3*H*)-dione (**V**)

Antimicrobial

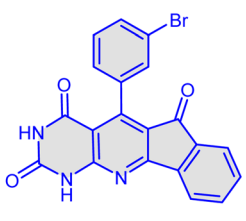

5-(3-bromophenyl)-1*H*-indeno[2',1':5,6]pyrido[2,3-*d*]pyrimidine-2,4,6(3*H*)-trione (**VI**)

Anti-dirrehea

Fig. 5 Structures of some biologically active and fused 6-aminouracil compounds V–VI.

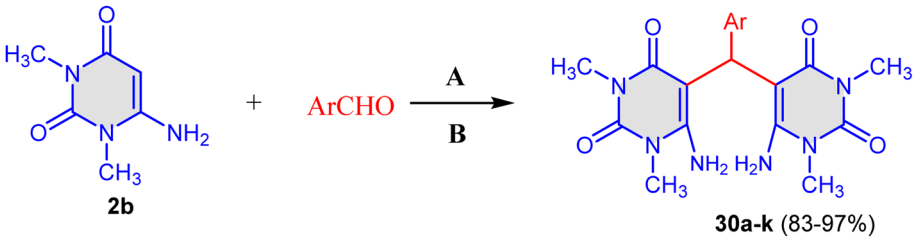

30a-k: **a**: Ar = Ph; **b**: Ar = 4-MeC_6H_5; **c**: Ar = 4-$PhCH_2OC_6H_4$; **d**: Ar = 3-$MeOC_6H_4$; **e**: Ar = 4-$MeOC_6H_4$; **f**: Ar = 2,5-$(MeO)_2C_6H_3$; **g**: Ar = 2-$NO_2C_6H_4$; **h**: Ar = 4-$NO_2C_6H_4$; **i**: Ar = 2-ClC_6H_4; **j**: Ar = 4-ClC_6H_4; **k**: Ar = 2,4-$Cl_2C_6H_3$

Scheme 8 Formation of bis uracils **30a–k**. Reagents and conditions: A; Nano-[FSRN][H_2PO_4]. B; solvent-free, 120 °C.

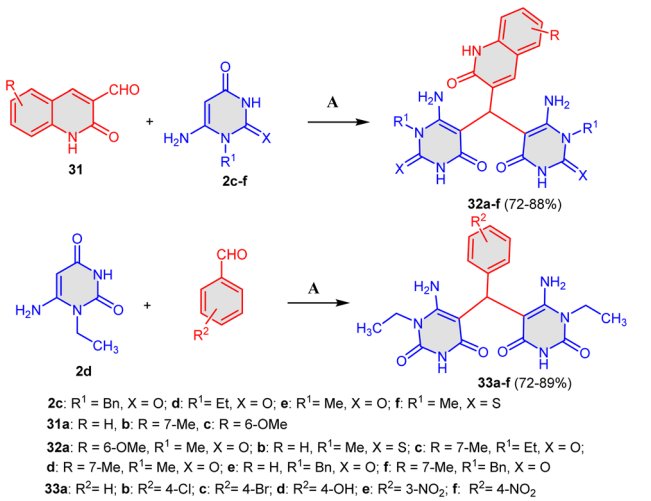

2c: R^1 = Bn, X = O; **d**: R^1= Et, X = O; **e**: R^1= Me, X = O; **f**: R^1 = Me, X = S
31a: R = H, **b**: R = 7-Me, **c**: R = 6-OMe
32a: R = 6-OMe, R^1 = Me, X = O; **b**: R = H, R^1= Me, X = S; **c**: R = 7-Me, R^1= Et, X = O;
d: R = 7-Me, R^1= Me, X = O; **e**: R = H, R^1= Bn, X = O; **f**: R = 7-Me, R^1= Bn, X = O
33a: R^2= H; **b**: R^2= 4-Cl; **c**: R^2= 4-Br; **d**: R^2= 4-OH; **e**: R^2= 3-NO_2; **f**: R^2= 4-NO_2

Scheme 9 Synthesis of quinoline-bis uracil compounds **32a–f** and **33a–f**. Reagents and conditions: A; AcOH, reflux, 3–4 h.

a series of bis(6-amino-1,3-dimethyluracil-5-yl)methane derivatives **30a–k**. The catalyst nano-[Fe_3O_4@SiO_2-R-$NHMe_2$][H_2PO_4] is magnetically recyclable. It was used during the reaction of 6-amino-1,3-dimethyluracil (**2b**) with different aldehydes. The formed products were obtained in excellent yield of 80–97%. Meanwhile, another nano catalyst was announced as *N*,*N*,*N*′,*N*′-tetramethyl-ethylenediaminium bisulfate ([TMEDA][HSO_4]$_2$), which was utilized to produce the final products **30a–k** (Scheme 8).[110]

In 2023, El-Kalyoubi *et al.*[111] reacted quinolone-3-carbaldehydes **31** with 6-aminouracil derivatives **2c–f** in refluxing acetic acid (AcOH) to obtain bis-uracils **32a–f**. Under the same conditions, 6-amino-1-ethyl-uracil (**2d**) reacted with aromatic aldehydes to produce bis-aminouracils **33a–f** (Scheme 9). The anti-proliferative activities of these compounds were screened against three distinct cancer cell lines (HepG-2

Table 6 Cytotoxic effects of the hybrids **32b**, **32c** and **32f** on both A549 and normal cell lines

	Cytotoxicity IC_{50} μM		
Compd	A549	Vero	SI
32b	49.13 ± 0.16	204.15 ± 0.49	4.15
32c	54 ± 0.41	251.79 ± 4.41	4.66
32f	2.49 ± 0.15	28.49 ± 3.12	11.44
Doxorubicin	43.11 ± 1.22	80.4 ± 0.73	1.86

Table 5 Anti-proliferative activity of bis-uracil/quinoline derivatives **32a–f** and **33a–f** against human cancer cell lines (IC_{50} [μM])

					IC_{50} values		
Compd	R	R^1	R^2	X	A549	MCF7	HepG-2
32a	6-OMe	Me	—	O	63.01 ± 0.9	129.8 ± 1.02	58.31 ± 1.26
32b	H	Me	—	S	49.13 ± 0.16	60.31 ± 0.62	59.55 ± 1.01
32c	7-Me	Et	—	O	54 ± 0.41	64.19 ± 0.34	92.68 ± 0.44
32d	7-Me	Me	—	O	66.84 ± 0.66	107.39 ± 2.17	185.99 ± 0.58
32e	H	Bz	—	O	52.92 ± 0.25	103.27 ± 1.73	97.08 ± 0.85
32f	7-Me	Bz	—	O	2.49 ± 0.15	5.00 ± 0.16	6.24 ± 0.04
33a	—	—	H	—	108.52 ± 1.77	77.97 ± 1.52	253.77 ± 4.37
33b	—	—	4-Cl	—	102.1 ± 0.23	199.28 ± 1.97	243.79 ± 1.04
33c	—	—	4-Br	—	53.52 ± 0.7	177.56 ± 1.26	107.66 ± 0.31
33d	—	—	4-OH	—	66.2 ± 1.55	230.17 ± 3.75	202.56 ± 7.34
33e	—	—	3-NO_2	—	127.41 ± 3.27	230.25 ± 1.83	203.7 ± 0.67
33f	—	—	4-NO_2	—	56.41 ± 0.87	219.33 ± 4.77	185.6 ± 8.04
Doxorubicin	—	—	—	—	43.11 ± 1.22	9.93 ± 0.57	35.5 ± 0.46

Table 7 Inhibitory efficacy of compounds (**32b**, **32c** and **32f**) against topoisomerases I and II

Compd	Topoisomerase I (IC_{50}) μM	Topoisomerase II (IC_{50}) μM
32b	12.17 ± 0.58	20.28 ± 0.94
32c	43.57 ± 2.09	32.42 ± 1.50
32f	2.83 ± 0.14	7.34 ± 0.34
Camptothecin	1.07 ± 0.05	—
Doxorubicin	—	4.22 ± 0.19

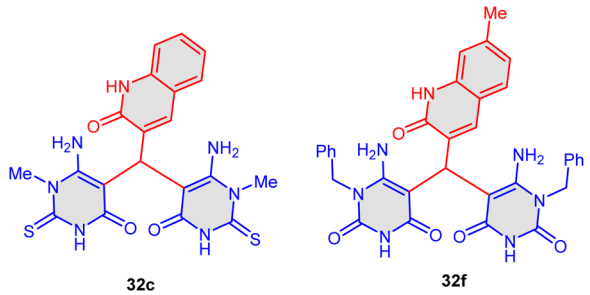

Fig. 6 Structures of antiproliferative compounds **32c** and **32f**.

hepatic carcinoma, MCF-7 breast adenocarcinoma, and A549 lung cancer) and compared with the standard reference doxorubicin (Tables 5 and 6).[111]

2.2.1.1 Structure activity relationship. Based on the results presented in Tables 5–7, compounds **32a** (R = 6-Me, R^1 = Me) and **32d** (R = 6-Me, R^1 = Me) revealed a moderate activity against the standard drug (doxorubicin). However, compound **32e**, which contains non-substituted quinoline and R^1 = benzyl, demonstrated non-selective efficacy against A549, MCF-7, and HepG-2 cell lines in the micromolar range with IC_{50} values of 52.92, 103.27 and 97.08 μM, which compared to 43.11, 9.93 and 35.50 μM for doxorubicin, respectively. The activity increased when additional electron-donating groups, where (R = Et) **32c** (Fig. 6), were substituted for the methyl group on the bisuracil unit (IC_{50} = 54.00, 64.19, and 92.68, respectively). It was also shown that biological effectiveness was significantly influenced by the type of heteroatom present on the uracil ring. When the oxygen atom was replaced with a sulfur atom, the antiproliferative activity was extremely improved, as observed in **32b** (IC_{50} values of 49.13, 60.31, and 59.55 μM in A549, MCF-7, and HepG-2 cell lines, respectively). The activity increased as a result of substituents at the uracil ring (R^1 = benzyl) and the electron-donating substituent's impact on the quinoline moiety (R = Me), as shown in compound **32f** (Fig. 6). An acceptable activity that appeared unlikely to be better for the activity was obtained by substituting the quinoline moiety into a substituted monoaryl system. Summarily, adding a rigid bulky group to the uracil moiety and/or a lipophilic electron donating group to the quinoline ring resulted in a significant improvement in antiproliferative inhibitory activity.

2.2.2. Synthesis of pyrrolo-pyrimidine derivatives. Bis-pyrrolo[2,3-*d*]pyrimidine derivatives **37a–e** or **38a–g** were obtained in 90–96% yields *via* a one-pot multicomponent reaction between 6-aminouracils (**2**), 1,4-phenylene-bis-glyoxal (**34**), and dimedone (**35**) or derivatives of barbituric acid (**36**), and the reaction was performed in 5% tetrapropylammonium bromide (TRAB) and EtOH at reflux temperature (Scheme 10).[112] In a trial of study, the reaction of 1,4-phenylene-bis-glyoxal (**34**), 6-aminouracil (**2**), and dimedone (**35**) was chosen as a model reaction

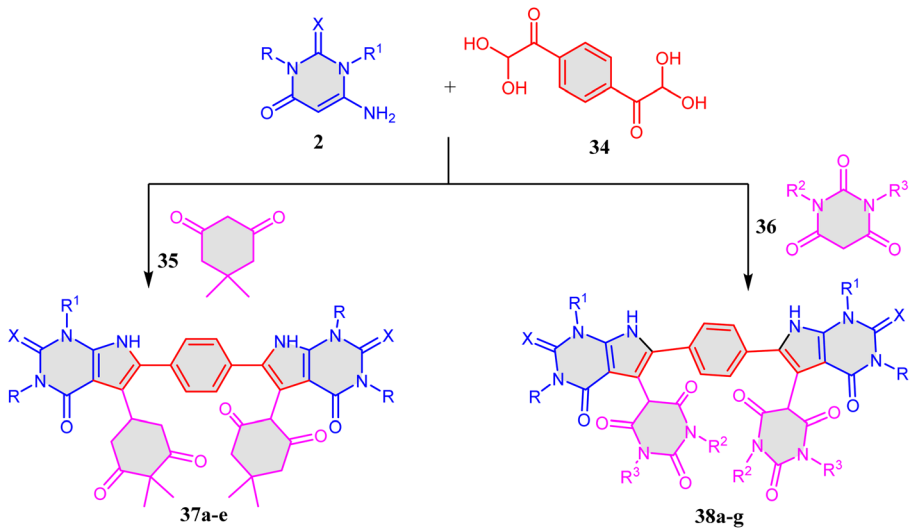

37a-e: **37a**: R = R^1= H; X = O; **b**: R = H; R^1= Me; X = O; **c**: R = R^1= Me; X = O; **d**: R = R^1= Et; X = O; **e**: R = R^1= Et; X = S

38a-g: **38a**: R = R^1= R^2= R^3= H, X = O; **b**: R = R^1= H; R^2= R^3 = Me, X = O; **c**: R = R^1= H, R^3 = R^2= Me, X = O; **d**: R = H, R^1=R^2=R^3 = Me, X = O; **e**: R = R^1= R^2= R^3 = Me, X = O; **f**: R = R^1= Et, R^2= R^3 = Me, X = O; **g**: R = R^1= H; R^2= R^3 = Me, X = S

Scheme 10 Synthesis of bispyrrolo[2,3-*d*]pyrimidines **37a–e** and **38a–g**. Reagents and conditions: A; TRAB, EtOH, reflux.

Table 8 Effects of several solvents, temperatures, and mol% of TPAB on the synthesis of **37a–e** and **38a–e**[a]

Entry	Catalyst	Temperature (°C)	Solvent	Time (h)	**37a** yield (%)	**38a** yield (%)
1	No catalyst	50	EtOH	4	No reaction	No reaction
2	No catalyst	Reflux	EtOH	2	48	41
3	TPAB (5 mol%)	RT	EtOH	1.5	51	47
4	TPAB (5 mol%)	50	EtOH	1.5	48	47
5	TPAB (5 mol%)	60	EtOH	1.5	55	50
6	TPAB (5 mol%)	Reflux	EtOH	1.5	95	92
7	TPAB (10 mol%)	Reflux	EtOH	1.5	94	90
8	TPAB (5 mol%)	Reflux	THF	1.5	40	40
9	TPAB (5 mol%)	Reflux	MeOH	1.5	55	50
10	TPAB (5 mol%)	Reflux	CH_2Cl_2	1.5	20	Trace
11	TPAB (5 mol%)	Reflux	CH_3CN	1.5	28	Trace
12	TPAB (5 mol%)	Reflux	DMF	1.5	45	43
13	TPAB (5 mol%)	Reflux	H_2O	1.5	61	58

[a] 1,4-Phenylene-bis-glyoxal (1 mmol), 6-aminouracil (2 mmol), and barbituric acid (2 mmol)/EtOH (5 mL). 1,4-phenylene-bis-glyoxal (1 mmol), 6-aminouracil (2 mmol), and dimedone (2 mmol)/EtOH (5 mL). RT, room temperature; TPAB, tetrapropylammonium bromide.

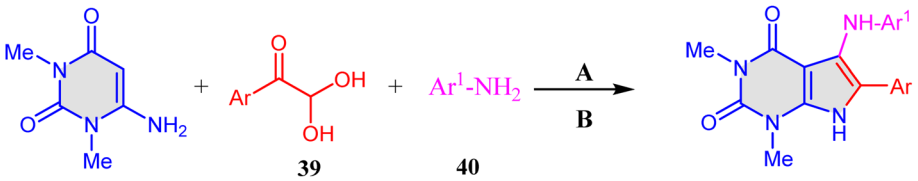

41a-m: **a**: Ar = Ar^1 = Ph, **b**: Ar = Ph, Ar^1 = 4-MeC_6H_4; **c**: Ar = Ph, Ar^1 = 4-ClC_6H_4; **d**: Ar = Ph, Ar^1 = 4-BrC_6H_4; **e**: Ar = 4-MeC_6H_4, Ar^1 = Ph; **f**: Ar = Ar^1 = 4-$CH_3C_6H_4$; **g**: Ar = 4-MeC_6H_5, Ar^1 = 4-ClC_6H_4; **h**: Ar = 4-MeC_6H_5, Ar^1 = 4-BrC_6H_4; **i** = Ar = 4-$MeOC_6H_5$, Ar^1 = Ph; **j**: Ar = 4-$MeOC_6H_5$, Ar^1 = 4-$CH_3C_6H_4$; k: Ar = 4-$MeOC_6H_5$, Ar^1 = 4-ClC_6H_4; **l**: Ar = 4-$MeOC_6H_5$, Ar^1 = 4-BrC_6H_4; **m**: Ar = 4-ClC_6H_5, Ar^1 = Ph

Scheme 11 Three-component reaction for the formation of pyrrolo[2,3-*d*]pyrimidines **41a–m**. Reagents and conditions: **A**; AcOH, MW 110 °C, 5 min.

to form products **38a–e**. However, the reaction of **34**, **2**, and barbituric acid (**36**) was chosen as a model reaction for products **38a–g** (Table 8). First, these model reactions were carried out in the absence of a catalyst, but no products were observed even after 4 h of stirring at 50 °C (Table 8, entry 1). It was found that the yields improved when the temperature was increased to reflux. The best result was obtained in terms of yield (95% and 92%) and reaction time (1.5 h) when the reaction was performed using 5 mol% of TPAB (Table 8, entry 6). The use of EtOH proved to be the best in terms of yield and reaction time (Table 8, entry 6).

In the same previous manner, a microwave-assisted one-pot reaction involving *N*,*N*-dimethyl-6-aminouracil (**2b**), aryl glyoxal monohydrates **39**, and aryl amines **40** was used to synthesize 5-arylamino-pyrrolo[2,3-*d*]pyrimidine derivatives **41a–m** (Scheme 11).[113] It is worth mentioning that the reaction proceeded efficiently in AcOH at 110 °C to give the corresponding product **41a** in 84% yield (Table 9, entry 8).

Scheme 12 illustrates the suggested mechanism in which AcOH would act as a solvent and promoter of Brønsted acid during the reaction as well. Initially, the condensation reaction

Table 9 Optimized conditions for a model example of **2b**, **39**, and aniline (**40a**) under microwave irradiation

Entry	Solvent	Catalyst	Temp (°C)	Time (min)	Yield (%)
1	EtOH	—	75	5	25
2	EtOH	PTSA	75	5	40
3	EtOH	$InCl_3$	75	5	35
4	EtOH	$Sc(OTf)_3$	75	5	30
5	CH_3CN	PTSA	80	5	Trace
6	Toluene	PTSA	100	5	Trace
7	DMF	PTSA	100	5	Trace
8	AcOH	—	100	5	84

occurs between aryl glyoxal (**39**) and aryl amines **40** to give compound **42**. The latter in the presence of acidic media was then converted into intermediate **43**, which would be nucleophilically attacked by C-5 of **2b** to give intermediate **44**. Then, the transformation of **44** into intermediate **45** was occurred, which was subsequently followed by an intermolecular cyclization to form intermediate **46**. Finally, the loss of a hydrogen proton from **46**, followed by dehydration, produces the targeted products **41a–m**.[113]

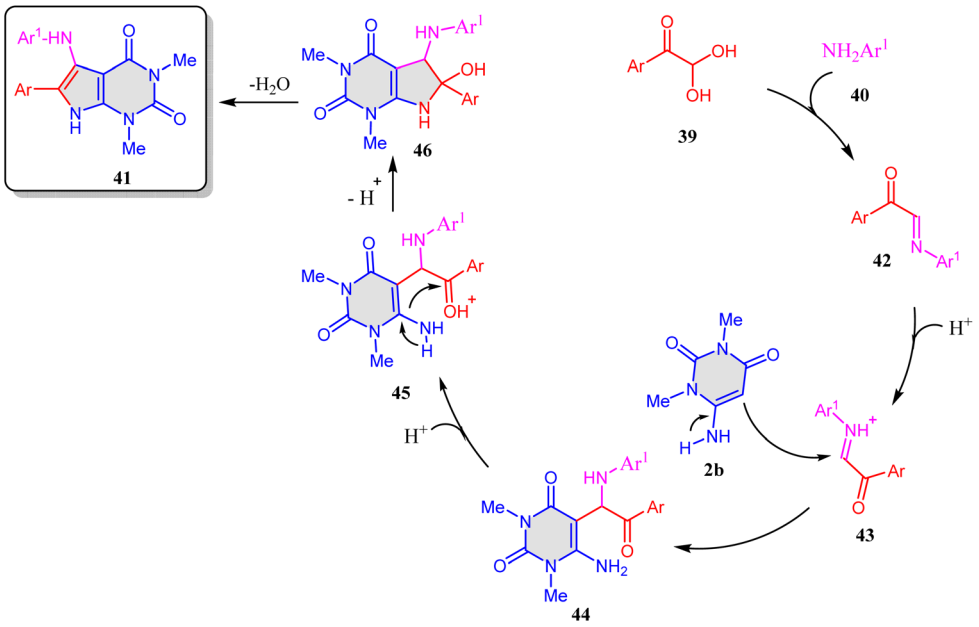

Scheme 12 Proposed mechanism for the formation of **41a–m**.

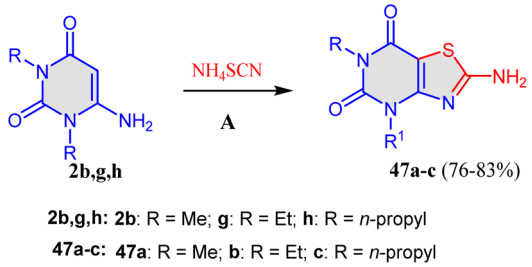

Scheme 13 Synthesis of uracil-fused 2-aminobenzothiazoles **47a–c**. Reagents and conditions: **A**; (i) H_2O_2, rt; (ii) NaOH, rt, 1 h.

2.2.3. Synthesis of thiazolo-pyrimidine derivatives. Interestingly, Ali *et al.*[47] successfully synthesized amino-thiazolo[4,5-*d*]pyrimidine-5,7-(4*H*,6*H*)-dione derivatives **47a–c** in good yields (76–83%) by treating 6-aminouracils **2b**, **g**, and **h** with ammonium thiocyanate (NH_4SCN) and catalyzed by H_2O_2 at room temperature (Scheme 13).

2.2.4. Synthesis of imidazo-pyrimidinedione (xanthine) derivatives. The nitrosation of 6-aminouracils **2b,e** directly produced 5-nitroso-6-aminouracils **48a** and **b** by employing sodium nitrite in 50% aqueous AcOH. In an aqueous ammonia solution and sodium dithionite ($Na_2S_2O_4$), reduction of **48a,b** produced 5,6-diamino-1,3-dimethyluracils **49a,b**. As shown in Scheme 14,[31] xanthine derivatives **50a,b** were produced by directly cyclizing 5,6-diamino-uracils **49a,b** using carbon disulfide (CS_2) in DMF under reflux for 5 h.[31]

In 2020, Han *et al.*[114] developed a synthesis of a series of 8,8′-disulfanediyl-bis(3-ethyl-1-substituted-3,7-dihydro-1*H*-purine-2,6-diones) **53a–k** (Scheme 15). Moreover, 5,6-diamino-uracils **51a–k** were prepared through the reaction of 6-aminouracils **2** with sodium nitrite ($NaNO_2$) in the presence of AcOH. Following

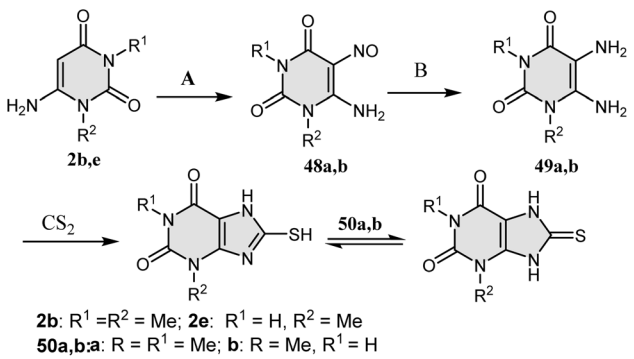

Scheme 14 Synthesis of xanthine derivatives **50a,b**. Reagents and conditions: **A**; $NaNO_2$/AcOH. **B**; $NH_3/Na_2S_2O_4$. **C**; CS_2/(DMF/EtOH), reflux.

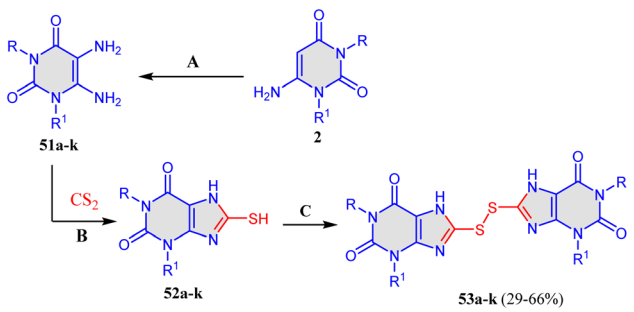

Scheme 15 Synthesis of 8,8′-disulfanediylbis(dihydro-1*H*-purine-2,6-diones) **53a–k**. Reagents and conditions: **A**; $NaNO_2$/AcOH, 70 °C, $Na_2S_2O_4$, NH_4OH, 70 °C. **B**; $NaHCO_3$, EtOH:H_2O, 65 °C, **C**; (i) I_2, KOH, EtOH, rt. (ii) reflux, overnight.

Table 10 Inhibitory activities of compound **53a–k** and their derivatives for SIRT1/2/3/5/6

Compd	R	R^1	IC_{50} (μM) SIRT3	SIRT1	SIRT2	SIRT5	SIRT6
53a	$-CH_2CH_3$	$-CH_2CH_3$	0.79 ± 0.06	0.10 ± 0.01	1.17 ± 0.04	0.42 ± 0.01	116.0 ± 6.2
53b	$-CH_2CH_2CH_3$	$-CH_2CH_2CH_3$	0.54 ± 0.05	0.12 ± 0.01	1.19 ± 0.06	0.39 ± 0.03	128.7 ± 16.1
53c	$-CH_2CH(CH_3)_2$	$-CH_2CH_3$	1.77 ± 0.05	0.43 ± 0.03	4.86 ± 0.08	1.51 ± 0.10	296.6 ± 11.3
53d		$-CH_2CH_3$	0.72 ± 0.06	0.17 ± 0.01	2.25 ± 0.12	0.50 ± 0.01	155.8 ± 6.5
53e		$-CH_2CH_3$	0.69 ± 0.12	0.15 ± 0.02	1.62 ± 0.05	0.54 ± 0.02	126.5 ± 10.2
53f	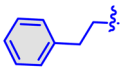	$-CH_2CH_3$	0.37 ± 0.05	0.17 ± 0.01	1.35 ± 0.05	0.45 ± 0.01	103.3 ± 6.3
53g	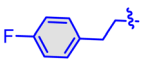	$-CH_2CH_3$	0.46 ± 0.04	0.19 ± 0.01	2.03 ± 0.04	0.84 ± 0.08	110.9 ± 2.6
53h	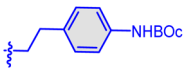	$-CH_2CH_3$	1.15 ± 0.08	0.41 ± 0.04	2.19 ± 0.08	1.00 ± 0.03	128.3 ± 4.1
53i	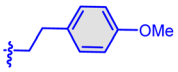	$-CH_2CH_3$	0.61 ± 0.03	0.21 ± 0.02	2.16 ± 0.08	0.61 ± 0.02	102.3 ± 9.1
53j	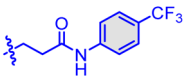	$-CH_2CH_3$	8.52 ± 0.22	1.87 ± 0.04	9.44 ± 0.19	26.12 ± 3.15	452.0 ± 9.8
53k	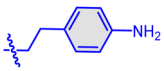	$-CH_2CH_3$	0.97 ± 0.06	0.49 ± 0.01	4.61 ± 0.13	0.92 ± 0.04	209.6 ± 5.9
ELT-31	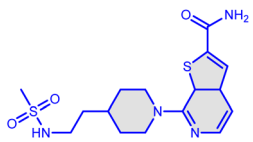		0.35 ± 0.02	0.27 ± 0.02	0.12 ± 0.01	>500	462.0 ± 14.9

that, 5,6-diaminouracils **51a–k** were treated with CS_2 in EtOH/H_2O in the presence of sodium bicarbonate ($NaHCO_3$) at 65 °C to give 8-mercapto-3,7-dihydro-1*H*-purine-2,6-diones **52a–k.** The resulting mercapto-purines were then refluxed in EtOH/KOH, and the reaction proceeded to give the final products **53a–k** (Scheme 15). The potential uses of sirtuin inhibitors include the treatment of several types of cancer and neurological diseases. The tested compounds **53a–k** showed that they are potent SIRT1/2/3/5 pan-inhibitors. Besides, compound **53f** (R = phenylethyl) exhibited the highest activity among all the examined derivatives. The results showed that **53f** was nontoxic at concentrations higher than 20 μM and stable in the assays, as shown in Table 10.[114]

2.2.4.1 Structure activity relationship. The data in Table 10 showed that compound **53b** (R = propyl) was more potent than compound **53a** (R = Et), demonstrating that the existence of

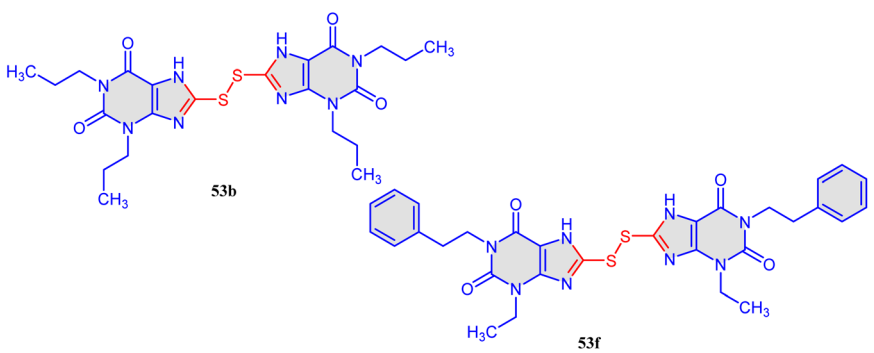

Fig. 7 Structures of sirtuin inhibitor compounds **53b** and **53f**.

long-chain alkyls at the R site improves the activity. Comparing the activities of **53a**, **53b**, and **53c** (R = *tert*-Bu), it was noted that the results in groups with branched chains were not satisfactory, indicating that there is a restricted space surrounding the R location in SIRT3. Correspondingly, derivatives **53d** (R = tetrahydropyran) and **53e** (R = tetrahydrofuran) cause a decrease in inhibitory activity compared to **53b**. Moreover, the presence of cycloalkanes at R (**53d** and **53e**) increased the hydrophobicity, leading to an improvement in activity compared to **53c**. Attempting to increase the activity of compound **53f** (R = phenethyl) (Fig. 7), the inhibitory action of SIRT3 was significantly increased. Besides, compounds **63g–i** and **53k**, which had a fluoro, Boc-protected amino, OMe, or NH_2 at the *p*-position of the phenethyl, respectively, showed a reduction in the activity. Furthermore, substituting the phenethyl with *N*-(3-(trifluoromethyl)phenyl)propionamide (compound **53j**) significantly decreased inhibitory action (23-fold) compared to **53f** (Fig. 7), suggesting that a larger group at the R position may cause steric hindrance with SIRT3.[114]

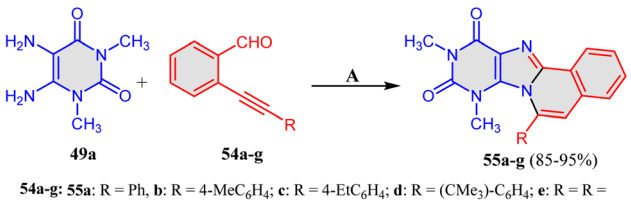

54a-g: **55a**: R = Ph, **b**: R = 4-MeC_6H_4; **c**: R = 4-EtC_6H_4; **d**: R = (CMe_3)-C_6H_4; **e**: R = R = C_6H_{13}; **f**: R = C_3H_7; **g**: R = 4-MeOC_6H_4

Scheme 16 Synthesis of 8,10-dimethyl-6-substituted purino[8,9-*a*]isoquinoline-9,11(8*H*,10*H*)-diones **55a–g**. Reagents and conditions: A; DMF, CuI, reflux.

Furthermore, 5,6-diamino-1,3-dimethylpyrimidine-2,4(1*H*,3*H*)-dione (**49a**) was allowed to react with 2-(ethynyl)-benzaldehydes **54a–g** catalyzed by CuI at refluxing DMF. The reaction proceeded to obtain 8,10-dimethyl-6-substituted-purino[8,9-*a*]isoquinoline-9,11-diones **55a–g** in good yields (Scheme 16).[115]

The suggested mechanism for the formation of compounds **55a–g** is illustrated in Scheme 17. Initially, imine **56** was produced through a reaction between 5,6-diamino-1,3-dimethyluracil (**49a**) and *o*-alkynyl aromatic aldehydes **54**. Subsequently, CuI promoted the nucleophilic attack of the NH_2 group on the imine carbon. Furthermore, aerial oxidation occurred on imine **56** to produce intermediate **57**. This was followed by a second intramolecular nucleophilic attack of the unsaturated imidazole nitrogen atom on the activated alkyne to form intermediate **58**, while the cyclized products **55a–g** were produced after the protonation process of intermediate **58**.[115]

A multi-step pot reaction for the synthesis of compounds **64a–g** was developed by Yang and co-workers,[32] as summarized in Scheme 18. They started by reacting 1-benzyl-6-aminouracil (**2c**) with 4-methoxypyridine in acetonitrile (MeCN) containing *N*-bromosuccinimide (NBS) to give 1-benzyl-8-methoxypyrido[2,1-*f*]purine-2,4(1*H*,3*H*)-dione (**59**). Compound **59** was then alkylated using *n*-propyl bromide (^{n}Pr-Br) to produce compound **60**. Subsequently, an elimination of the benzyl group using

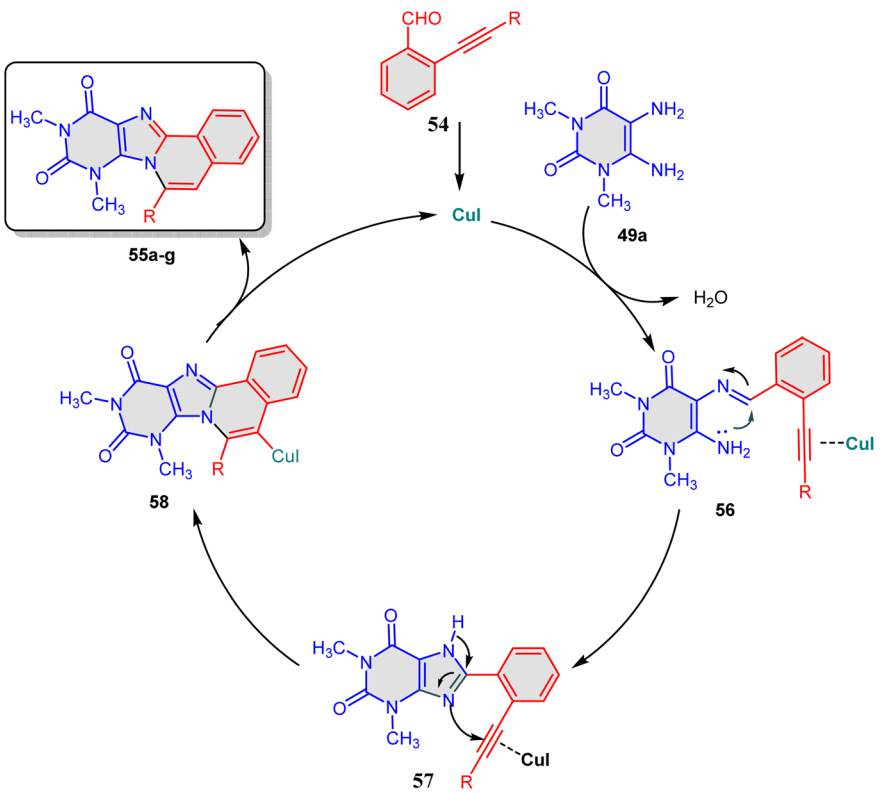

Scheme 17 Suggested mechanism for the formation of 6-substituted purino[8,9-*a*]isoquinoline-9,11-diones **55a–g**.

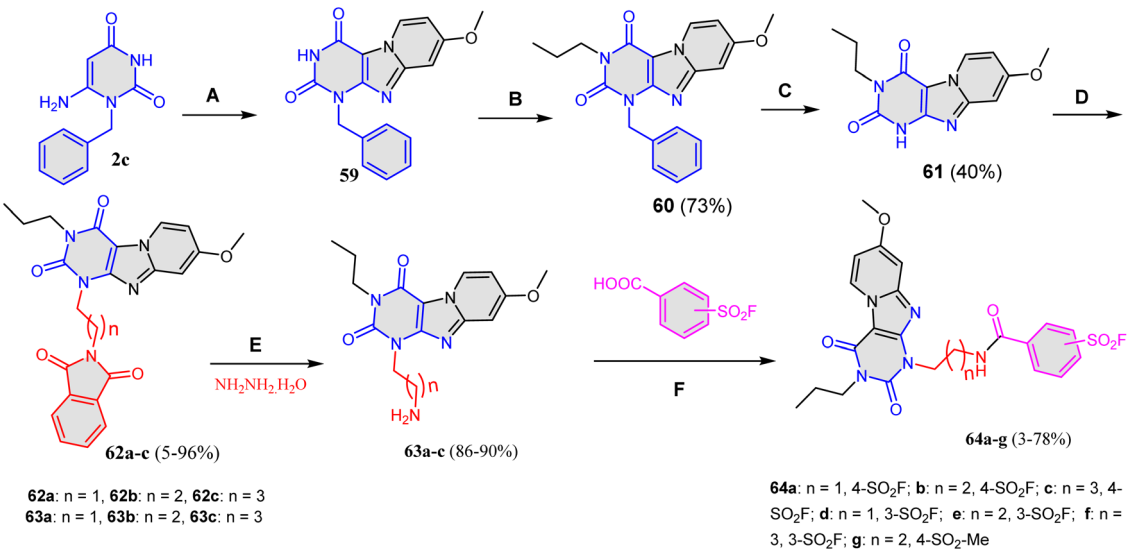

Scheme 18 Multistep reaction for the synthesis of hybrids **64a–g**. Reagents and conditions: **A**; (i) NBS, MeCN, 80 °C, 1 h. (ii) 4-methoxypyridine, 80 °C, overnight. **B**; ^{n}Pr-Br, DBU, MeCN, 80 °C. **C**; $Pd(OH)_2/C$, $HCOONH_4$, EtOH, reflux. **D**; *N*-bromoalkyl phthalamide, K_2CO_3, DMF, 100 °C, **E**; $N_2H_4 \cdot H_2O$, MeOH, reflux. **F**; $SOCl_2$, K_2CO_3, dry DMF, 40 °C.

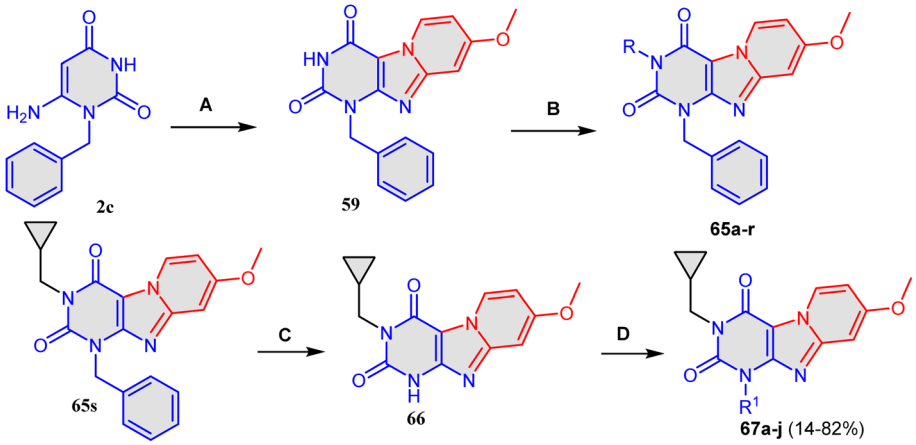

Scheme 19 Synthesis of xanthine derivatives **67a–j**. Reagents and conditions: **A**; (i) NBS, MeCN, 80°°C, 1 h. (ii) 4-methoxypyridine, 80 °C, overnight. **B**; R–Br, DBU, MeCN, 80 °C. **C**; $Pd(OH)_2$, ammonium formate, EtOH, reflux, overnight. **D**; R^1-Br, K_2CO_3, DMF, overnight.

palladium hydroxide ($Pd(OH)_2$) gave the corresponding xanthine scaffold **61** in 40% yield. Thereafter, compound **61** was allowed to react with *N*-bromoalkyl phthalamide in DMF at 100 °C to give compounds **62a–c**. The reaction of **62a–c** with hydrazine hydrate led to the formation of the corresponding amines **63a–c**. Eventually, the reaction of compounds **63a–c** with various benzoic acids afforded the desired products of **64a–g** (Scheme 18).[32]

Xia *et al.*[116] prepared compound **59**, which was further alkylated using different alkyl bromides with 1,8-diazabicyclo[5.4.0] undec-7-ene (DBU) and MeCN at 80 °C, followed by heating in 4-

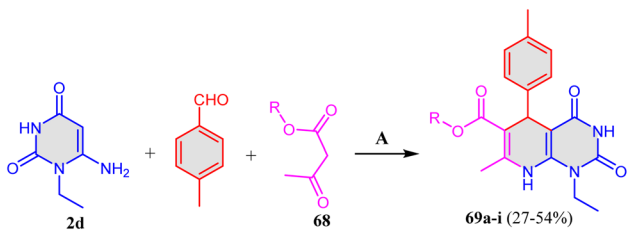

Scheme 20 Synthesis of pyrido[2,3-*d*]pyrimidine-6-carboxylates **69a–i**. Reagents and conditions: **A**; AcOH, reflux.

Table 11 Structures and affinity profiles for compounds 69a–i

Compd	R	IC_{50} (μM) BRDT-1	IC_{50} (μM) BRD4-1
69a	Me	5.9	5.4
69b	Propyl	7.9	5.5
69c	Allyl	4.7	3.1
69d	*t* Bu	10	5.5
69e	Bn	0.79	0.97
69f	4-$ClC_6H_4CH_2$	14	9.4
69g	4-$OMeC_6H_4CH_2$	15	11
69h	3,4-$(OMe)_2C_6H_4CH_2$	7.0	4.5
69i	4-$OMeC_6H_4CH_2CH_2$	11	9.1
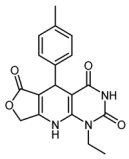		5.4	4.1
(+)-JQ1[a]		0.16	0.050

[a] (+)-JQ1 was used as the positive control. All compounds were tested once in duplicate.

methoxypyridine at 80 °C, to give 1-benzyl-8-methoxypyrido[2,1-*f*]purine-2,4(1*H*,3*H*)-dione (**59**). Alkylation of *N*-3 in **59** by various alkyl halides using DBU as a catalyst afforded **65a–r** (Scheme 19). In the case of 3-(cyclopropylmethyl)pyrido[2,1-*f*] purine (**65s**), the benzyl group in *N*-1 was removed *via* the reaction with $Pd(OH)_2$ and ammonium formate in refluxing EtOH to give 3-(cyclopropylmethyl)-8-methoxypyrido[2,1-*f*] purine-2,4(1*H*,3*H*)-dione (**66**). Compounds **67a–j** were then obtained, and *N*-1 was alkylated by treating **66** with different alkyl bromides in a mixture of DMF and K_2CO_3 (Scheme 19). Benzyl-3-propyl-1*H*,3*H*-pyrido[2,1-*f*]purine-2,4-dione derivative **65c** was illustrated as a lead compound of **65a–s** since it exhibits a K_i value of 4.0 ± 0.3 nM against the hA_3 receptor. Generally, pyrido [2,1-*f*]purine-2,4-dione derivatives **65a–s** have been described as a family of adenosine receptor antagonists.

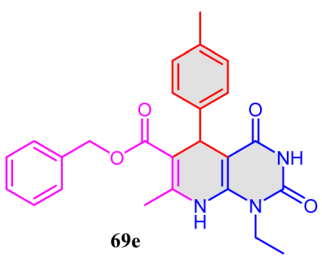

Fig. 8 Structure of compound **69e** with high affinity for BRDT-1 and BRD4-1.

2.2.5. Synthesis of pyrido[2,3-*d*]pyrimidine derivatives. A three-component one pot synthesis succeeded in obtaining substituted 1-ethyl-*N*-7-methyl-2,4-dioxo-5-*p*-tolyl-1,2,3,4,5,8-hexahydropyrido[2,3-*d*]pyrimidine-6-carboxamides **69a–i** in 27–54% yields.[117] The latter series was established *via* the reaction of a mixture of 6-amino-1-ethyluracil (**2d**), 4-methyl-benzaldehyde and 3-oxobutanoate ester derivatives **68** in refluxing AcOH (Scheme 20).[117] The formed compounds **69a–i** were examined for BRDT-1 and BRD4-1 inhibition (*i.e.* these proteins are involved in regulating gene expression, and their inhibition is explored as a potential therapeutic strategy for various diseases) using an Alpha Screen assay. Benzyl ester derivatives **69e** revealed the greatest affinity for BRD4-1 and BRDT-1. Profiling across bromodomains showed a high selectivity of **69e**, where R = Bn in case of the BET bromodomain family (Table 11).[117]

2.2.5.1 Structure activity relationship. The results in Table 11 show that compounds **69a**, **69b**, and **69c**, which have linear aliphatic chains, exhibited moderate activity, while the *tert*-butyl substituent **69d** decreased 2 times in BRDT-1 affinity compared with the lactone. In the case of the benzyl group **69e** (Fig. 8), the affinity was extremely enhanced for BRDT-1 and BRD4-1 (IC_{50} = 0.79 and 0.97, respectively). In addition, adding an (OMe) group or a chlorine atom to the aryl ring resulted in a reduction in affinity, as in the **69f** and **69g** derivatives. Furthermore, a comparison between **69g**, **69h**, and **69i** demonstrated that di-substitution and linker extension had only a small impact on affinity.[117]

In 2024, Yaragorla,[118] developed a simple reaction for the synthesis of pyrido[2,3-*d*]pyrimidine scaffolds **72a–k** during the reaction of 6-aminouracils **2** with propargyl alcohols **70**. The

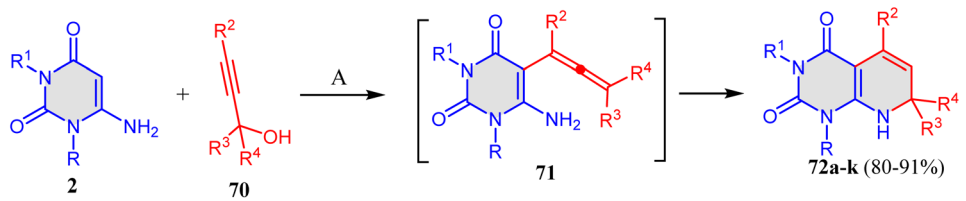

72a: R = R^1= Me, R^2= R^3=R^4= Ph; **b**: R = R^1= Me, R^2= Ph, R^4= R^3= 4-MeC_5H_4; **c**: R = R^1= Me, R^2= Ph, R^4= R^3= 4-$OMeC_5H_4$; **d**: R = R^1= Me, R^2= Ph, R^4= R^3= 4-ClC_5H_4; **e**: R = R^1= Me, R^2= Ph, R^4= R^3= 4-FC_5H_4; **f**: R = R^1= Me, R^2= R^3= Ph, R^4= 4-BrC_5H_4; **g**: R = R^1= Me, R^2= R^3= Ph, R^4= 4-ClC_5H_4; **h**: R = R^1= Me, R^2= R^3= Ph, R^4= 4-$OMeC_5H_4$; **i**: R = R^1= Me, R^2= R^3= Ph, R^4= 2-MeC_5H_4; **j**: R = R^1= R^4= Me, R^2= R^3= Ph; **k**: R = R^1= Me, R^2= Ph, R^4= R^3= Et

Scheme 21 Mechanochemical reaction between 6-aminouracil **2** and propargyl alcohols **70**. Reagents and conditions: A; HFIP/*p*-TsOH, 1–2 h.

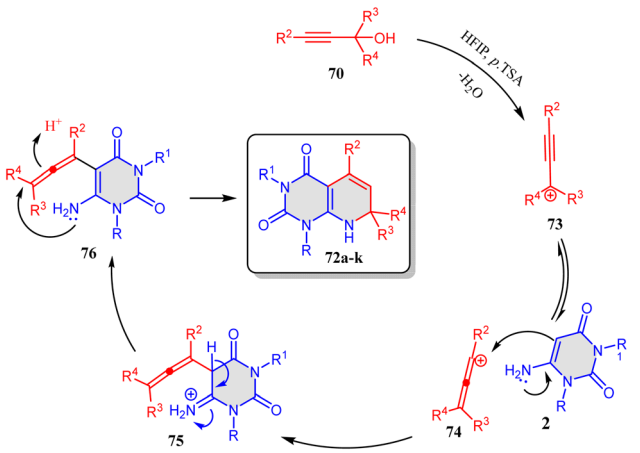

Scheme 22 Suggested mechanism for the formation of compounds 72a–k.

reaction proceeded *via* a [3 + 3] cascade annulation through the allenylation of uracil, followed by 6-*endo* trig cyclization in the presence of hexafluoroisopropanol (HFIP) and *p*-toluene sulfonic acid (*p*-TsOH). The final products were obtained through the formation of intermediate **71**, as illustrated in Scheme 21.[118]

A plausible mechanism for the synthesis of compounds **72a–k** is shown in Scheme 22. First, the catalyst mixture (HFIP/*p*-TSA) acts as a Brønsted acid and protonates propargyl alcohols **70** to produce propargylic cation **73** through the elimination of a water molecule. Intermediate **73** was then converted to an allenyl cation (**74**). Subsequently, the alkylation of uracil proceeded to afford the allene intermediate **75**. Finally, the targeted pyrido[2,3-*d*]pyrimidines **72a–k** were formed through the intramolecular 6-*endo-trig*-cyclization of **76** (Scheme 22).[118]

Hussain *et al.*[50] utilized 6-amino-5-formyluracil (**77**) as a precursor for several heterocyclic compounds. Scheme 23 described the reaction of **77** with several active methylene compounds, such as cyclohexane-1,3-dione (**78**), dimedone (**35**) and 1*H*-indene-1,3(2*H*)-dione (**79**), to form pyrido[2,3-*d*]pyrimidine scaffolds **80**, **81**, and **82**, respectively. However, compound **77** was allowed to react with pyrazole derivatives **83a–d** to obtain the corresponding pyrazolo[4′,3′:5,6]pyrido[2,3-*d*]pyrimidines derivatives **84a–d** (Scheme 23). All the reactions were performed in DMF and catalyzed by DBU.[51]

The same group utilized compound **77** in the synthesis of other heterocycles during its reaction with various compounds, such as thiazolidine-2,4-dione (**85**) and 2-thioxo-dihydropyrimidine-4,6(1*H*,5*H*)-dione (**86a**). The corresponding 5,7-dimethylthiazolo[5′,4′:5,6]-pyrido[2,3-*d*]pyrimidine-2,6,8(3*H*,5*H*,7*H*)-trione (**87**) and 2-thioxodihydropyrimidine-4,6-(1*H*,5*H*)-dione (**88**) were obtained, respectively. When compound **77** was reacted with 3-methyl-1*H*-pyrazol-5-amine (**89**), the reaction afforded 3,6,8-trimethyl-1,8-dihydro-5*H*-pyrazolo[4′,3′:5,6]pyrido[2,3-*d*]pyrimidine-5,7(6*H*)-dione (**90**). The reaction of **77** with **2a,b** afforded pyrido[2,3-*d*:6,5-*d*′]dipyrimidines **91a,b** (Scheme 24).[50]

In continuation, the reactions of 6-amino-5-formyluracil (**77**) with 4-hydroxy-2*H*-chromen-2-one (**92**), 1-ethyl-4-

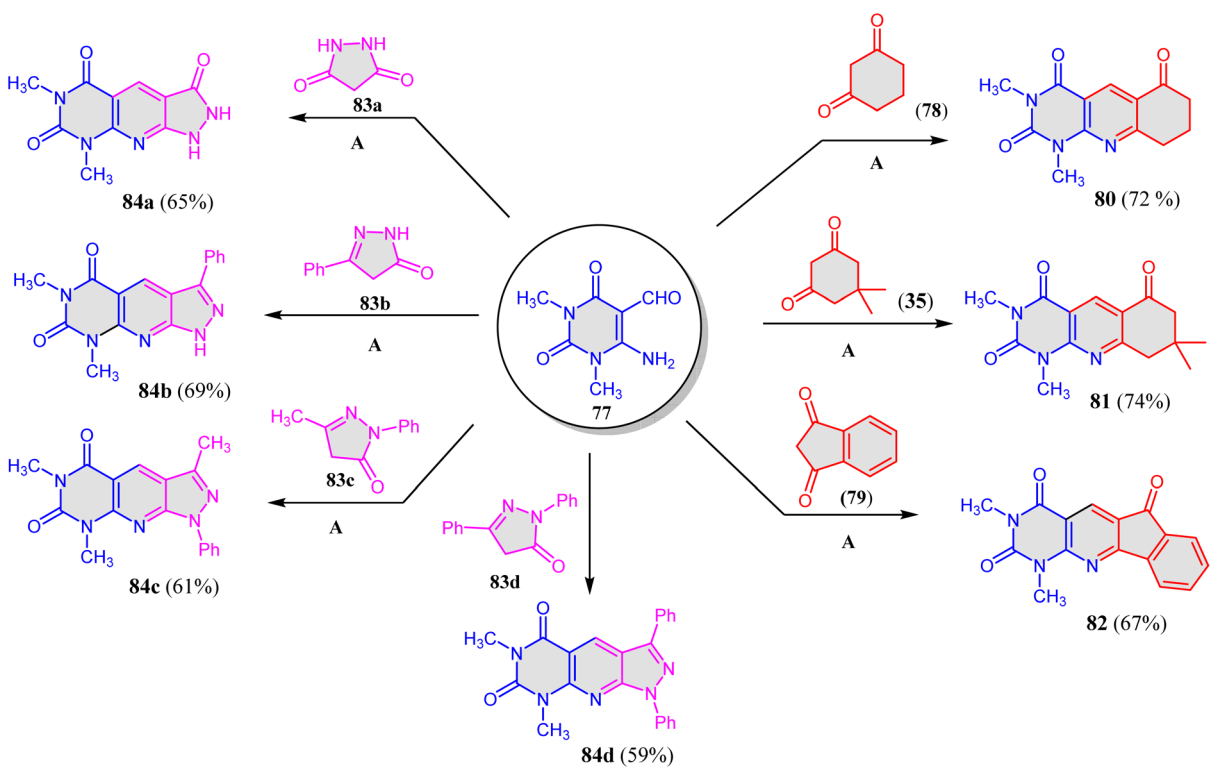

Scheme 23 Reaction of 6-amino-5-formyluracil **77** with cyclic carbon nucleophiles. Reagents and conditions: **A**; DMF/DBU, reflux. 120 min.

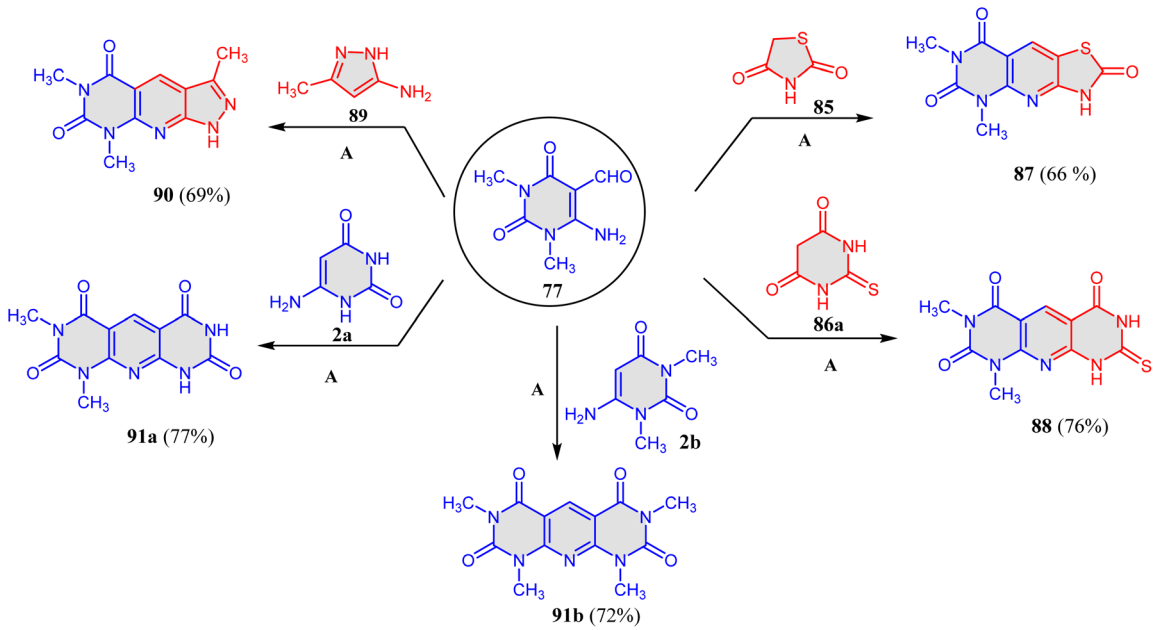

Scheme 24 Synthesis of compounds **87**, **88**, **90** and **91a**,**b**. Reagents and conditions: **A**; DMF/DBU, reflux. 120 min.

hydroxyquinolin-2(1*H*)-one (**93**) and 2-hydroxy-4*H*-pyrido[1,2-*a*] pyrimidin-4-one (**94**) in DMF and DBU for 30 min produce pyrido[2,3-*d*]pyrimidine building blocks **95**, **96** and **97**, respectively, as depicted in Scheme 25.[50]

The formed products were evaluated owing to their antimicrobial activity against Gram-positive bacteria, namely *Bacillus subtilis* (ATCC6635) and *Staphylococcus aureus* (ATCC25923), as well as Gram-negative bacteria, namely *E. coli* (ATCC 25922) and *Salmonella typhimurium* (ATCC 14028). Moreover, they were tested for yeast (*Candida albicans* ATCC 10231) and fungus (*Asperigillus fumigatus*). The majority of the compounds demonstrated good to excellent activities against human hepatocellular carcinoma cell lines (HePG-2) and colon carcinoma cell lines (HCT-116) (Tables 12 and 13). Compounds **84a** and **88**, **90** and **91a** displayed higher antiproliferative activity (from 2.68 to 16.82 μg mL^{-1}) against two types of cancer cell lines compared to the standard drug (5-fluorouracil).[50]

2.2.5.2 Structure activity relationship. The existence of an annulated system, namely thiazolo[5,4:5,6]pyrido[2,3-*d*]pyrimidine, may be the reason why compound **87** (Fig. 9) exhibited an inhibitory action that was closer to that of the reference drug. Compound **96** had significant action against Gram-negative bacteria, but compounds **96** and **97** (Fig. 9) demonstrated outstanding antimicrobial activity against Gram-positive bacteria. Additionally, compound **97** showed a significant level of effectiveness against *Candida albicans*, a kind of yeast. Compounds **88**, **91a**, and **91b** (Fig. 9) had strong inhibitory impacts on fungus *A. fumigatus* and yeast *C. albicans*, which was attributed to the existence of a fused system called pyrimidopyridopyrimidine. It is interesting to note that compounds **88**, **90**, and **91a** (Fig. 9) had more cytotoxic activity against both types of cancer cell lines than the standard drug. This might be explained by the fact that the same molecular frame contains pyrazole and pyrimidine annulated with a pyrido[2,3-*d*]pyrimidine backbone. Additionally, compounds **80**, **81**, **87**, and **91a** (Fig. 9) showed greater cytotoxic action against colon cancer (HCT-116) than the reference drug. Due to the presence of quinoline, pyrazolopyridine, thiazolopyridine, and pyrimidopyridine coupled with a 1,3-dimethyl-pyrimidine moiety, these compounds showed a moderately inhibiting impact on HepG-2 cells. More activity is displayed by free hydrogen in pyrazole and pyrimidine rings than by methyl or phenyl groups. Derivatives **96** and **97** (Fig. 9) had moderate efficacy against two of the cancer cell lines. The presence of indenopyridine, pyrazolopyridine, chromenopyridine, benzonaphthyridine, and pyrimidodipyridine moieties fused with the 1,3-dimethylpyrimidine moiety may be the cause of this.

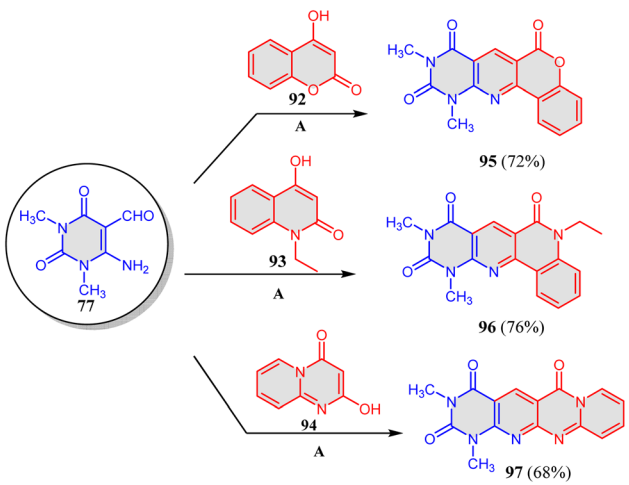

Scheme 25 Reaction of 6-amino-5-formyluracil **79** with heterocyclic compounds. Reagents and conditions: **A**; DMF/DBU, reflux, 30 min.

Table 12 *In vitro* antimicrobial evaluations of synthesized products (Schemes 23–25) at 500 and 1000 μg mL^{-1}[a]

	Mean of zone diameter (mm)											
	Gram-positive bacteria				Gram-negative bacteria				Yeasts and fungi			
	S. aureus		*B. subtilis*		*S. typhimurium*		*E. coli*		*C. albicans*		*A. fumigatus*	
Compd	1000 μg mL^{-1}	500 μg mL^{-1}	1000 μg mL^{-1}	500 μg mL^{-1}	1000 μg mL	500 μg mL^{-1}	1000 μg mL^{-1}	500 μg mL^{-1}	1000 μg mL^{-1}	500 μg mL^{-1}	1000 μg mL^{-1}	500 μg mL^{-1}
80	15 I	12 I	17 I	13 I	13 I	10 I	11 L	8 L	16 I	13 I	14 I	10 I
81	18 I	14 I	15 I	12 I	16 I	12 I	10 L	7 L	13 I	10 I	17 I	12 I
82	16 I	10 I	19 I	15 I	15 I	12 I	12 L	8 L	15 I	11 I	16 I	12 I
84a	20 I	15 I	17 I	13 I	18 I	13 I	16 I	13 I	17 I	13 I	17 I	11 I
84b	17 I	12 I	14 I	10 I	12 I	9 I	14 I	10 I	14 I	10 I	13 I	9 I
84c	14 I	11 I	19 I	15 I	17 I	13 I	10 L	6 L	16 I	11 I	18 I	13 I
84d	13 I	10 I	14 I	10 I	15 I	11 I	13 I	10 I	18 I	14 I	14 I	10 I
87	33 H	23 H	32 H	21 H	34 H	25 H	33 H	24 H	30 H	22 H	33 H	24 H
88	18 I	13 I	18 I	13 I	19 I	14 I	11 L	8 L	26 H	19 H	26 H	18 H
90	16 I	11 I	17 I	15 I	16 I	12 I	14 I	10 I	19 I	14 I	18 I	14 I
91a	19 I	15 I	14 I	10 I	13 I	10 I	16 I	12 I	24 H	19 H	27 H	20 H
91b	15 I	10 I	16 I	11 I	15 I	11 I	15 I	10 I	28 H	21 H	25 H	19 H
95	22 I	16 I	19 I	15 I	17 I	14 I	13 I	9 I	19 I	15 I	15 I	12 I
96	30 H	21 H	27 H	21 H	27 H	20 H	26 H	18 H	20 I	16 I	17 I	13 I
97	31 H	22 H	26 H	19 H	19 I	14 I	18 I	13 I	26 H	20 H	21 I	15 I
S	35	26	35	25	36	28	38	27	35	28	37	26

[a] S: Standard drugs such as chloramphencol in the case of Gram-positive bacteria, cephalothinin in the case of Gram-negative bacteria and cycloheximide in the case of yeast and fungi.

Table 13 IC_{50} values of the synthesized compounds in Schemes 23–25 against human tumor cells after 24 h of incubation

Compd	(HepG-2 cells) IC_{50}(μg mL^{-1})	HCT-116 cells IC_{50}(μg mL^{-1})
80	26.55 ± 1.76	21.10 ± 1.36
81	23.07 ± 1.45	14.62 ± 1.01
82	12.54 ± 0.95	35.45 ± 2.34
84a	2.68 ± 0.24	13.58 ± 0.96
84b	9.16 ± 0.76	15.78 ± 1.12
84c	14.62 ± 1.00	19.03 ± 1.32
84d	25.52 ± 1.56	35.25 ± 2.31
87	11.37 ± 0.88	15.78 ± 1.11
88	5.92 ± 0.59	10.33 ± 0.82
90	5.81 ± 0.57	16.82 ± 1.21
91a	4.88 ± 0.41	11.37 ± 0.87
91b	11.39 ± 0.90	14.61 ± 1.02
95	26.55 ± 1.66	47.18 ± 2.94
96	15.78 ± 1.09	28.76 ± 1.87
97	12.54 ± 0.93	44.98 ± 2.86
5-FU	6.44 ± 0.61	21.5 ± 1.35

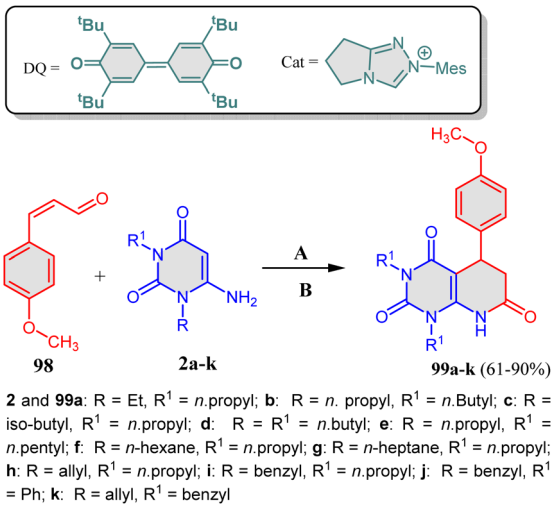

Scheme 26 Synthesis of dihydropyrido[2,3-*d*]pyrimidines **99a–k**. Reagents and conditions: **A**; DQ, cat. K_3PO_4, **B**; toluene, rt, 20 h.

Furthermore, a series of dihydropyrido[2,3-*d*]pyrimidines **99a–k** were obtained in good yields (61–90%) *via* aza-Claisen rearrangement between 3-(4-methoxyphenyl)acrylaldehyde (**98**) and 6-amino-uracils **2**. The reaction was catalyzed by K_3PO_4, and DQ was used as an oxidant reagent (Scheme 26).[119]

Scheme 27 illustrates the suggested mechanism. The organo-catalyst was initially provided by the deprotonation of the triazolium salt. When catalyst **I** and compound **98** were added nucleophilically, intermediate **100** was obtained. This intermediate was then oxidized to form α,β-unsaturated acyl azolium **101**. The 1,2-addition of cyclic enamine to acyl azolium **101** subsequently resulted in the formation of an *N*-acylation product. Through transition state intermediate **103**, hemiaminal **102** then underwent aza-Claisen rearrangement. After this rearrangement, the catalyst was regenerated *via* intramolecular lactamization to afford adduct **105** and yield the end product **99**. The nucleophilic addition of uracil enamine as a Michael acceptor in a 1,4-fashion to the α,β-unsaturated acyl azolium intermediate may also account for this catalyzed annulation. Subsequently, enol intermediate **106** underwent intramolecular acylation and proton transfer to yield targeted compounds **99a–k** (Scheme 27).[119]

Additionally, Dongre *et al.*[120] used another environmentally friendly protocol to synthesize another series of pyrido[2,3-*d*] pyrimidine-6-carbonitrile derivatives **108a–h** in excellent yields (85–95%) using EtOH/H_2O and Et_3N (Scheme 28).[120]

The antibacterial activity of compounds **108a–h** was evaluated *in vitro* against Gram-positive bacteria, such as *Staphylococcus* and *Bacillus cereus*, as well as against Gram-negative bacteria, such as *P. merabitis* and *S. maresens*. Maximum antibacterial efficacy against *Staphylococcus*, *B. cereus*, *P. merabitis*, and *S. maresens* was demonstrated by pyrido[2,3-*d*]pyrimidines **108a–d** (Table 14). Electron-donating functionalities, such as benzaldehyde, –OH, –Me, and –OMe, attached to the phenyl ring of the fused pyridine skeleton of the annulated pyrido[2,3-*d*]pyrimidines were responsible for the extensive effects on the membrane potential associated with the bactericidal activity

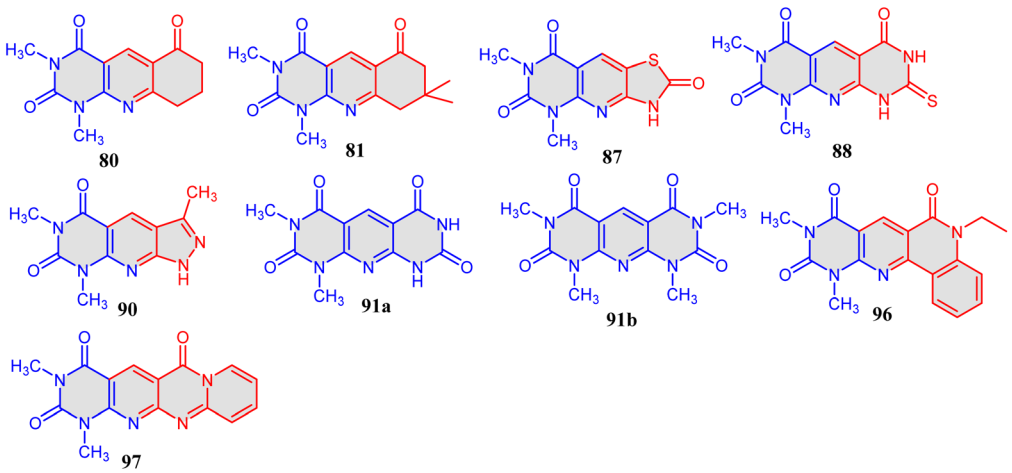

Fig. 9 Structures of antimicrobial and anticancer compounds **90**, **91a**, **91b**, **96** and **97**.

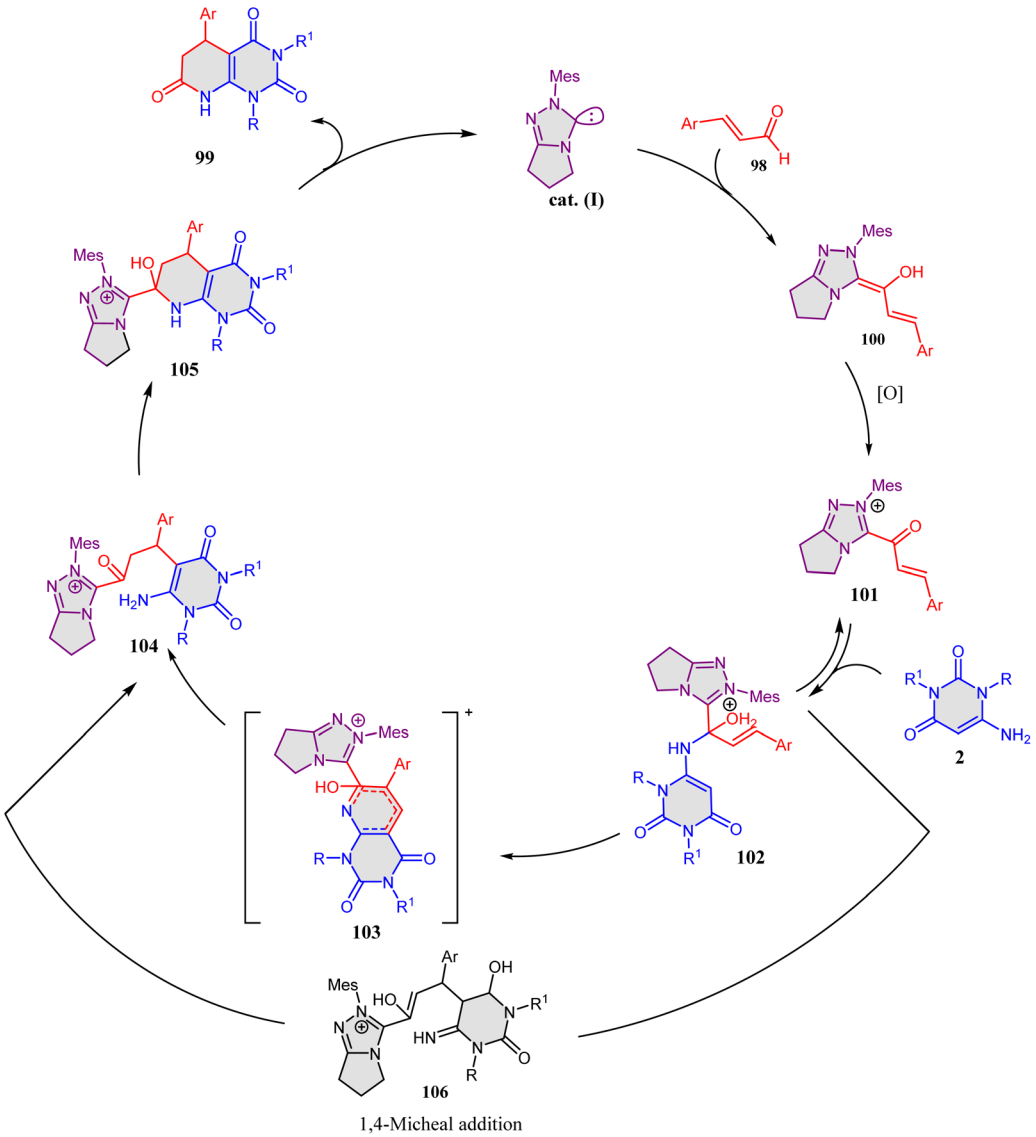

Scheme 27 Suggested mechanism for the formation of compounds **99a–k**.

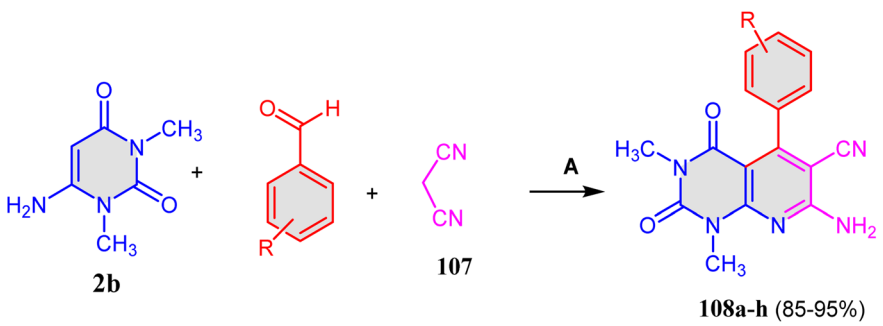

108a-h: **a**: R = 4-Me; **b**: R = H; **c**: R = 4-OMe; **d**: R = 4-OH; **e**: R = 4-Cl; **f**: R = 4-NO_2; **g**: R = 3-NO_2; **h**: R = 2-NO_2

Scheme 28 Synthesis of biologically active pyridopyrimidines **108a–h**. Reagents and conditions: A = $EtOH/H_2O$, Et_3N.

Table 14 Antibacterial activity values of pyrido[2,3-*d*]pyrimidines [minimum inhibitory concentration (MIC) in mg mL^{-1}]

			Gram-positive bacteria		Gram-negative bacteria	
Compd	Ar	log *P*	*B. cereus*	*Staphylococcus*	*P. merabitis*	*S. maresens*
108a	4-Me	1.54	12	11	14	13
108b	H	1.10	11	12	12	14
108c	4-OMe	1.15	12	11	13	17
108d	4-OH	0.62	18	15	16	17
108e	4-Cl	1.77	13	10	10	1
108f	4-NO_2	1.05	11	9	8	10
108g	3-NO_2	1.03	9	7	11	9
108h	2-NO_2	1.01	7	6	10	7
SD1:standard drug (streptomycin)		—	21	23	22	22

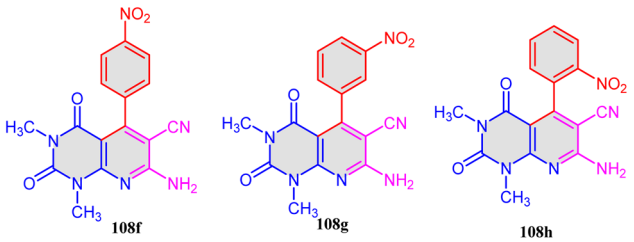

Fig. 10 Structures of antibacterial molecules **108f–h**.

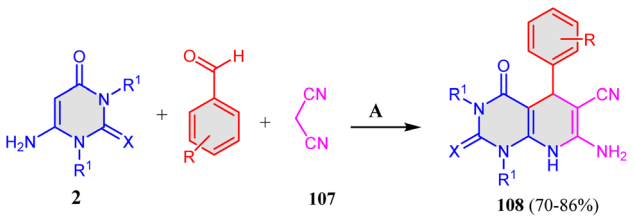

R = 4-Cl, R^1= Me, X = O; R = 4-NO_2, R^1= Me, X = O; R = 3-NO_2, R^1= Me, X = O; R = 2-NO_2, R^1= Me, X = O; R = 4-Cl, R^1= H, X = O; R = 4-OCH_3, R^1= H, X = O; R = 3-NO_2, R^1= H, X = O; R = 4-NO_2, R^1= H, X = O; R = 4-Cl, R^1= H, X = S; R = 4-NO_2, R^1= H, X = S

Scheme 29 Three-component reaction for the synthesis of **108**. Reagents and conditions: A; urea, EtOH:H_2O, 60 °C.

attributed to pharmacologically active compounds. However, compound **108f** (R = 4-NO_2) exhibited moderate activity, while compounds **108g** (R = 3-NO_2) and **108h** (R = 2-NO_2) decreased the inhibition activity due to their electron withdrawing groups (Fig. 10).[120]

Meanwhile, Javahershenas and Khalafy[121] developed a three-component reaction between various 6-aminouracils (**2**), malononitrile (**107**), and aromatic aldehydes, which afforded the final products of pyrido[2,3-*d*]pyrimidine-6-carbonitrile derivatives **108** in 70–86% yields. The reaction was performed in EtOH:H_2O at 60 °C with urea as an organo-catalyst (Scheme 29).[121]

With regard to the methods for the synthesis of pyridopyrimidine frameworks, Anbhule *et al.*,[122] utilized green solvents, specifically a glycerol–water system, in the synthesis of pyrido[2,3-*d*]pyrimidine derivatives **108** in high yields (83–96%) through a multicomponent reaction between 6-aminouracil **2**, various aldehydes, and malononitrile (**107**) (Scheme 30).[122]

In 2020, Hashemian *et al.*,[123] also prepared a diversity of pyrido[2,3-*d*]pyrimidines skeletons using Mn-ZIF-8@$ZnTiO_3$ nanoparticles as a catalyst (Scheme 31). The three-component reaction between aromatic aldehydes, various substituted 6-aminouracil **2a,b**, and malononitrile (**107**) was performed in a H_2O/EtOH system at 70 °C, and the final products **108** were formed in good to excellent yields (87–95%).[123]

Table 15 shows the utility of various solvents in the synthesis of **108** (R = 4-Me, R^1 = Me) as a model example. The mixture solvent of H_2O and EtOH in a ratio of 1 : 1 was found to give the highest yield and lowest reaction time.[123]

When 6-aminouracil (**2a**) reacted with aromatic aldehydes and **107** in water at 80 °C and catalyzed by Fe_3O_4-ZnO-NH_2-$PW_{12}O_{40}$ nanocatalyst, the reaction proceeded to give 7-amino-pyrido[2,3-*d*]pyrimidine-6-carbonitriles **108** in 75–95% yields (Scheme 32).[124]

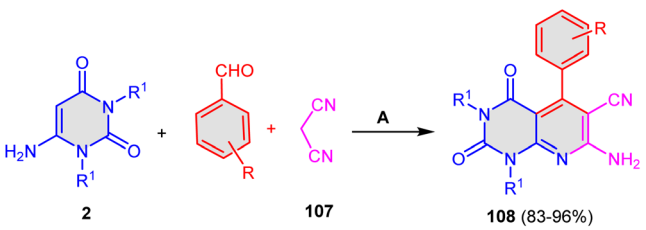

R = 4-Cl, R^1= Me; R = 4-NO_2, R^1= Me; R = 3-NO_2, R^1= Me; R = 2-NO_2, R^1= Me; R = 4-NO_2, R^1 = H; R = 4-CF_3, R^1 = Me; R = 3,4-Cl_2, R^1= H; R = 4-OH, R^1 = H

Scheme 30 Green synthesis of pyridopyrimidine **108**. Reagents and conditions: A; glycerol: H_2O, 95 °C.

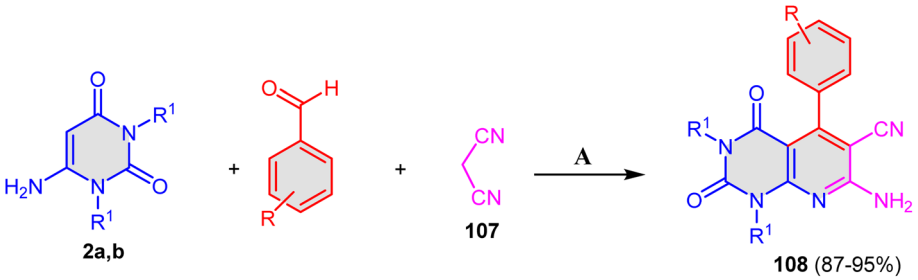

R = 4-Me, R^1 = Me; R = 4-OMe, R^1 = Me;R= 4-OH, R^1 = H; R = R^1 = H; R = 2,4-Cl, R^1 = H; R = 2-OH,3-OMe, R^1 = H; R = 2-Cl, R^1 = Me

Scheme 31 Mn nano catalyst-mediated synthesis of pyrido[2,3-*d*]pyrimidines **108**. Reagents and conditions: A; Mn-Zif-8@$ZnTiO_3$ NPs, B; EtOH:H_2O.

Table 15 Effects of different solvents on the reaction yield for the synthesis of **108**

			108 (R = 4-Me, R^1 = Me)	
Entry	Solvent	Condition	Time (min)	Yield[a] (%)
	Solvent-free	120	100	50
1	CH_3CN	Reflux	80	44
2	$CHCl_3$	Reflux	70	46
3	Acetone	Reflux	80	55
4	MeOH	Reflux	50	70
5	EtOH	Reflux	40	85
7	H_2O	Reflux	30	90
8	EtOH/H_2O(1 : 1)	Reflux	15	97

[a] Isolated yield reaction conditions: benzaldehyde (1 mmol), malononitrile (1 mmol) and pyrimidines, Mn-ZIF-8@$ZnTiO_3$, temp. 70 °C.

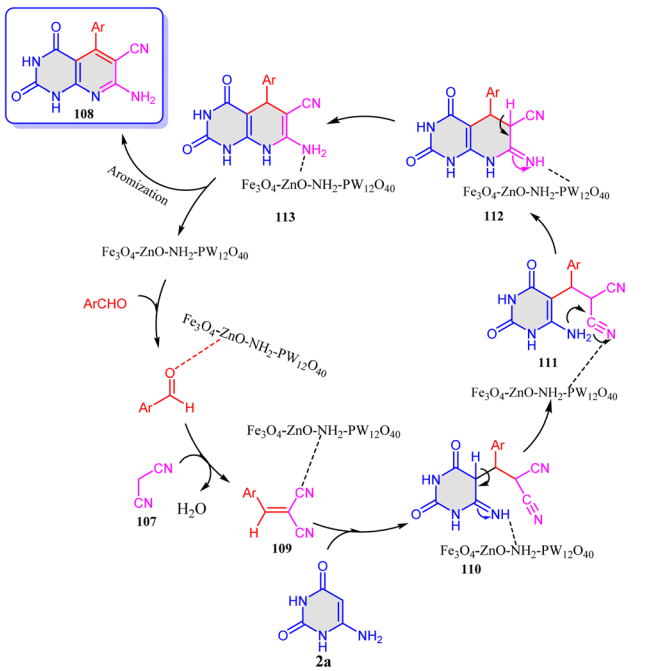

Scheme 33 Plausible mechanism for the synthesis of compound **108**.

The plausible reaction mechanism is shown in Scheme 33. First, intermediate **109** was formed *via* Knoevenagel condensation between arylaldehyde and malononitrile (**107**). Second, 6-aminouracil (**2a**) was added to intermediate **109** *via* Michael's addition to generate intermediate **110**. After that, intermediate **110** was converted into tautomer **111**, which underwent intermolecular cyclization to produce **112**. Following this, the tautomerization process was achieved *via* the interconversion of intermediate **112** into **113**. Eventually, aromatization of **113** afforded the final products **108** (Scheme 33).[124]

Moreover, Rad and Mokhtary[125] used MgO nanoparticles in the synthesis of pyrido[2,3-*d*]pyrimidine derivatives **108** by reacting aminouracil derivatives **2**, various aromatic aldehydes and **107**. The reaction was performed in H_2O at 80 °C, and MgO nano-particles (NP) were applied as a catalyst to obtain the final products **108** in good to excellent yields (84–92%) (Scheme 34).

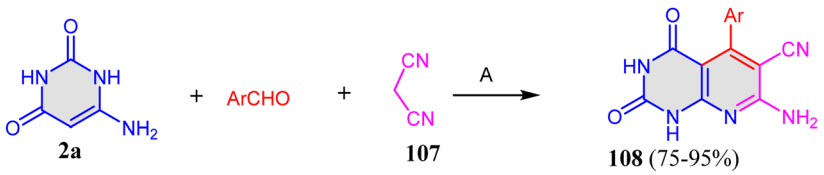

Ar = 3-NO_2-C_6H_4; Ar = 4-NO_2-C_6H_4; Ar = 4-HO-C_6H_4; Ar = Ph; Ar = 4-MeC_6H_4; Ar = 3-HO-C_6H_4: Ar = 4-CF_3-C_6H_4; Ar = 2-furyl;

Scheme 32 Nano-catalyzed synthesis of tetrahydropyrido[2,3-*d*]pyrimidine-6-carbonitriles **108**. Reagents and conditions: A; Fe_3O_4-ZnO-NH_2-$PW_{12}O_{40}$. B; H_2O, 80 °C.

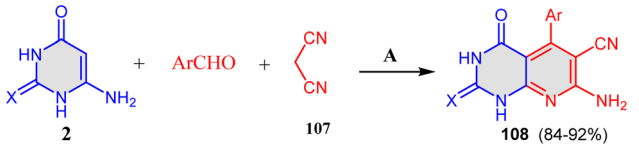

X = S, O

Ar = 3-$NO_2C_6H_4$; Ar = 4-ClC_6H_4; Ar = 2-MeO-C_6H_3; Ar = 2,4-$Cl_2C_6H_3$; Ar =4-$NO_2C_6H_4$; Ar = 3-$MeOC_6H_4$; Ar = 4-BrC_6H_4; Ar = 2,6-$Cl_2C_6H_3$; Ar = 4-OHC_6H_4

Scheme 34 MgO catalytic synthesis of pyrido[2,3-*d*]pyrimidine-6-carbonitriles **108**. Reagents and conditions: A = MgO NPs. B = H_2O, 80 °C.

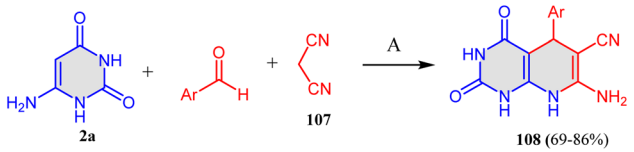

Ar = C_6H_5, 3-NO_2-C_6H_4, 4-OMe-C_6H_4, 4-Cl-C_6H_4, 4-Me-C_6H_4, 4-F-C_6H_4, 2,6-Cl_2-C_6H_3, 2,3$(OMe)_2$-C_6H_3, 2,4-Cl_2-C_6H_3

Scheme 36 Synthetic pathway for compound **108**. Reagents and conditions: A; SBA-Pr-SO_3H, solvent-free, 60 °C.

The mechanism for the formation of the final products is shown in Scheme 35. The reaction between the **107** and the aryl aldehydes was promoted by MgO nano particles and afforded intermediate **115**, which reacted with **2** *via* Michael addition to form intermediate **116**. Following that, **116** underwent a rearrangement to give intermediate **117**. Next, intermolecular cyclization occurred in **117** to produce **118**. Finally, proton transfer and aromatization occurred to intermediate **118** to obtain the final products **108**.[125]

Similarly, Ziarani *et al.*[126] reported an interesting approach for the formation of pyrido[2,3-*d*]pyrimidine derivatives **108** by utilizing SBA-15-Pr-SO_3H nano-catalyst (NP) under solvent free conditions in the reaction between 6-aminouracil (**2a**), **107**, and aromatic aldehydes to obtain 7-amino-5-aryl-2,4-dioxo-1,2,3,4-tetrahydropyrido[2,3-*d*]pyrimidine-6-carbonitriles **108** in 69–86% yields (Scheme 36).[126]

The antimicrobial activity for synthesized products showed potent activities (Scheme 36) with Ar = C_6H_5 (28 and 23 mm), 4-ClC_6H_4 (26 and 30 mm), 4-$CH_3C_6H_4$ (28 and 20 mm), 4-FC_6H_4 (30 and 24 mm) and 2,6-$Cl_2C_6H_3$ (28 and 18 mm) along with inactivity for the compounds with 3-$NO_2C_6H_4$, 4-$OCH_3C_6H_4$, and 2,3-$(OCH_3)_2C_6H_3$ against *B. subtilis* and *S. aureus* species compared to chloramphenicol and gentamicin standards antibiotics. Thus, the introduction of nitro and methoxy substituents in the phenyl ring is not favored for potent antimicrobial consequences. Additionally, compounds 4-ClC_6H_4 (8 and 12 mm) and 4-$CH_3C_6H_4$ (9 and 10 mm) showed good activities against *E. coli* and *C. albicans* species, respectively. The only recorded activity against the growth inhibition of *P. aeruginosa* was observed for the compound featuring a 4-ClC_6H_4 substituted group (10 mm). The compound with an unsubstituted phenyl ring presented the most potent antifungal activity against the *C. albicans* species (14 mm). The MIC values of the different assessments presented potent values for compounds with Ar = C_6H_5, 4-$CH_3C_6H_4$, and 4-FC_6H_4 against *B. subtilis* species, along with 4-ClC_6H_4 against *S. aureus* species, with MIC values of 2 mg mL^{-1} (Table 16).[126]

Furthermore, in 2018, Moradi *et al.*[127] developed another synthesis of pyrido[2,3-*d*]pyrimidines core **120a–p** utilizing Fe_3O_4@SiO_2@$(CH_2)_3$S-SO_3H nano-magnetic catalyst by reacting 2,6-diamino-pyrimidin-4-ol (**119**), **107**, and various aldehydes under neat conditions at 100 °C to afford 2,7-diamino-5-oxo-4-phenyl-1,8-naphthyridine-3-carbonitriles **120a–p** in 84–94% yield (Scheme 37).[127] Meanwhile, using the same catalyst, a three component reaction of **119** with alkyl 2-cyanoacetates **121** and aldehydes afforded 7-amino-2,5-dioxo-4-phenyl-1,2,3,4,5,6-hexahydro-1,8-naphthyridine-3-carbonitriles **122a–c** in 81–87% yields (Scheme 37).[127]

Additionally, Saberikhah *et al.*[128] developed a simple reaction for synthesizing pyrido[2,3-*d*]pyrimidines **108** through the reaction between aromatic aldehydes **107** and amino-thiouracil **2** to produce the targeted products **108** (Scheme 38). The reaction was achieved under green conditions utilizing Fe_3O_4@TiO_2@NH_2@$PMo_{12}O_{40}$ as a catalyst (Scheme 38). However, the reactions of 6-amino-2-(alkylthio)uracil (**123**) with aryl aldehydes and **107** under the same conditions afforded 7-amino-2-(alkylthio)-4-oxo-3,4-dihydropyrido[2,3-*d*]pyrimidine-6-carbonitrile derivatives **124a–j** (Scheme 38).[128]

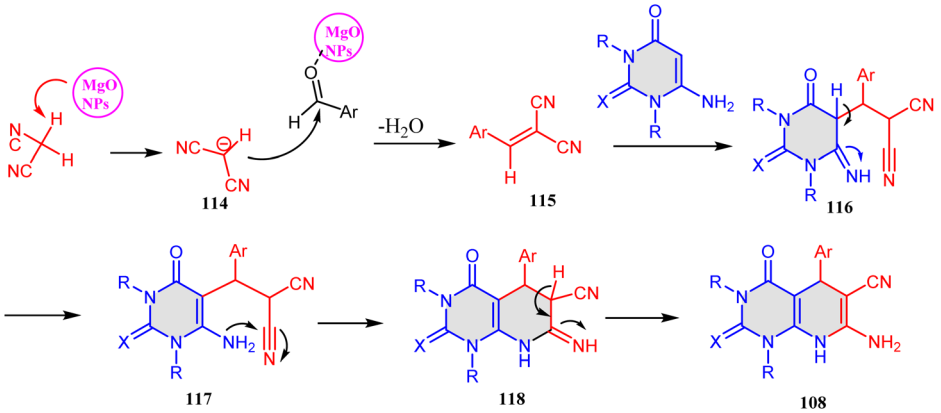

Scheme 35 Plausible mechanism for the formation of pyrido[2,3-*d*]pyrimidine-6-carbonitriles **108**.

Table 16 Minimum inhibitory concentrations (lg mL^{-1}) of synthesized pyrido[2,3-*d*]pyrimidines against fungi and Gram-positive and Gram-negative bacteria

Ar	*B. subtilis*	*S. aureus*	*E. coli*	*P. aeruginosa*	*C. 2albicans*
Ph	2	8	—	—	128
3-$NO_2C_6H_4$	—	—	—	—	—
4-$OCH_3C_6H_4$	—	—	—	—	—
4-ClC_6H_4	8	2	512	512	256
4-$CH_3C_6H_4$	2	32	512	—	512
4-FC_6H_4	2	8	—	—	—
2,6-$Cl_2C_6H_3$	4	64	—	—	—
2,3-$(OCH_3)_2C_6H_3$	—	—	—	—	—
Chloramphenicol	4	8	4	256	—
Gentamicin	0.125	0.5	0.5	1	—
Nystatin	—	—	—	—	8

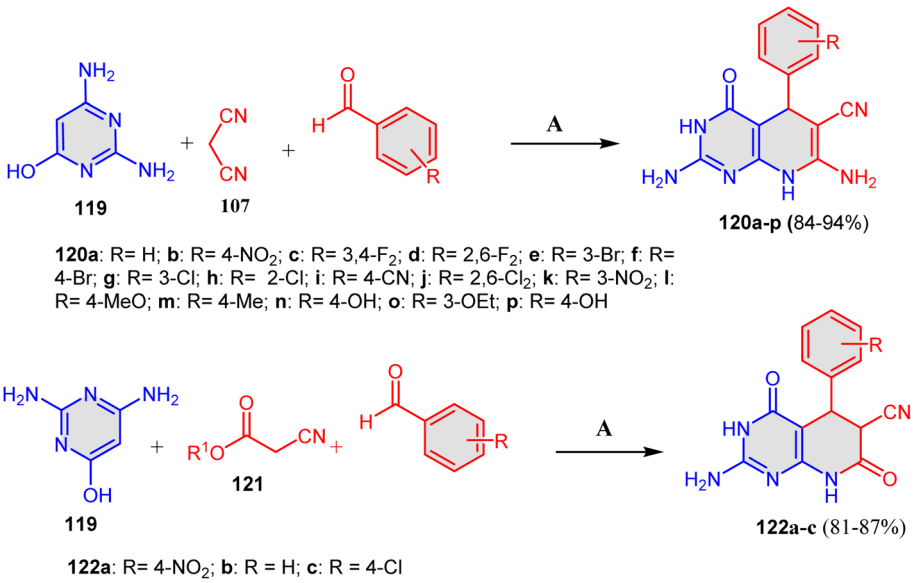

Scheme 37 Reaction of 2,6-diaminopyrimidin-4-ol (**119**) with active methylene compounds. Reagents and conditions: **A**; Fe_3O_4@SiO_2@(-$CH_2)_3$S-SO_3H, neat, 100 °C.

Another series of pyrido[2,3-*d*]pyrimidines **108** was synthesized by Esmaili *et al.*[129] through a multicomponent reaction between 6-amino-1,3-dimethyluracil (**2b**), aryl aldehydes and **107** in refluxing EtOH and catalyzed by nano-[Fe_3O_4@SiO_2/*N*-propyl-1-(thiophen-2-yl) ethanimine][$ZnCl_2$] as a catalyst (Scheme 39).[129]

In summary, Scheme 40 depicts the conditions listed in Schemes 28–32, 34, 36, and 39 detailed for the synthesis of the derivatives of compound **108** from the reaction of 6-aminouracil derivatives **2**, aromatic aldehydes, and **107**. The same kind of conversion under various reaction circumstances is depicted in Scheme 40. It is worth mentioning that the most intriguing circumstance resulted from the use of nano-catalysts. The nanocatalysts that achieved the best yields were Fe_3O_4@-TiO_2@NH_2@$PMo_{12}O_{40}$ nanocatalyst (92–98%), MgO NPs (90–97%), and Mn-ZIF-8@$ZnTiO_3$ (87–95%).

In addition, the role of the catalyst is described in the formation of **108** from the reaction of 6-aminouracil derivatives **2** with aryl aldehydes and **107**, as it enhances the abstraction of a hydrogen proton from **107** to form its anion (**A**, Scheme 41). The second role of the catalyst is to enhance the electrophilicity of the carbon of the carbonyl group of the aldehydes. The latter enables the previously formed anion **A** to attack the carbonyl group to form the corresponding ylidene. Furthermore, nucleophilic attack of the nucleophilic carbon CH-5 of **2** to the ylidene forms intermediate **B**. The neutralization of **B** then gives intermediate **C**. The third role of the catalyst is to enhance the 1,3-H shift so as to facilitate the subsequent sequence and cyclization process, which would then occur (Scheme 41).

Additionally, the reaction of (phenylsulfonyl)acetonitrile (**125**), aromatic aldehydes and 6-aminouracil (**2**) in glycerol as a green solvent at 80 °C yielded the desired products of 7-amino-5-aryl-6-(phenylsulfonyl)-6,8*a*-dihydropyrido[2,3-*d*]pyrimidine-2,4-diones **126a–n** in excellent yields (88–95%), as depicted in Scheme 42.[130]

Table 17 shows that glycerol acts well and produces 7-amino-5-phenyl-6-(phenylsulfonyl)-6,8a-dihydropyrido[2,3-*d*]pyrimidine-2,4(1*H*,3*H*)-dione (**126a**) at 80 °C for 2 h with 90% yield (entry 10).[129]

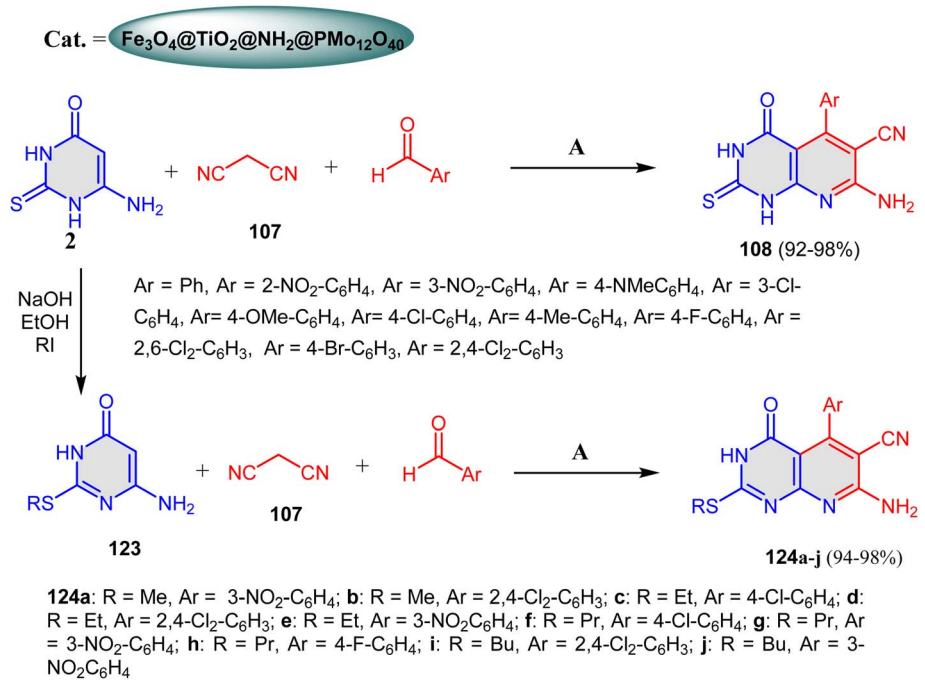

Scheme 38 Synthesis of compounds **108** and **124a–j**. Reagents and conditions: A; Fe_3O_4@TiO_2@NH_2@$PMo_{12}O_{40}$, H_2O, 80 °C.

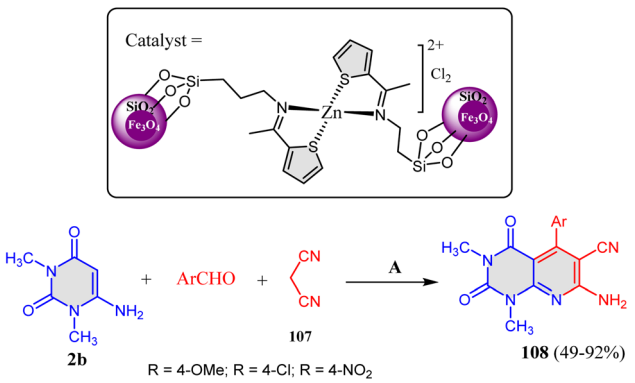

Scheme 39 Synthetic pathway for compound **108**. Reagents and conditions: A; EtOH, reflux, nano-[Fe_3O_4@SiO_2/*N*-propyl-1-(thiophen-2-yl)ethanimine][$ZnCl_2$].

In the same manner, Saberikhah *et al.*[131] reported the synthesis of 1-methyl-1*H*-pyrrolyl-hexahydropyrido[2,3-*d*] pyrimidine scaffolds **128a–i** through multicomponent reaction between 6-amino-thiouracil, 1-methyl-2-cyanoacetyl-1*H*-pyrrole (**127**), and aryl aldehydes in EtOH and catalyzed by γ-Fe_2O_3@-HAp@PBABMD@Cu magnetic nanoparticles to give the targeted products **128a–i** in 90–97% yields (Scheme 43).[131] Due to the multi-step process of the nano-catalyst preparation, the catalyst's remarkable productivity and recyclability gave this procedure additional significance. Incorporating the pyrrole ring into bicyclic pyridopyrimidines is advantageous for the potential activity of biological potency.[130]

The proposed mechanism of the synthesis of pyrrolyl-hexahydropyridopyrimidines **128a–i** is shown in Scheme 44. Initially, the carbonyl group of aldehydes was activated by the nano-catalyst during Knoevenagel condensation between aldehydes and compound **127** to give arylidene **129**. Subsequently, intermediate **130** was formed *via* the Michael addition reaction between **129** and **2**. Finally, intermediate **130** went through intramolecular cyclization to produce intermediate **131**, which lost a molecule of water to produce the desired products **128a–i** (Scheme 44).[131]

In 2020, Dastmard *et al.*[132] reported green efficient synthesis of pyridopyrimidine-indole hybrid molecules **133a–m** *via* multicomponent reaction between 6-amino-1,3-dimethyl-pyrimidine-2,4-dione (**2b**) with 3-cyanoacetyl-indole (**132**) and aromatic aldehydes in EtOH, catalyzed by Fe_3O_4@FAp@Ni nano catalyst (Scheme 45). The possible mechanistic pathway for the formation of **133a–m** is shown in Scheme 46. The presence of Fe_3O_4@FAp@Ni nano catalyst activated the reaction between compound **132** and aldehydes to form intermediate **134**. Next, a Michael addition between **134** and **2b** occurred and afforded **135**. Subsequently, the intermolecular cyclization and elimination of a molecule of water afforded adduct **136**. Following that, the oxidation and aromatization of **136** occurred to obtain pyridopyrimidine compounds **133a–m** (Scheme 46).[132]

A diversity of pyrrolo[3′,4′:5,6]pyrido[2,3-*d*]pyrimidine-2,4,6(3*H*)-trione compounds **139a–j** were successfully synthesized by Jiang and coworkers.[28] The reaction occurred between 6-amino-1-ethyluracil **2d** and ethyl-4-chloro-2-(4-methylbenzylidene)-3-oxobutanoate (**137**) in MeOH at 45 °C in the presence of $MgSO_4$ to produce ethyl-7-(chloromethyl)-1-ethyl-2,4-dioxo-5-(*p*-tolyl)-1,2,3,4,5,8-hexahydro-pyrido[2,3-*d*] pyrimidine-6-carboxylate (**138**), which then reacted with primary amines in EtOH at MW irradiation to produce the final

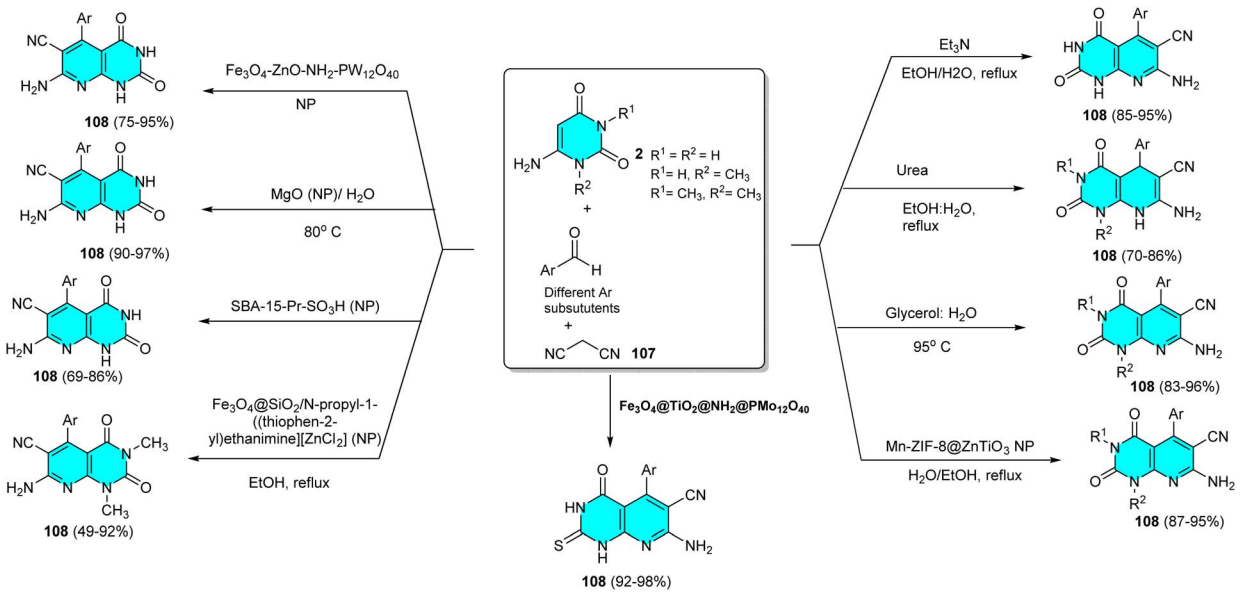

Scheme 40 Synthetic pathways for compound **108** under the conditions mentioned in Schemes 28–32, 34, 36, and 39.

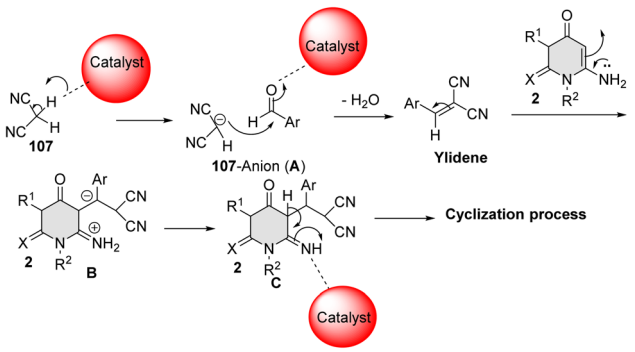

Scheme 41 General features of the role of a catalyst in the pathways describing the formation of **108**.

Table 17 Optimization conditions for the preparation of **126a** under various solvents and temperatures

Entry	Solvent	Temperature (°C)	Time (h)	Yield (%)
1	Acetonitrile	80	12	NR
2	DMF	80	12	NR
3	Toluene	80	12	NR
4	DMSO	80	12	NR
5	EtOH	80	12	NR
6	H_2O	80	12	NR
7	Neat	80	12	NR
8	Glycerol	RT	7	72
9	Glycerol	60	3	85
10	Glycerol	80	2	90
11	Glycerol	100	2	90

products **139a–k** in 10–45% yields, as depicted in Scheme 47.[28] Structural changes in the dihydropyridine lactam side chain of compound **139** were investigated to study its impact on both BET affinity (the BET affinity constant describes the material's adsorption characteristics) and selectivity. All derivatives demonstrated a slight preference for BRD4-1 over BRDT-1 (Table 18), including **139k** and **139f**. According to the results, compound **139f** was highly selective for the bromodomain and extra terminal (BET) bromodomains.[28]

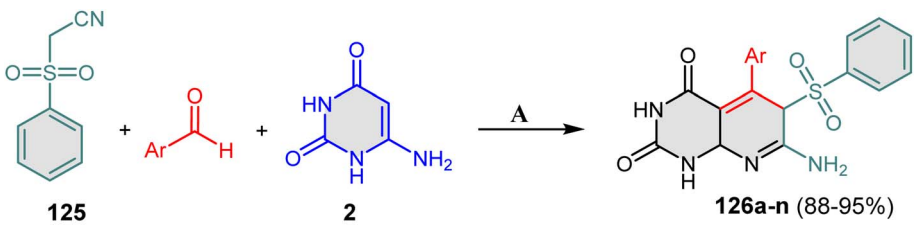

126a: Ar = Ph; **b**: Ar = 4-Br-C_6H_4; **c**: Ar = 3,4-Cl_2-C_6H_3; **d**: Ar = 4-Me-C_6H_4; **e**: Ar = 2,6-Cl_2-C_6H_3; **f**: Ar = 4-MeO-C_6H_4; **g**: Ar = 2-thiophene; **h**: Ar = 2-Br-C_6H_4; **i** = MeS-C_6H_4; **j** = Ar = 2-Cl-C_6H_4; **k**: Ar = 4-Cl-C_6H_4; **l**: Ar = 2-NO_2-C_6H_4; **m**: Ar = 4-NO_2-C_6H_4; **n**: Ar = 3-Pyridyl

Scheme 42 Synthesis of pyrido[2,3-*d*]pyrimidines **126a–n**. Reagents and conditions: A = Glycerol, 80 °C.

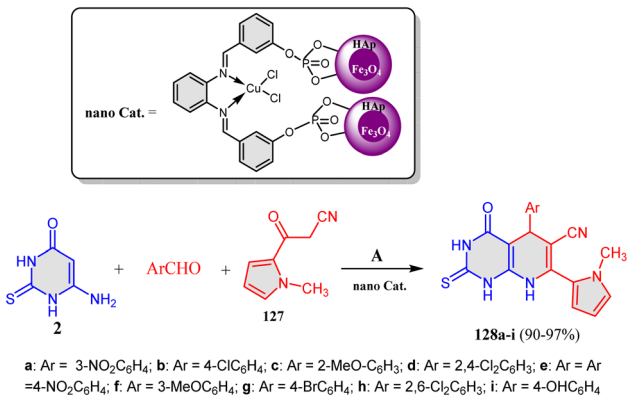

a: Ar = 3-$NO_2C_6H_4$; **b**: Ar = 4-ClC_6H_4; **c**: Ar = 2-MeO-C_6H_3; **d**: Ar = 2,4-$Cl_2C_6H_3$; **e**: Ar = Ar =4-$NO_2C_6H_4$; **f**: Ar = 3-$MeOC_6H_4$; **g**: Ar = 4-BrC_6H_4; **h**: Ar = 2,6-$Cl_2C_6H_3$; **i**: Ar = 4-OHC_6H_4

Scheme 43 Synthesis of pyrido[2,3-*d*]pyrimidines **128a–n**. Reagents and conditions: A; EtOH, 80 °C, 8–13 min.

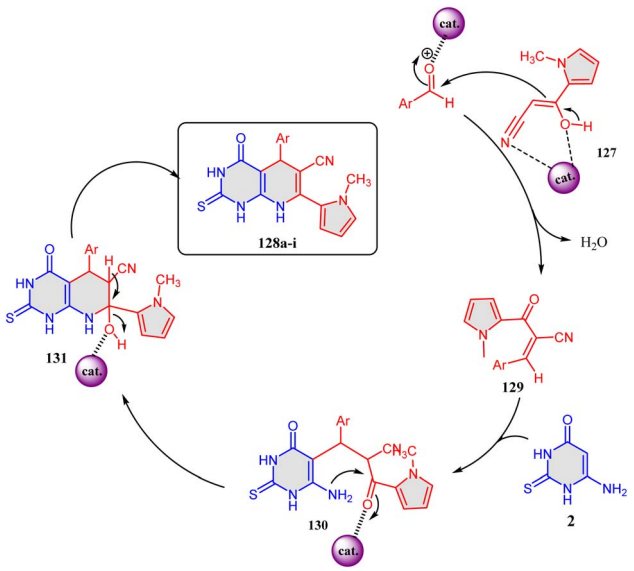

Scheme 44 Suggested mechanism for the synthesis of compound **128**.

2.2.5.3 Structure activity relationship. Table 18 shows that an electron-rich aromatic ring may interact with special R54 in BRDT-1 through a cation-pi process. Overall, aromatic substitution had no discernible impact on affinity. Fig. 11 shows that the structures of compounds **139b** (R = Me), **139d** (R = 4-OH), and **139e** (R = 4-OMe), containing electron-donating groups, were slightly more potent than that of compound **139c** (R = 4-Cl) with an electron withdrawing group. Compounds **139e**, **139f**, and **139g** containing OMe groups were investigated, and compound **139e** (R = 4-OMe) had the highest inhibition activity, followed by 2-OMe and 3-OMe substitutions. BET activity was not improved by disubstitution with OMe or chlorine moieties, as shown in (**139h**, **139i**, and **139j**). However, **139h** (R = 3,4-$(OMe)_2$) revealed the least inhibition activity against BRDT-1. None of the aryl changes significantly affected BRDT-1 specificity. Furthermore, this subset of analogs showed similar activities for BRD4-1 and BRD4-2.[28]

Patil *et al.*[133] also synthesized another series of substituted pyrido[2,3-*d*:6,5-*d*]dipyrimidines **140a–k** in good yields (80–88%) through the reaction between thiobarbituric acid or barbituric acid **86a,b**, aromatic aldehydes, and 1,3-dimethyl-6-aminouracil (**2b**) (Scheme 48). The reaction was catalyzed by phosphorous pentoxide (P_2O_5) and carried out in EtOH as a solvent.

All synthetic products were examined for their antituberculosis activity. The majority of the products demonstrated moderate to good activity against the *M. tuberculosis* H37RV strain according to the results (Table 19). Using standard drugs, such as pyrazinamide, ciprofloxacin, and streptomycin, for comparison purposes, the synthesized compounds were screened for their antimycobacterial activity at concentrations of 0.8, 1.6, 3.12, 6.25, 12.5, 25, 50, and 100 μg mL^{-1}. The results showed that all the compounds demonstrated activity at 50 μg mL^{-1} (Table 19).[126]

Moreover, El-Kalyoubi *et al.*[100] fortunately reacted 6-aminouracils **2** with 5-(substituted-1-yl-sulfonyl)indoline-2,3-diones **141a–c** in AcOH under reflux conditions to give the final products of spiro-oxindole-pyrido[2,3-*d*:6,5-*d*′]dipyrimidines **142–144** in good yields, as illustrated in Scheme 49.[100] The antiviral activity of the synthesized compounds against SARS-CoV-2 was examined. All products were evaluated for the percentage of inhibition using the plaque reduction assay, which demonstrated that compounds **142a**, **143b**, **143d**, and **143e** had a high activity. The four compounds exhibited potent inhibitory activity ranging from 40.23 ± 0.09 to 44.90 ± 0.08 nM and from 40.27 ± 0.17 to 44.83 ± 0.16 nM, respectively, when compared with chloroquine as a reference standard, which showed 45 ± 0.02 and 45 ± 0.06 nM

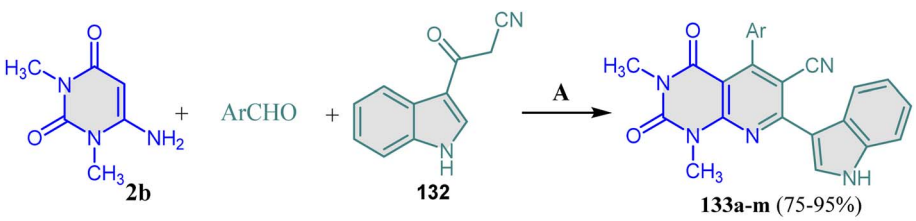

133a: Ar = 4-$NO_2C_6H_4$; **b**: Ar = 4-MeC_6H_3; **c**: Ar = 4-MeO-C_6H_3; **d**: Ar = 4-ClC_6H_4; **e**: Ar = Ar = 2-ClC_6H_4; **f**: Ar = 2,4-$Cl_2C_6H_3$; **g**: Ar = 3-BrC_6H_3; **h**: Ar = 1-naphthyl; **i**: Ar = 3-OHC_6H_4; **j**: Ar = 4-nicotinyl; **k**: Ar = 3-NO_2-C_6H_4; **l**: Ar = 4-CNC_6H_4; **m**: Ar = 4-$NMeC_6H_4$

Scheme 45 Synthesis of pyridopyrimidine-indole hybrids **133a–m**. Reagents and conditions: A; EtOH, Fe_3O_4@FAp@Ni.

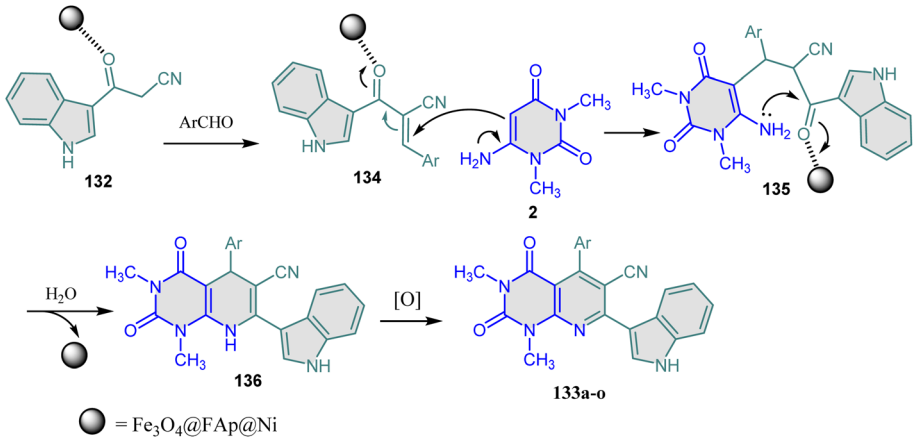

Scheme 46 Possible mechanistic pathway for the formation of **133a–m**.

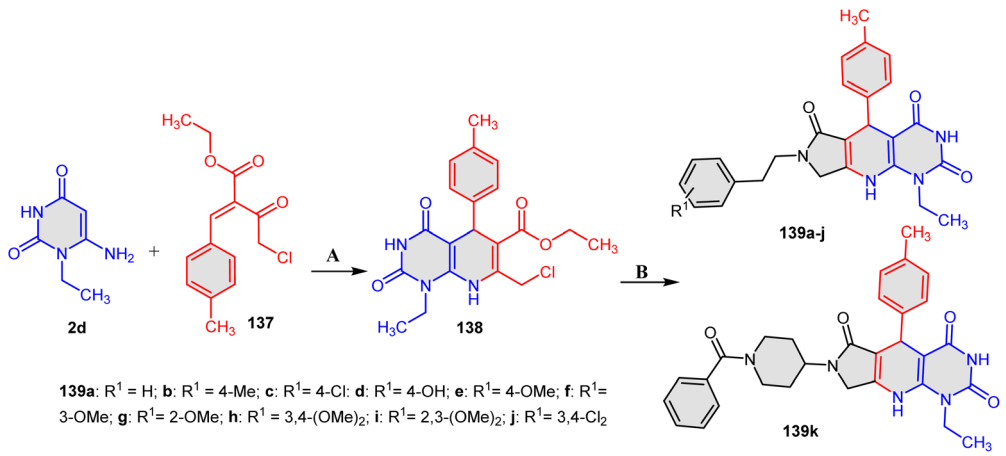

Scheme 47 Formation of pyrrolo[3′,4′:5,6]pyrido[2,3-*d*]pyrimidine-2,4,6(3*H*)-triones **139a–k**. Reagents and conditions: A; $MgSO_4$, MeOH, 45 °C. B; RNH_2, EtOH, Microwave, 120 °C.

Table 18 Structure and inhibitory profile of second-round modifications

Compd		R^1	IC_{50} [μM] BRDT-1	IC_{50} [μM] BRDT-2	IC_{50} [μM] BRD4-1	IC_{50} [μM] BRD4-2
139a	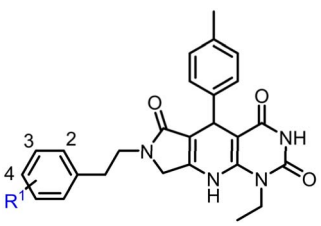	H	7.6 ± 1.7	1.2 ± 0.08	2.3 ± 0.48	1.4 ± 0.12
139b		4-Me	12 ± 1.9	2.2 ± 0.07	3.5 ± 0.93	2.1 ± 0.16
139c		4-Cl	25 ± 4.1	3.1 ± 0.24	6.3 ± 2.1	3.0 ± 0.49
139d		4-OH	2.2 ± 0.76	0.61 ± 0.06	1.3 ± 0.20	0.82 ± 0.03
139e		4-OMe	4.3 ± 0.26	104 ± 13	0.60 ± 0.15	0.98 ± 0.04
139f		3-OMe	18 ± 3.6	1.2 ± 0.08	1.9 ± 0.42	1.3 ± 0.09
139g		2-OMe	9.4 ± 1.1	1.5 ± 0.07	2.3 ± 0.40	1.6 ± 0.08
139h		3,4-$(OMe)_2$	103 ± 12	14 ± 2	23 ± 0.79	17 ± 2.84
139i		2,3-$(OMe)_2$	69 ± 8.7	13 ± 2.8	20 ± 1.2	11 ± 3.5
139j		3,4-Cl_2	35 ± 3.64	8.4 ± 1.7	13 ± 3.8	6.0 ± 1.5
(+)-JQ1[a]		—	1.0 ± 0.1	1.1 ± 0.8	0.37 ± 0.1	0.30 ± 0.01

[a] (+)-JQ1 was used as a positive control in the AlphaScreen assay. All compounds were tested in quadruplicate; ± indicates standard deviation.

against RdRp and spike glycoprotein, respectively. These four substances were used to further study their mechanisms of action on spike glycoprotein and RNA-dependent RNA polymerase (RdRp). The results were quite encouraging, demonstrating effectiveness comparable to that of chloroquine, which was previously used in the treatment of COVID-19.

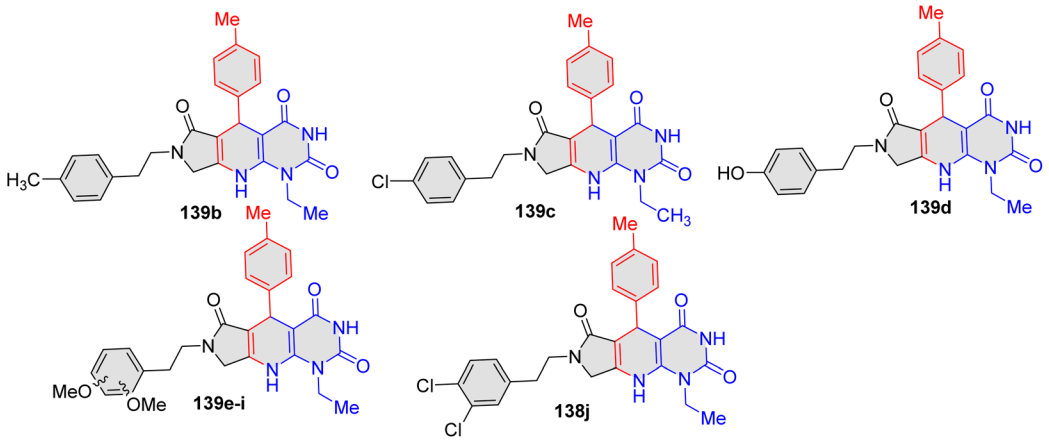

Fig. 11 Structure of compounds **139b–h** with inhibition activity against BRDT-1.

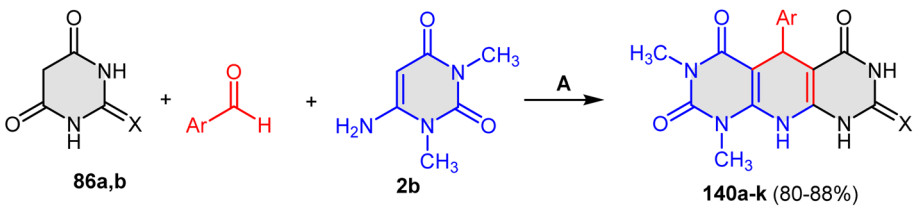

140a: Ar = 3-ClC$_6$H$_4$, X = O; **b**: Ar = 4-CNC$_6$H$_4$, X = O; **c**: Ar = 2-NO$_2$C$_6$H$_4$, X = O; **d**: Ar = 3-ClC$_6$H$_4$, X = S; **e**: Ar = 3-NO$_2$C$_6$H$_4$, X = S; **f**: Ar = 2-ClC$_6$H$_4$, X = O; **g**: Ar = 2-ClC$_6$H$_4$, X = S; **h**: Ar = 4-NO$_2$C$_6$H$_4$, X = S; **i**: Ar = 2-NO$_2$C$_6$H$_4$, X = S; **j**: Ar = 4-ClC$_6$H$_4$, X = S; **k**: Ar = 4-ClC$_6$H$_4$, X = O

Scheme 48 P_2O_5-mediated synthesis of **140a–k**. Reagents and conditions: **A** = P_2O_5/EtOH.

Table 19 Antituberculosis activity of compounds **140a–k** against *Mycobacterium tuberculosis*[a]

Compd	100 μg mL^{-1}	50 μg mL^{-1}	25 μg mL^{-1}	12.5 μg mL^{-1}	6.25 μg mL^{-1}	3.12 μg mL^{-1}	1.6 μg mL^{-1}	0.8 μg mL^{-1}
140a	S	S	R	R	R	R	R	R
140b	S	S	R	R	R	R	R	R
140c	S	S	R	R	R	R	R	R
140d	S	S	R	R	R	R	R	R
140e	S	S	R	R	R	R	R	R
140f	S	S	R	R	R	R	R	R
140g	S	S	R	R	R	R	R	R
140h	S	S	R	R	R	R	R	R
140i	S	S	R	R	R	R	R	R
140j	S	S	R	R	R	R	R	R
140k	S	S	R	R	R	R	R	R
Minimum inhibitory concentration	Pyrazinamide Streptomycin Ciprofloxacin				3.125 μg mL^{-1} 6.25 μg mL^{-1} 3.125 μg mL^{-1}			

[a] S, susceptible; R; resistant.

2.2.5.4 Structure activity relationship. SAR of compounds **142a**, **143b**, **143d** and **143e** (Fig. 12) indicates that **142a**, which has R = Me and X = O, is the most active derivative among these series **142a–d** against replication of the virus, with the percentage of inhibition = 84%. Additionally, replacing the methyl group with a benzyl or 4-Cl-Bn moiety, as in compounds **143b** and **143c**, the activity decreased to 75% and 0%, respectively. This decreases in activity is because of the presence of the benzylidene moiety in general, and the substitution of one hydrogen bond by a chlorine atom at position four in the benzylidene moiety leads to the removal of the activity. Furthermore, 5-(piperidin-1-ylsulfonyl)-1′*H*-spiroindoline derivatives **143b** and **143e** with a methyl moiety and carbonyl or thiocarbonyl (X = O or S) showed the highest activity among the

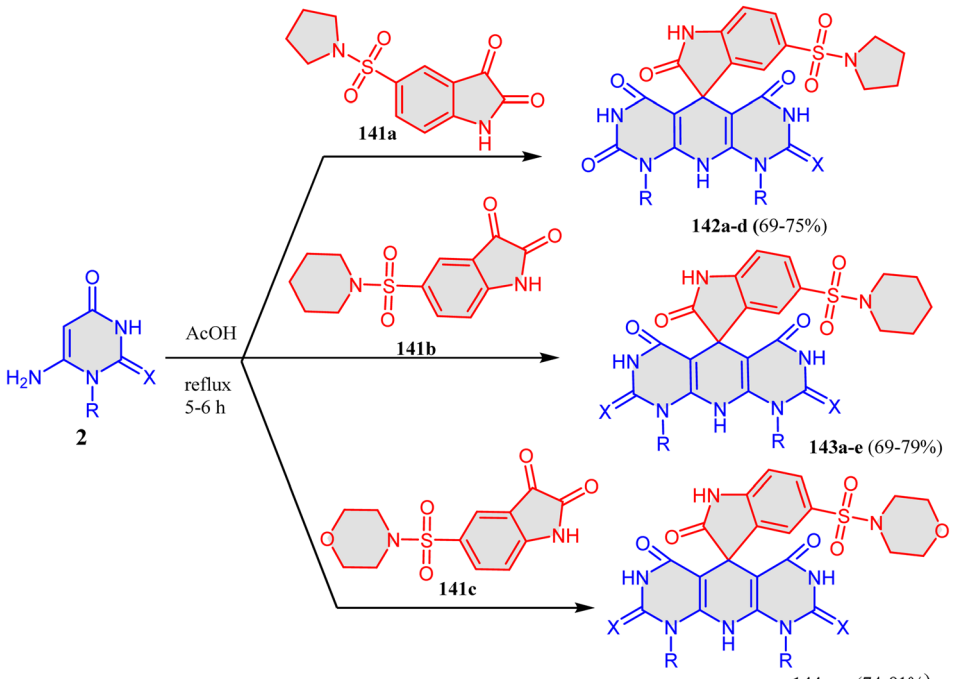

142a: R= Me, X = O; **b**: R = C_6H_4-CH_2, X = O; **c**: R = **4-Cl**-C_6H_4-CH_2, X = O; **d**: R = Me, X = S

143 and 144a-d: a: R = H, X = O; **b**: R= Me, X = O; **c**: R = C_6H_4-CH_2, X = O; **d**: R =**4-Cl**-C_6H_4-CH_2, X = O; **e**: R = Me, X = S

Scheme 49 Reaction of 6-aminouracil **2** with 5-(substituted-1-yl-sulfonyl)indoline-2,3-diones **141a–c**.

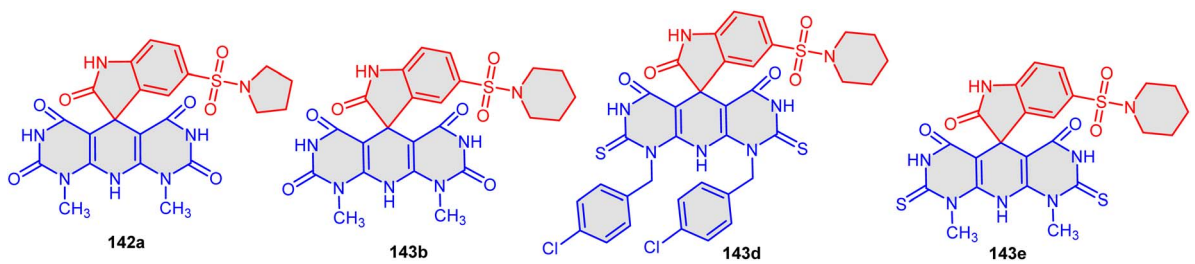

Fig. 12 Structures of compounds **142a**, **143b**, **143d** and **143e**.

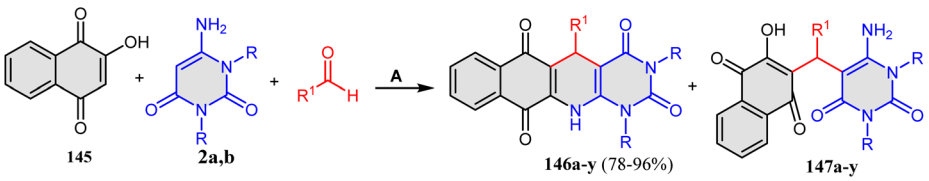

146 and 147a-y: a: R=Me, R^1= Ph; **b**: R=Me,R^1= 4-Cl-C_6H_4; **c**: R=Me,R^1= 4-Me-C_6H_4, **d**: R=Me, R^1= 4-OMe-C_6H_4; **e**: R=Me,R^1= 4-CH(Me)$_2$-C_6H_4; **f**: R=Me, R^1= 4-NO_2-C_6H_4; **g**: R=Me,R^1= 4-F-C_6H_4, **h**: R=Me,R^1= 2-Cl-C_6H_4; **i**: R=Me, R^1= 3-Br-C_6H_4, **j**: R=Me,R^1= Naphthyl; **k**: R=Me, R^1= 2-OMe-C_6H_4, **l**: R= H, R^1= C_6H_5; **m**: R= H, R^1= 4-OMe-C_6H_4; **n**: R=H, R^1= 4-CH(Me)$_2$-C_6H_4; **o**: R=H, R^1= 4-F-C_6H_4, **p**: R= H, R^1= 2-Cl-C_6H_4; **q**: R=H, R^1= 3-Br-C_6H_4, **r**: R=H ,R^1= 2-OMe-C_6H_4; **s**: R=H, R^1= 2-OMe-C_6H_4; **t**: R=H,R^1= 2,6-Me$_2$-C_6H_3; **v**: R=H, R^1= 4-Br-C_6H_4; **w**: R=H ,R^1= 4-CN-C_6H_4; **x**: R=Me,R^1= Cyclohexyl, **y**: R= Me, R^1= Butyl

Scheme 50 Microwave-assisted synthesis of pyridopyrimidines **146a–y**. Reagents and conditions: A; MW, AcOH/H_2O.

tested derivatives against the replication of SARS-CoV-2, with a percentage of inhibition of 99% and 91%, respectively. Moreover, 1′*H*-spiroindoline derivative **143c** demonstrated an inhibition percentage of 74%, and this decrease in activity may be related to the presence of the benzyl moiety. Additionally, compound **143d** exhibited good activity with an inhibition percentage of 80% when the substitutions were R = 4-Cl-Bn and X = O.

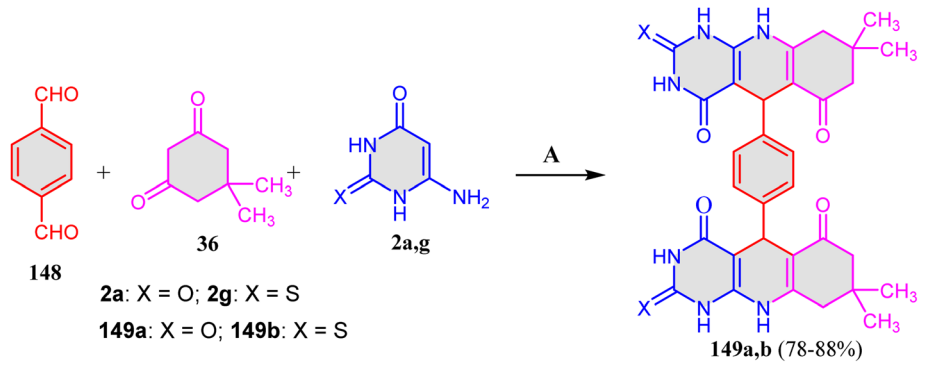

Scheme 51 Synthesis of bis pyrido[2,3-*d*]pyrimidine scaffolds **149a,b**. Reagents and conditions: A; MW, 5 min, AcOH.

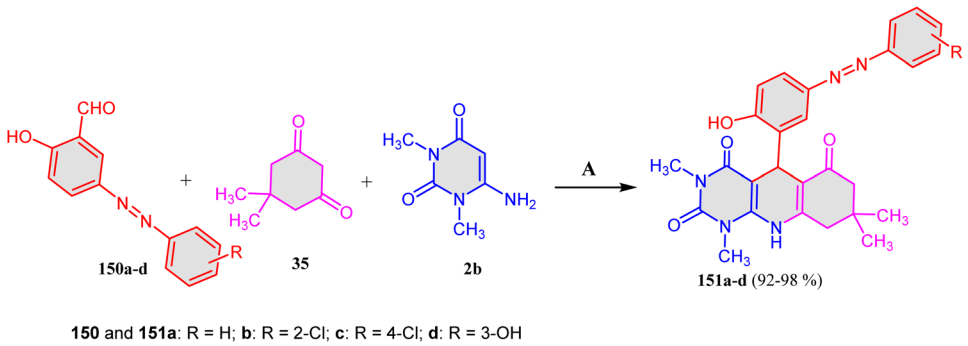

Scheme 52 Three-component synthesis of pyrimido[4,5-*b*]quinolines **151a–d**. Reagents and conditions: A; choline chloride, oxalic, B = DESs, 80 °C.

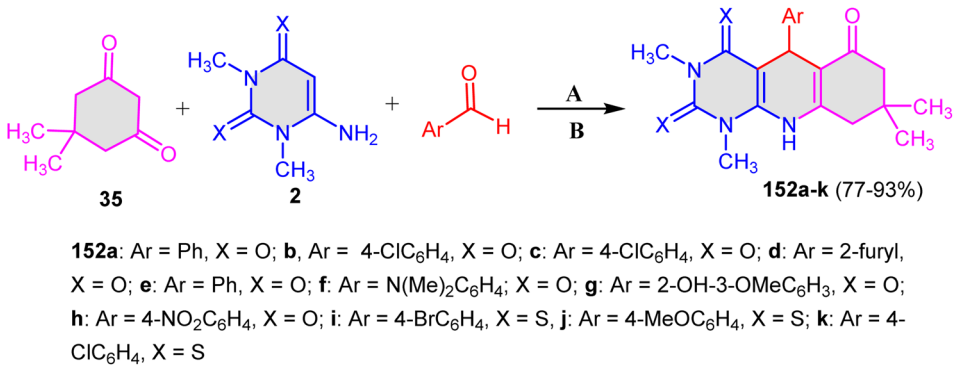

Scheme 53 Synthesis of naphthyridines **152a–k**. Reagents and conditions: A; MIL-100(Cr)/NHEtN($CH_2PO_3H_2$)$_2$; B; DMF, 100 °C.

Under microwave irradiation, the reaction of aminouracil derivatives **2a,b**, 2-hydroxy-1,4-naphthaquinone (**145**) and different aldehydes in AcOH/H_2O for 25 min afforded pyrimido[4,5-*b*]quinolines **146a–y**. Minor products of compound **147a–y** were also formed and isolated during the reaction, as shown in Scheme 50.[134]

Recently, in 2025, Alatawi *et al.*[135] reacted 6-aminouracil derivatives **2a,g**, terephthalaldehyde (**148**) and dimedone (**35**) in AcOH under microwave irradiation for 5 min to form bis-pyrido[2,3-*d*]pyrimidine derivatives **149a,b** in 78–88% yield (Scheme 51).[135] Compounds **149a** and **b** displayed great efficiency in inhibiting the *candida albicans* fungus's growth, with MIC levels between 51 and 74 mg mL^{-1}, which is similar to the positive control. MIC levels range from 62 to 82 mg mL^{-1}. Meanwhile, in 2020, Masoumi *et al.*[136] performed the same reactions in EtOH in a catalyst-free reaction condition to obtain the same scaffolds.

Moreover, Gholami and his group[136] reported a multicomponent reaction with azo aldehydes **150**, dimedone (**35**) and 6-amino-1,3-dimethyluracil (**2b**) to obtain pyrimido[4,5-*b*]quinoline derivatives **151a–d** in 92–98% yields. The reaction was carried out in deep eutectic solvents (a class of solvents formed by the eutectic mixture of two or more compounds, resulting in a liquid with a melting point significantly lower than that of its

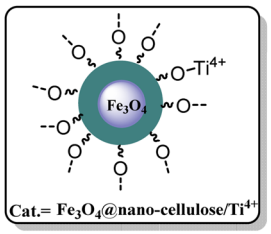

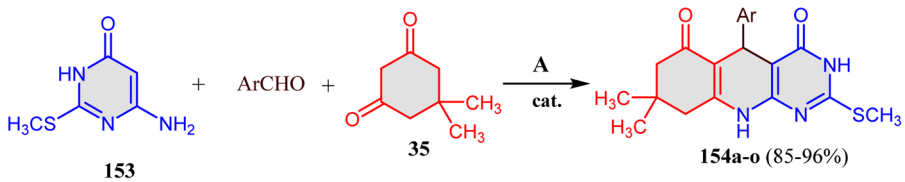

153 35 **154a-o** (85-96%)

a: Ar = 4-$MeOC_6H_4$; **b**, Ar = 2,4-$(MeO)_2C_6H_3$; **c**: Ar = 2,4-$Cl_2C_6H_3$; **d**: Ar = 4-$NO_2C_6H_4$; **e**: Ar = Ph; **f**: Ar = 4-OH-3-$OMeC_6H_3$; **g**: Ar = 4-$CO_2MeC_6H_4$; **h**: Ar = 3,4,5-F_3-C_6H_2; **i**: Ar = 3-BrC_6H_4; **j**: Ar = 4-MeC_6H_4; **k**: Ar = 4-ClC_6H_4; **l**: Ar = 3-$NO_2C_6H_4$; **m**: Ar = 3,4-$(OH)_2C_6H_3$; **n**: Ar = 4-BrC_6H_4; **o**: Ar = 4-CO_2H-C_6H_4

Scheme 54 Synthesis of naphthyridines **154a–k**. Reagents and conditions: **A**; Cat. H_2O, 70 °C.

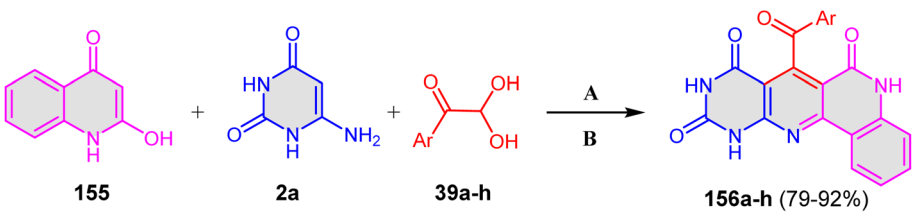

155 **2a** **39a-h** **156a-h** (79-92%)

156 and **39**:**a-h:** **a**: Ar = Ph, **b**: Ar = 4-BrC_6H_4; **c**: Ar = 4-$ClOC_6H_4$; **d**: Ar = 4-FC_6H_4; **e**: Ar = 4-MeC_6H_4; **f**: Ar = 4-$MeOC_6H_4$; **g**: Ar = 3-MeO-4-OHC_6H_3; **h**: Ar = 3,4-$(MeO)_2C_6H_4$

Scheme 55 Ag NP-mediated synthesis of pyrimido[4,5-*b*][1,6]naphthyridines **156a–h**. Reagents and conditions: **A**; Ag NPs; **B**; EtOH/H_2O/60 °C.

Table 20 Various solvents and catalysts used in the synthesis of compounds **156a–h**

Entry	Solvent	Temp. (°C)	Catalyst (mol%)	Time (h)	Yield **156e** (%)
1	EtOH/H_2O (1 : 1)	Reflux	L-proline (20 mol%)	7	52
2	EtOH	Reflux	L-proline (20 mol%)	7	58
3	EtOH	Reflux	*p*-TSA (20 mol%)	6	57
4	EtOH/H_2O (1 : 1)	Reflux	*p*-TSA (20 mol%)	6	50
5	EtOH/H_2O (1 : 1)	60	AgNPs (5 ppm)	3	74
6	EtOH/H_2O (1 : 1)	60	AgNPs (20 ppm)	3	92
7	H_2O	60	AgNPs (10 ppm)	24	—
8	AcOH	70	L-proline (20 mol%)	10	79
9	AcOH	Reflux	L-proline (20 mol%)	10	70

Table 21 Time of reaction for **39a–h**, **2a** and **155** and the yield (%) for the synthesis of products **156a–h**

Entry	Ar	Time (min)	Yields (%)
1	Ph	300	**156a** (79)
2	4-BrC_6H_4	240	**156b** (88)
3	4-ClC_6H_4	270	**156c** (82)
4	4-FC_6H_4	240	**156d** (87)
5	4-Tol	180	**156e** (91)
6	4-$MeOC_6H_4$	150	**156f** (92)
7	3-MeO-4-HOC_6H_3	180	**156g** (89)
8	3,4-$(MeO)_2C_6H_3$	210	**156h** (90)

individual components) and choline chloride/oxalic acid (ChCl/Oxa) at 80 °C was present (Scheme 52).[137]

In continuation to previous discussion about the synthesis of pyrido-pyrimidine frameworks, tetrahydropyrimido[4,5-*b*]quinolines **152a–k** were obtained in high yields (77–93%) through a three-component reaction between dimedone (**35**), 6-aminouracil derivatives **2** and different aldehydes under reflux conditions in the presence of MIL-125(Ti)–$N(CH_2PO_3H_2)_2$ as a catalyst (Scheme 53).[138] Interestingly, the preparation of **152a–k** was achieved *via* a vinylogous anomeric-based oxidation mechanism with a high yield and short reaction time.[138]

Mirjalili *et al.*[139] reported the synthesis of tetrahydropyrimido[4,5-*b*]quinoline analogs **154a–o** *via* the utilization of Fe_3O_4@nano-cellulose/Ti(IV) as a nanocatalyst. Therefore, a one-pot technique was applied in the reactions of 6-amino-2-(methylthio) pyrimidin-4(3*H*)-one (**153**) with aryl aldehydes and dimedone (**35**) under H_2O at 70 °C (Scheme 54).

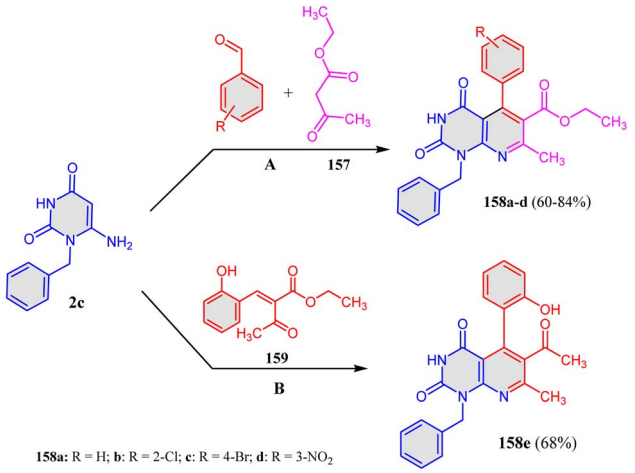

Scheme 56 Reaction of 1-benzyl-6-aminouracil with compound ethyl acetoacetates **157** and **159**. Reagents and conditions: **A**; EtOH, TEA, reflux, 12 h. **B**; DMF, TEA, reflux, 4 h.

It was also reported[140] that silver nanoparticles were used to catalyze the reaction between 2-hydroxyquinoline-4(1*H*)-one (**155**), 6-aminouracil (**2a**) and arylglyoxal monohydrates **39a–h** in a mixture solvent of EtOH/H_2O at 60 °C, affording pyrimido[4,5-*b*][1,6]naphthyridines **156a–h** as the final products in 79–92% yields (Scheme 55).[140]

The reactions of **39e**, **2a** and **155** were chosen as optimized reactions (Table 20). The reaction mixture was stirred using various catalysts and, in a mixture, solvent systems. A solid precipitate separated out in 50–92% yields of substituted pyrimido[4,5-*b*][1,6]naphthyridine (**156e**). The highest yield (91%) was achieved when the reaction was performed using 10 ppm of AgNPs as a nanocatalyst in H_2O/EtOH (1 : 1) after 3 h of reaction time (Table 20, entry 6). To investigate the effect of the catalyst amount, the reaction was repeated in the presence of various amounts of AgNPs, as increasing the amount of catalyst did not significantly affect the reaction yield.[140]

The one-pot, three-component reaction of aryl **39a–h**, **2a** and **155** in the presence of AgNPs (10 ppm) using H_2O/EtOH (1 : 1) as a solvent afforded the desired compounds **156a–h** in high yields (Table 21).[140]

El-Kalyoubi *et al.*[141] reacted 1-benzyl-6-aminouracil **2c**, aromatic aldehydes and ethyl acetoacetate (**157**) in EtOH/Et_3N at reflux temperature for 12 h to give tetrahydropyrido[2,3-*d*]

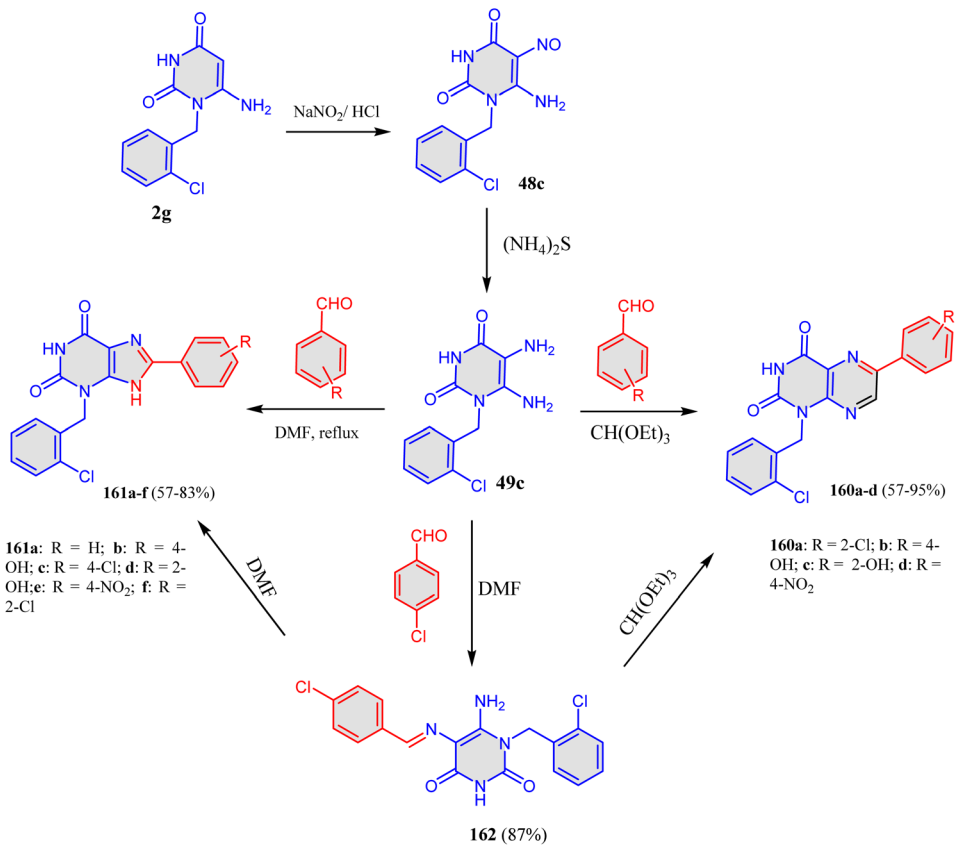

Scheme 57 Synthesis of pteridines **160a–d** and purine compounds **161a–f**.

Table 22 *In vitro* inhibitory activity of tested compounds against the human lung carcinoma cell line (A549) expressed as IC_{50} values μM ± standard deviation

Tested Compd	Structure	IC_{50} values (μM)	Tested compounds	Structure	IC_{50} values (μM)
158a	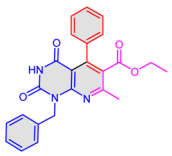	237 ± 6.3	**161c**	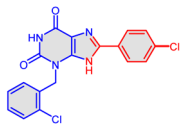	27.0 ± 1.1
158b	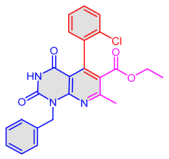	10.3 ± 0.2	**161d**	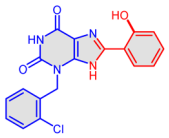	23.1 ± 0.6
158c	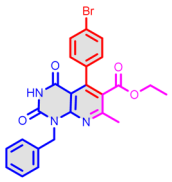	349 ± 7.8	**161e**	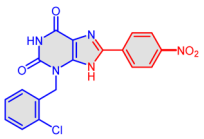	26.3 ± 1.3
158d	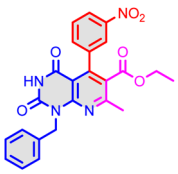	59.5 ± 2.5	**161f**	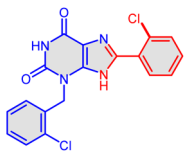	141 ± 3.9
158e	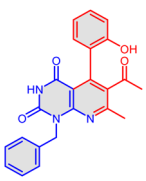	246 ± 7.1	**160a**	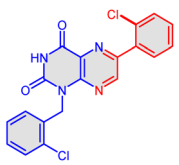	86.1 ± 2.8
162	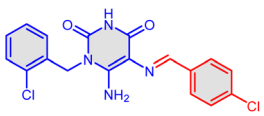	62.0 ± 2.4	**160b**	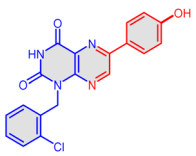	84.8 ± 3.4
161a	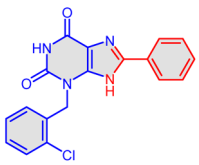	54.0 ± 1.8	**160c**	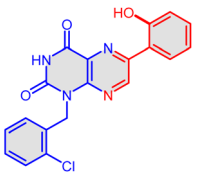	24.9 ± 1.2
161b	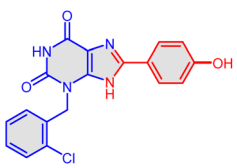	58.5 ± 1.7	**160d**	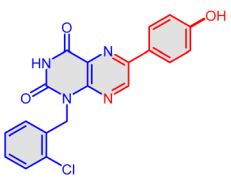	12.2 ± 0.3
Methotrexate		**36.3 ±3.9**			

pyrimidine-6-carboxylates **58a–d** in 60–84% yields. During the reaction of 1-benzyl-6-aminouracil **2c** with ethyl 2-(2-hydroxybenzylidene)acetoacetate (**159**) under the same conditions for 4 h, the reaction proceeded to give 6-acetyl-1-benzyl-5-(2-hydroxyphenyl)-7-methylpyrido[2,3-*d*]pyrimidine-2,4(1*H*,3*H*)-dione (**158e**), as shown in Scheme 56.[141]

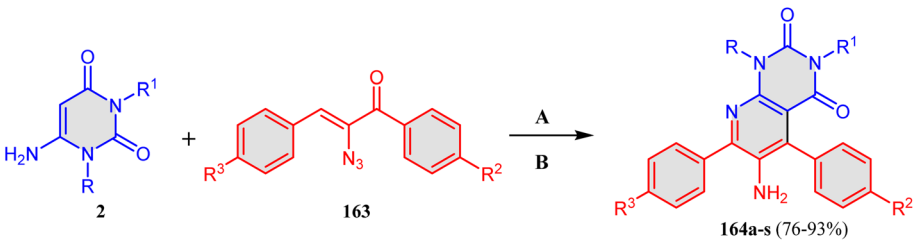

164a-s:a: R = R^1= H, R^2= H, R^3 = Me; **b**: R = R^1= H, R^2= R^3 =Cl; **c**: R = R^1= H, R^2= H, R^3 = Br; **d**: R = R^1= H, R^2= Me, R^3 = Br; **e**: R = Me, R^1= H, R^2= OMe, R^3 = H; **f**: R = Me, R^1= H, R^2= H, R^3 = Cl; **g**: R = Me, R^1= H, R^2= R^3 = Cl; **h**: R = Me, R^1= H, R^2= H, R^3 = Br: **i**: R = Me, R^1= H, R^2= Me, R^3 = Br; **j**: R = R^1= Me, R^2= R^3 = H; **k**: R = R^1= R^3= Me, R^2= H; **l**: R = R^1= Me, R^2= OMe, R^3 = H; **m**: R = R^1= Me, R^2= H, R^3 = Cl; **n**: R = R^1= Me, R^2= Me, R^3 = Cl; **o**: R = R^1= Me, R^2= OMe, R^3 = Cl; **p**: R = R^1= Me, R^2= R^3 = Cl; **q**: R = R^1= Me, R^2= H, R^3 = Br; **r**: R = R^1= Me, R^2= Br, R^3 = Me; **s**: R = R^1= Me, R^2= Me, R^3 = Br

Scheme 58 Reaction of α-azidochalcones **163** with 6-amiouracils **2**. Reagents and conditions: A = DMF, Et_3N; B = 50 °C, 30 min.

The same authors[141] also prepared compounds containing pteridine and purine frameworks. The strategy started with nitrosation of 1-(2-chlorobenzyl)-6-aminouracil **2g** to give 6-amino-1-(2-chlorobenzyl)-5-nitrosopyrimidine-2,4-dione (**48c**), which was treated with ammonium sulfide $(NH_4)_2S$ to produce 5,6-diamino-1-(2-chlorobenzyl)-pyrimidinedione (**49c**) (Scheme 57), when compound **49c** reacted with triethyl orthoformate and various aromatic aldehydes afforded pteridine derivatives **160a–d.** However, when it reacted only with aromatic aldehydes, it afforded purine **161a–f.** On the other hand, when diaminouracil **49c** reacted with 4-chlorobenzaldhyde, it gave ylidene form **162**, which produced the corresponding pteridine **160** when it was treated with triethyl orthoformate. Besides, refluxing ylidene **162** in DMF gave the corresponding purine (Scheme 57).[141]

The formed products were examined for *in vitro* lung carcinoma inhibitory activity against the cell line A549. The results showed that the most effective compounds against lung carcinoma are **158b**, **161c**, **161d**, **161e**, **160c** and **160d** (Table 22) using methotrexate as a drug reference. The pteridine scaffold containing the 2-Cl-Bn group **158b** exhibited good inhibitory activity ($IC_{50} = 10.3 \pm 0.2$). Purine compounds **161c**, **161d**, and **161e**, which have R = 4-Cl, 2-OH and 4-NO_2, displayed IC_{50} = 27.0 ± 1.1, 23.1 ± 0.6, and 26.3 ± 1.3, respectively. Moreover, pteridine compounds **160c** and **160d** with an OH group in positions 2 and 4 demonstrated a significant increase in inhibition activity (IC_{50} = 24.9 ± 1.2 and 12.2 ± 0.3) compared to the reference methotrexate (IC_{50} = 36.3 ± 3.9).[141]

The synthesis of 6-amino-pyrido[2,3-*d*]pyrimidine-2,4-diones **164a–s** was reported by Adib *et al.*[142] through the reaction between α-azidochalcones **163** and 6-amiouracil derivatives in DMF/Et_3N at 50 °C for 30 min (Scheme 58). The corresponding products were formed in high yields (79–93%). α-Glucosidase inhibitory activity of the products **164a–s** was investigated and displayed significant *in vitro* yeast α-glucosidase inhibition with IC_{50} values between 78.0 ± 2.0 and 252.4 ± 1.0 μM. According to the results, the compound with the highest significant activity was **164o** and was around 10-fold more potent than the reference drug, acarbose (IC_{50} = 750.0 ± 1.5 μM).[142] Compound **164a** with 4-Me substituent on the 7-phenyl ring showed the most inhibitory activity in this series ($IC_{50} = 164.5 \pm 1.5$ mM). The replacement of the methyl group with a Br atom in the mentioned position (compound **164c**) decreases the inhibitory activity. Moreover, the anti-α-glucosidase activity decreased in compound **164b** ($R^2 = R^3$ = Cl). In the case of derivatives **164e–i** (R = Me), a better result was obtained for compound **164i** with (R^2 = 4-CH_3 and R^3 = 4-Br). The absence of a methyl group in compound **164h** decreased the inhibitory effect. The activity of compound **164f** (R^3 = Cl) decreased ($IC_{50} = 224.0 \pm 1.5$ mM). The presence of a chlorine atom (R = Me, $R^2 = R^3$ = Cl) in compound **164g** results in a significant increase in inhibition ($IC_{50} = 187.0 \pm 1.0$ mM). Compound **164e** (R^3 = 4-OMe) was the second most potent compound in this series. A comparison of the IC_{50} values of derivatives with R = Me **164g–i** with their analogs (R = H) **164b–d** showed that the derivatives containing the Me group were more potent than the others. Furthermore, in **164j–s** derivatives, compound **164o** with (R^2 = 4-OCH_3 and R^3 = 4-Cl) was the most potent compound among all the synthesized compounds ($IC_{50} = 78.0 \pm 2.0$ mM) (Table 23).[142]

A plausible mechanism for the synthesis of 6-amino-pyrido[2,3-*d*]pyrimidine-2,4-diones **164a–s** is illustrated in Scheme 59. The mechanism could be explained by the presence of base C-5 of 6-aminouracil **2**, which would undergo a Michael addition to α-azidochalcone **163**, and the nitrogen molecule was eliminated to produce adduct **165**. Next, cyclic form **166** was formed *via* a nucleophilic attack of the imine on the adjacent carbonyl. The adduct **166** then loses a molecule of H_2O to form intermediate **167**. Finally, a proton shift occurred, leading to the generation of the final products **164a–s.**[142]

Shaddel *et al.*[143] developed a green synthetic technique for the synthesis of dihydropyrido[2,3-*d*]pyrimidine **169a–k**. The reaction proceeded between Meldrum's acid **168**, **2a** and aldehydes in H_2O at 70 °C in the presence of L-tyrosinium hydrogen sulfate IL ($Mn_{0.5}Fe_{0.25}Ca_{0.25}Fe_2O_4$–$SiO_2$@[L-Tyr]

Table 23 *In vitro* α-glucosidase inhibitory activity of compounds **164a–s** and acarbose (as a reference drug)

Compd	Structure	IC_{50} (μM)	Compd	Structure	IC_{50} (μM)
164a	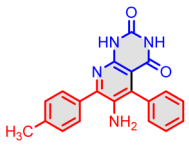	164.5 ± 1.5	**164k**	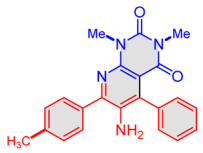	145.0 ± 1.5
164b	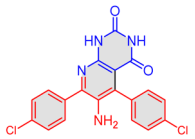	237.0 ± 1.0	**164l**	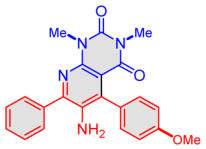	185.0 ± 1.0
164c	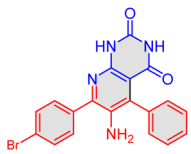	223.2 ± 1.5	**164m**	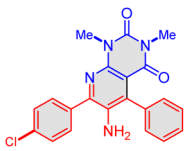	122.3 ± 2.5
164d	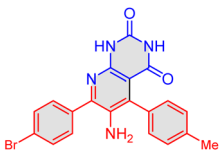	222.0 ± 2.0	**164n**	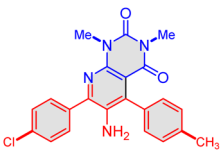	177 ± 1.0
164e	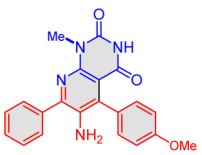	112.5 ± 1.0	**164o**	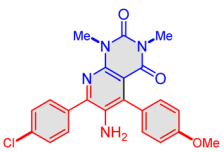	78.0 ± 2.0
164f	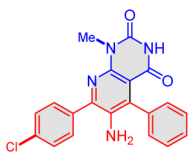	224.0 ± 1.5	**164p**	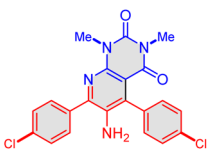	215.0 ± 1.0
164g	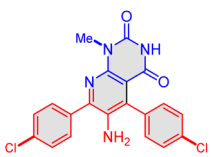	187.0 ± 1.0	**164q**	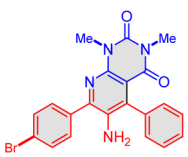	132.0 ± 1.5
164h	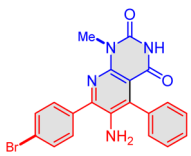	177.1 ± 1.0	**164r**	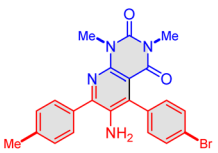	193.0 ± 1.5
164i	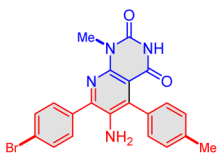	91.0 ± 1.0	**164s**	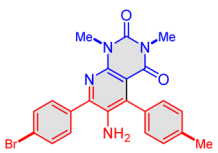	236.0 ± 1.3
164j	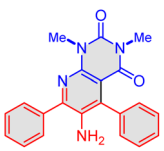	252.4 ± 1.0			
Acarbose		**750.0 ±1.5**			

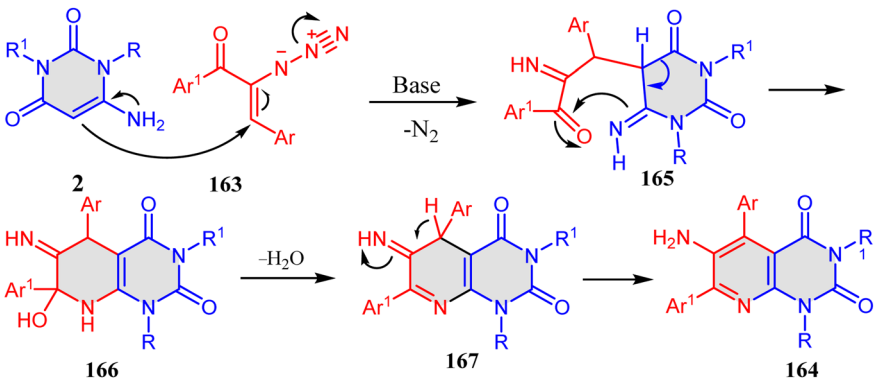

Scheme 59 Suggested mechanism for the formation of compound **164a–s**.

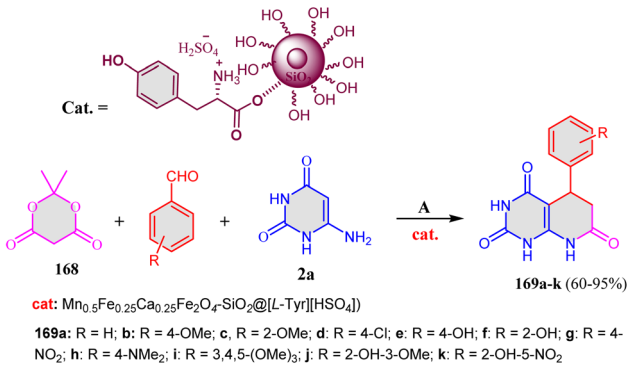

Scheme 60 Formation of dihydropyrido[2,3-*d*]pyrimidines **169a–k**. Reagents and conditions: **A**; H_2O, 70 °C.

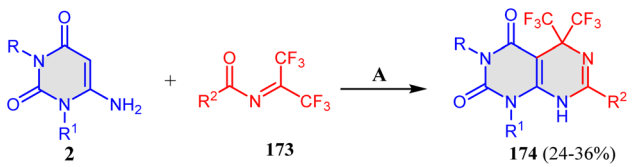

Scheme 62 Reaction of 6-aminouracils **2** with compound **173**. Reagents and conditions: **A** = DMF, Et_3N.

[HSO_4]) as a catalyst to obtain the final products **169a–k** (Scheme 60).

Recently, Abdelaal *et al.*[144] synthesized pyrido[2,3-*d*]pyrimidine **172a–d** bearing coumarin ring through the reaction of 3-(3-(dimethylamino)acryloyl)-2*H*-chromen-2-one (**170**) with 6-aminouracil derivatives **2** in AcOH at reflux temperature for 5–6 h (Scheme 61). Compound **172a** demonstrated a potent and selective activity against CNS cancer cell lines U251 and SF-295 (80.51% and 96.86%, respectively). Compound **172c** displayed lethal activity (GI > 100%) toward 41 tumor cell lines that belong to all the nine subpanels except leukemia (GI = 23.13–97.50%). This broad activity was narrowed to non-small cell lung cancer NCI-H226 (GI = 64.09%) and ovarian cancer cell line OVCAR-3 (75.53%) by the addition of a 4-methoxy group to the appended phenyl ring at N−1 (compound **172d**).[144]

2.2.6. Synthesis of pyrimido[4,5-*d*]pyrimidine-2,4-dione derivatives. On mixing substituted 6-aminouracils **2** with *N*-acylimines of hexafluoroacetone (**173**) in DMF and using Et_3N as a catalyst, the reaction afforded substituted 5,5-bis(trifluoromethyl)-5,8-dihydro-pyrimido[4,5-*d*]pyrimidine-2,4-

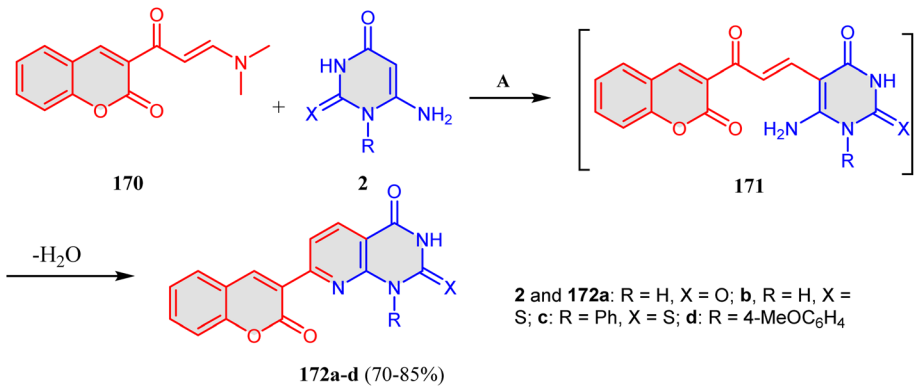

Scheme 61 Reaction of 3-(3-(dimethylamino)acryloyl)-2*H*-chromen-2-one **170** with 6-aminouracils **2**. Reagents and conditions: **A**; AcOH, reflux, 5–6 h.

Table 24 Structures and activities of compounds **174a–e**

Entry	R	R^1	R^2	GLP-1R IC_{50} (μM)[a,b]	GLP-1R p IC_{50}	GLP-1 min (%)
174a	H	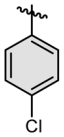	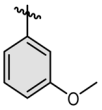	5.9[a] 5.8[b]	5.23 ± 0.09[a] 5.24 ± 0.08[b]	16.8 ± 6.3[a] 23.9 ± 5.5[b]
174b	H			1.3[a] 1.5[b]	5.89 ± 0.04[a] 5.82 ± 0.06[b]	36.2 ± 1.9[a] 32.0 ± 2.4[b]
174c	H		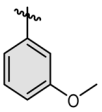	7.2[a] 7.2[b]	5.14 ± 0.08[a] 5.14 ± 0.08[b]	22.7 ± 6.2[a] 26.4 ± 6.2[b]
174d	Me	Me	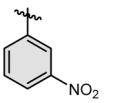	0.61[a] 0.69[b]	6.22 ± 0.03[a] 6.16 ± 0.04[b]	16.4 ± 1.5[a] 15.5 ± 1.7[b]
174e	Me	Me		0.65[a] 0.69[b]	6.19 ± 0.03[a] 6.16 ± 0.05[b]	20.9 ± 1.4[a] 19.7 ± 2.1[b]

[a] GLP-1R IC_{50}, pIC_{50} and GLP-1 min (%) in TREx293 HEK cell line with GloSensor cAMP assay upon activation with an EC_{80} of GLP-1 (7–36) amide; $n = 3$. [b] GLP-1R IC_{50}, pIC_{50} and GLP-1 min (%) in TREx293 HEK cell line with GloSensor.

diones **174a–e** in 24–36% yields (Scheme 62 and Table 24). The glucagon-like peptide-1 receptor (GLP-1R) is a major area of interest in the treatment of type II diabetes. It is essential for increasing insulin secretion and decreasing glucagon secretion.[145] The results showed that 7-(4-chlorophenyl)-1,3-dimethyl-5,5-bis(trifluoromethyl)-5,8-dihydropyrimido-[4,5-*d*] pyrimidine-2,4(1*H*,3*H*)-dione (**174e**) is an effective GLP-1R antagonist. Compound **174e** inhibited Exendin-4 (EX-4) simulation, which blocked insulin release in islets; moreover, it decreased insulin levels while increasing blood glucose. The structures and GLP-1R antagonist activities of representative analogs **174a–e** are highlighted in Table 24; when R = H (**174a**, **174b**, and **174c**), the compounds were inactive (IC_{50} > 10 μM), resulting in weak partial antagonists, while in **174b** (R^1 = benzyl and R^2 = 2-thienyl), more GLP-1R antagonist potency was observed (GLP-1 (7–36) amide, IC_{50} = 1.3 μM, pIC_{50} = 5.89 ± 0.04, 36.2 ± 1.9 GLP-1 min; exendin-4, IC_{50} = 1.5 μM, pIC_{50} = 5.82 ± 0.06, 32.0 ± 2.4 GLP-1 min) than the lead **174a**. GLP-1 antagonist potency increased when Me was substituted for hydrogen at R (Table 24).[145]

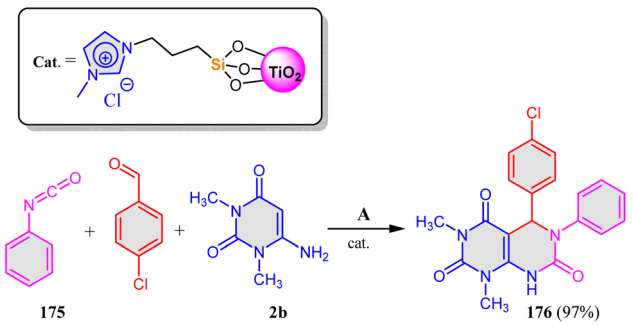

Scheme 63 Synthesis of compound **176** using TiO_2@LLs nanocatalyst. Reagent and conditions: A; EtOH:H_2O, reflux, cat.

In 2020, Bakhshali-Dehkordi *et al.*[146] utilized TiO_2 nanoparticles to synthesize 5-(4-chlorophenyl)-1,3-dimethyl-6-phenyl-5,8-dihydropyrimido[4,5-*d*]pyrimidine-trione (**176**) in 97% yield. A three-component reaction was performed between phenyl isocyanate (**175**), 4-chlorobenzaldhyde and 1,3-dimethyl-6-aminouracil (**2b**) in EtOH/H_2O containing TiO_2 nanoparticles immobilized by an ionic liquid based on imidazole at reflux temperature (Scheme 63).[146]

The suggested mechanism is illustrated in Scheme 64. First, the nitrogen atom of 6-amino-*N*,*N*-dimethyluracil **2b** attacked the carbonyl of **175** to obtain intermediate **177**. The presence of TiO_2@ILs promoted the nucleophilic attack of C-5 in intermediate **177** on the aldehyde to produce intermediate **178**, which underwent a proton shift and rearrangement to yield intermediate **179**. Finally, **179** intermolecular cyclization and dehydration were undergone to give the final product **176** (Scheme 64).[146]

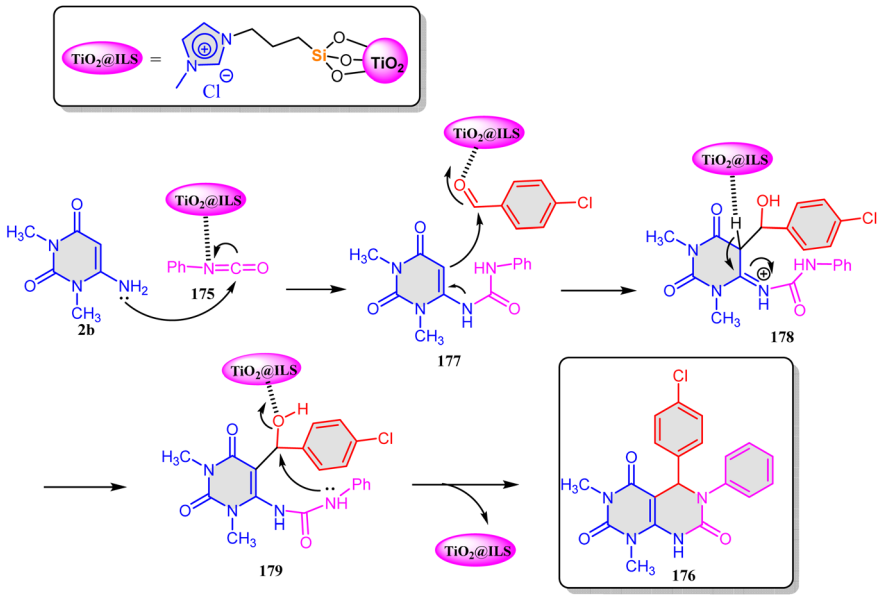

Scheme 64 Proposed mechanism for the synthesis of compound **176**.

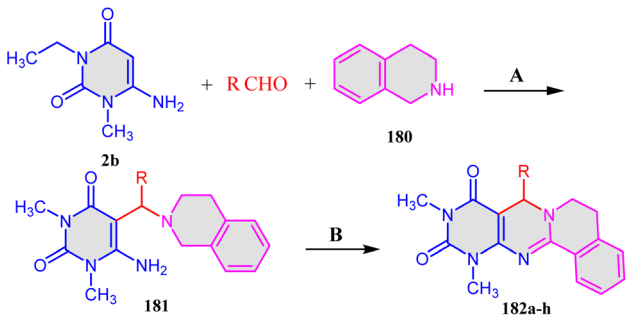

182a: R = Ph; **b**: R = 4-ClC_6H_4; **c**: R = R = 3-ClC_6H_4; **d**: R = 2-ClC_6H_4; **e**: R = 4-$NO_2C_6H_4$; **f**: R = 4-MeC_6H_4; **g**: R = 4-$MeOC_6H_4$; **h**: R = 3,4-$(MeO)_2C_6H_4$

Scheme 65 Synthesis of pyrimido[4,5-*d*]pyrimidines **182a–h**. Reagents and conditions: **A**; EtOH, AcOH, rt; **B**; I_2, TBHP, EtOH, rt.

Furthermore, Borpatra *et al.*[147] reported an interesting approach for the formation of pyrimido[4,5-*d*]pyrimidine derivatives **182a–h** *via* the reaction between 1,3-dimethyl-6-aminouracil (**2b**), various aldehydes and 1,2,3,4-tetrahydroisoquinoline (**180**) in EtOH and AcOH at room temperature to give compound **153.** Following that, compound **181** was stirred in EtOH at room temperature in the presence of *t*-butyl hydroperoxide (TBHP) and I_2 to obtain the cyclic form of pyrimido[4,5-*d*]pyrimidines **182a–h** (Scheme 65).

The multicomponent reaction between anilines **183**, 6-amino-1,3-dimethyluracil (**2b**), 1-phenyl-3-(4-substituted-phenyl)-4-formyl-1*H*-pyrazoles **184**, and *N*,*N*-dimethylformamide dimethylacetal (**185**) was performed in the presence of [Bmim]$FeCl_4$ to obtain pyrazolo-pyrimido[4,5-*d*]

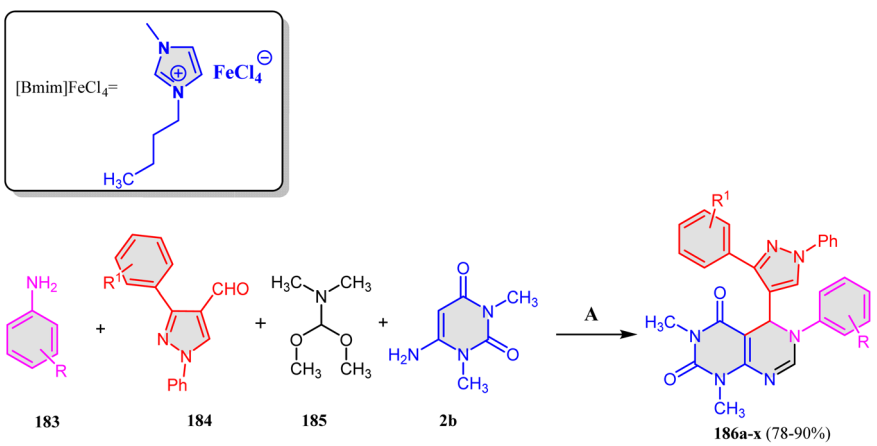

186a: R = 4-NO_2, R^1= H; **b**: R = 4-NO_2, R^1= 4-Cl; **c**: R = 4-NO_2, R^1= 4-Me; **d**: R = 4-NO_2, R^1= 4-OMe; **e**: R = 4-NO_2, R^1= 3-NO_2; **f**: R = 4-Cl, R^1= H; **g**: R = R^1= 4-Cl; **h**: R = 4-Cl, R^1= 4-Me; **i**: R = 4-Cl, R^1= 4-OMe; **j**: R = 4-Cl, R^1= 3-NO_2; **k**: R = 4-Me, R^1= H; **l**: R = 4-Me, R^1= 4-Cl; **m**: R = R^1= 4-Me; **n**: R = 4-Me, R^1= 4-OMe; **o**: R = 4-Me, R^1= 3-NO_3; **p**: R = R^1= H; **q**: R = H, R^1= 4-Cl; **r**: R = H, R^1= 4-Me; **s**: R = H, R^1= 4-OMe; **t**: R = thiophene, R^1= H; **u**: R = thiophene, R^1= 4-Cl; **v**: R = thiophene, R^1= 4-Me; **w**: R = thiophene, R^1= 4-OMe; **x**: R = thiophene, R^1= 3-NO_2

Scheme 66 Formation of pyrazolo-pyrimido[4,5-*d*]pyrimidine hybrids **186a–x**. Reagents and conditions: **A**; [Bmim]$FeCl_4$, 80 °C.

Table 25 Antibacterial activity of pyrazolo-pyrimido[4,5-*d*]pyrimidines **186a–x**

	Minimum inhibitory concentration (lg mL^{-1})						
Compd	*Bacillus subtilis* MTCC121	*Staphylococcus aureus* MTCC 96	*S. aureus* MLS16 MTCC 2940	*Micrococcus luteus* MTCC 2470	*Klebsiella planticola* MTCC 530	*Escherichia coli* MTCC 739	*Pseudomonas aeruginosa* MTCC 2453
186a	>125	>125	>125	>125	>125	>125	>125
186b	>125	>125	>125	>125	>125	>125	>125
186c	7.8	15.6	7.8	15.6	>125	>125	>125
186d	31.2	31.2	31.2	15.6	>125	>125	>125
186e	>125	>125	>125	31.2	>125	>125	>125
186f	>125	>125	>125	>125	>125	>125	>125
186g	>125	>125	>125	>125	>125	>125	>125
186h	>125	>125	>125	15.6	>125	>125	>125
186i	31.2	15.6	15.6	7.8	>125	>125	>125
186j	>125	>125	>125	>125	>125	>125	>125
186k	>125	>125	>125	>125	>125	>125	>125
186l	7.8	7.8	7.8	3.9	>125	>125	>125
186m	7.8	7.8	15.6	7.8	>125	>125	>125
186n	>125	>125	>125	>125	>125	>125	>125
186o	>125	>125	>125	>125	>125	>125	>125
186p	62.5	31.2	15.6	7.8	>125	>125	>125
186q	>125	>125	>125	>125	>125	>125	>125
186r	>125	>125	>125	>125	>125	>125	>125
186s	>125	>125	>125	>125	>125	>125	>125
186t	31.2	31.2	15.6	15.6	>125	>125	>125
186u	15.6	31.2	15.6	15.6	>125	>125	>125
186v	31.2	15.6	15.6	15.6	>125	>125	>125
186w	31.2	15.6	15.6	15.6	>125	>125	>125
186x	>125	>125	>125	>125	>125	>125	>125
Ciprofloxacin	0.9	0.9	0.9	0.9	0.9	0.9	0.9

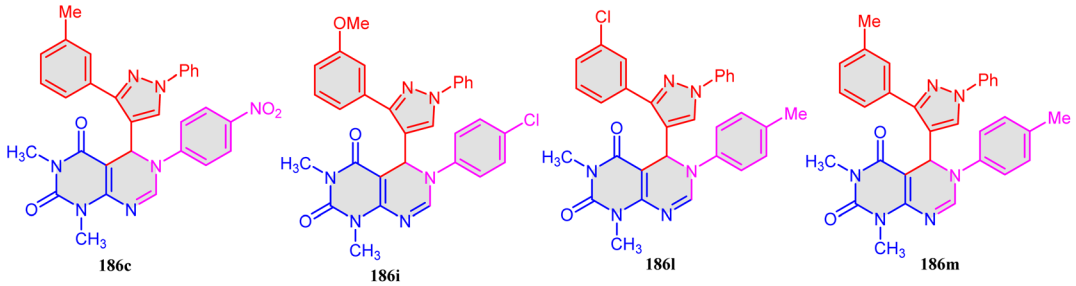

Fig. 13 Structures of antibacterial compounds **186c**, **186i**, **186l** and **186m**.

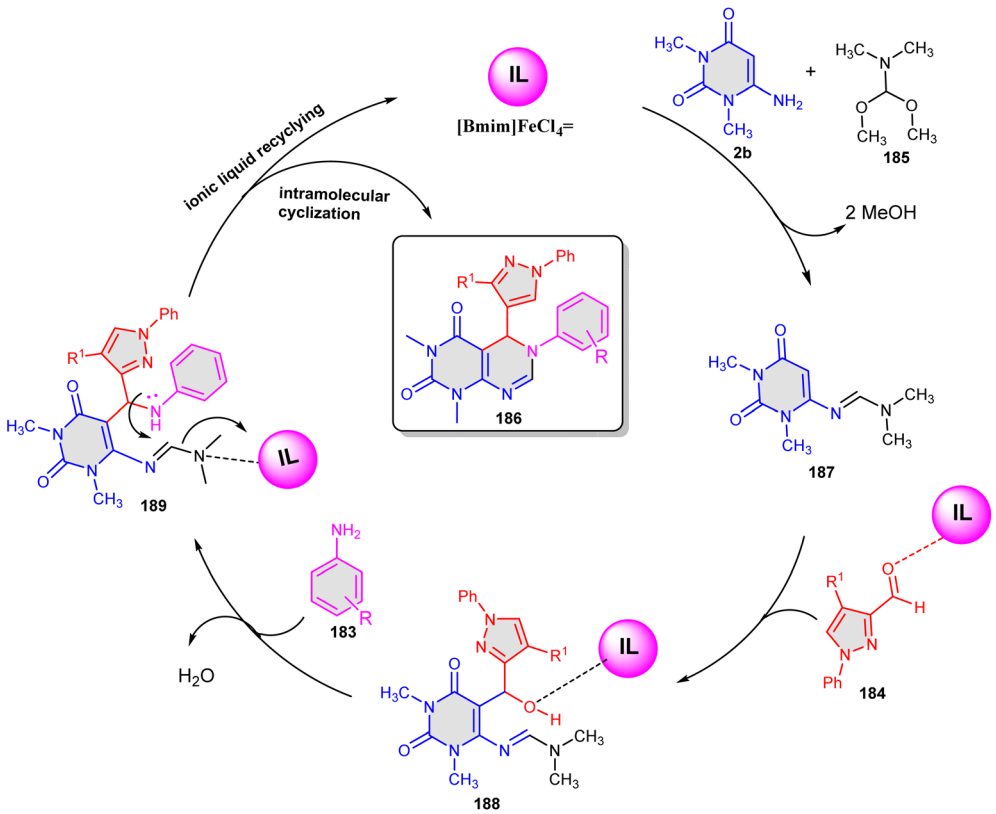

Scheme 67 Suggested mechanism for the synthesis of pyrazolo-pyrimido[4,5-*d*]pyrimidines **186a–x**.

pyrimidines **186a–x** in 78–90% yields (Scheme 66).[148] The formed products were investigated for their antibacterial activity (Table 25). Among all the tested compounds, compounds **186d**, **186t**, **186u**, **186v**, and **186w** had good activity with MIC values ranging from 15.6 to 31.2 μg mL^{-1}, while compounds **186c**, **186i**, **186l**, and **186m** were of nearly promising activity with MIC values ranging from 3.9 to 15.6 μg mL^{-1} (Table 25).[148]

2.2.6.1 Structure activity relationship. Based on the data presented in Table 25, derivatives **186c**, **186i**, **186l** and **186m** containing (–NO_2), (–Cl), (–Me) and (–OMe) groups, respectively, increased the activity considerably (Fig. 13). It was observed that compound **186f** (R = 4-Cl, R^1 = H) has a simple hydrogen atom attached to the basic pyrazolo-pyrimido[4,5-*d*]pyrimidines scaffold, which has neutral properties and may probably contribute to the antibacterial activity. However, compound **186l** (R = 4-Me, R^1 = 4-Cl) contains an electron withdrawing chlorine atom, which probably may contribute to the antibacterial activity.

Scheme 67 illustrates the suggested mechanism for the reaction. As amidine **187** was formed *via* the reaction between 6-amino-1,3-dimethyluracil **2b** and *N*,*N*-dimethylformamide dimethyl acetal (**185**). Next, 1-phenyl-3-(4-substituted-phenyl)-4-formyl-1*H*-pyrazoles **184** underwent a reaction with compound **187** to produce intermediate **188**. Intermediate **188** likely reacted with the aromatic amines **183** and lost a molecule of water to give intermediate **189**. Finally, a nucleophilic attack occurred in intermediate **189** to the imino carbon atom; accordingly,

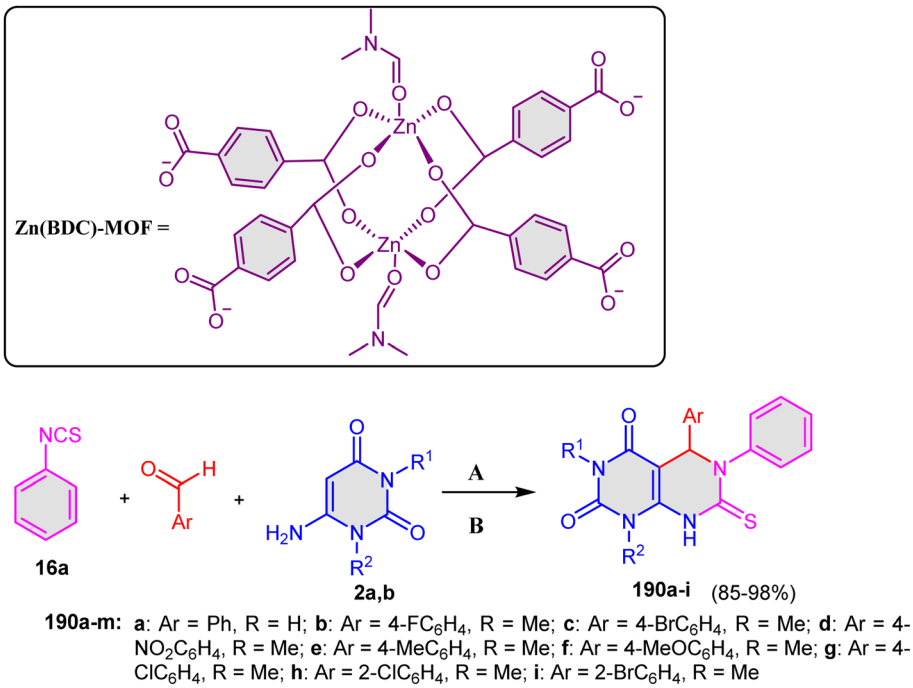

Scheme 68 Synthesis of pyrimidopyrimidine derivatives **190a–i**. Reagents and conditions: **A**; Zn(BDC)-MOF, solvent-free; **B**; ultrasound.

dimethylamine was removed and subsequently intermolecular cyclized to produce the desired products **186a–x**.[148]

Shirini *et al.*[149] established a series of pyrimido[4,5-*d*]pyrimidine frameworks **190a–i** through a solvent free three-component reaction between phenyl isothiocyanate (**16a**), aromatic aldehydes, and 6-aminouracil derivatives **2a,b** under US irradiation, using Zn(BDC)-MOFs-(BDC,1,4-benzenedicarboxylic acid) as a catalyst. MOFs (metal–organic frameworks) were utilized as a catalyst in 5–10 min (Scheme 68). The final products **190a–i** were formed in high yields (85–98%).[149]

Additionally, Ghorbani-Vaghei *et al.*[150] utilized 7-aminonaphthalene-1,3-disulfonic acid (ANDSA)-functionalized magnetic Fe_3O_4@SiO_2 particles as a catalyst in the formation of pyrimido[4,5-*d*]pyrimidine derivatives **190a–p** (Scheme 69).[150]

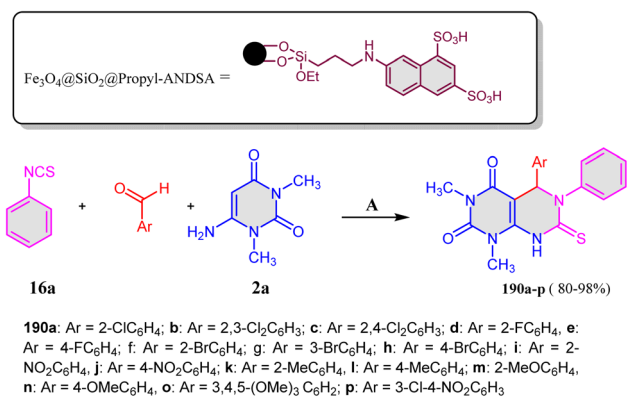

Scheme 69 One-pot multicomponent reaction for the synthesis of pyrimido[4,5-*d*]pyrimidines **190a–p**. Reagents and conditions: **A**; Fe_3O_4@SiO_2@Propyl-ANDSA, H_2O/reflux.

Abdollahi-Basir *et al.*[35] also synthesized a diversity of pyrimido[4,5-*d*]pyrimidine scaffolds **190a–i** *via* solvent free reaction between 6-aminouracils **2a,b**, aromatic aldehydes and isothiocyanate **16a**, and MIL-53(Fe) was employed as a catalyst at 110 °C (Scheme 70).

The suggested mechanism for the synthesis of **192** is shown in Scheme 71.[35] Initially, 6-aminouracil **2a** interacted *in situ* with phenyl isothiocyanate (**16a**) to produce intermediate **191**. Subsequently, with the MIL-53(Fe) present, intermediate **192** underwent a nucleophilic attack on the aldehyde to obtain intermediate **193**, which was converted into **194** *via* a hydrogen shift. After dehydration and intermolecular cyclization, the final product **190** was formed.[35]

The reaction conditions shown in Schemes 66–68 depict comparable conversion under various reaction conditions, which are summed together in Scheme 72. The reaction of aminouracil derivative **2** with aromatic aldehydes and phenyl isothiocyanate (**16a**), catalyzed by either **A**, **B**, or **C**, produced comparable products **190** in very good to excellent yields. Scheme 70 shows the same type of conversion under different reaction conditions. It is important to note that catalysis with catalyst **A** can be applied generally to various uracil derivatives **2**. In addition, methods employing catalysis by **A** perform methods **B** or **C** in the yields of the obtained products under the preceding conditions (Scheme 72).

A series of pyrimidopyrimidines **196a–o** were obtained in high yields (85–98%) *via* a multi component reaction between urea derivatives **195a,b** and substituted aromatic aldehydes, and 6-aminouracils **2**. The reaction was performed in EtOH at

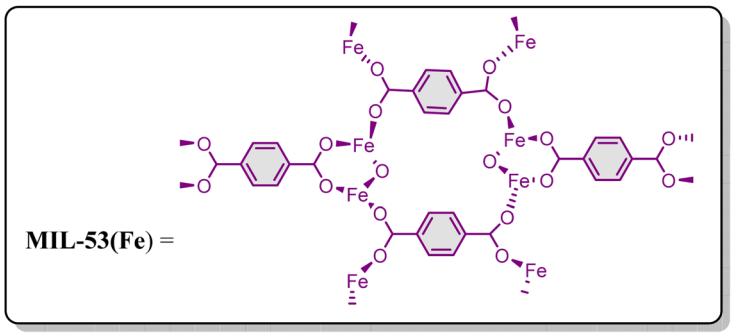

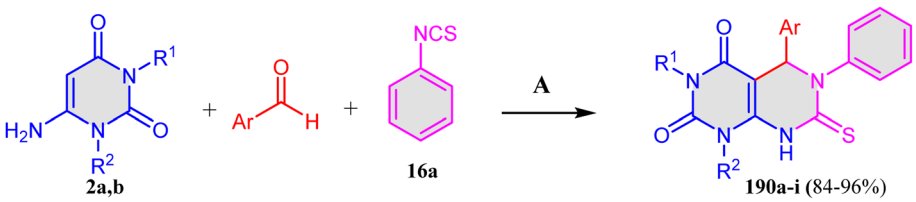

190a: R = H, Ar = Ph; **b**: R = Me, Ar = 4-FC_6H_4; **c**: R = Me, Ar = 4-BrC_6H_4; **d**: R = Me, Ar = 4-$O_2NC_6H_4$; **e**: R = Me, Ar = 4-MeC_6H_4; **f**: R = Me, Ar = 4-$MeOC_6H_4$; **g**: R = Me, Ar = 4-ClC_6H_4; **h**: R = Me, Ar = 2-ClC_6H_4; **i**: R = Me, Ar = 2-BrC_6H_4

Scheme 70 Synthesis of pyrimido[4,5-*d*]pyrimidine **190a–i**. Reagents and conditions: A; MIL-53(Fe), solvent free, 110 °C.

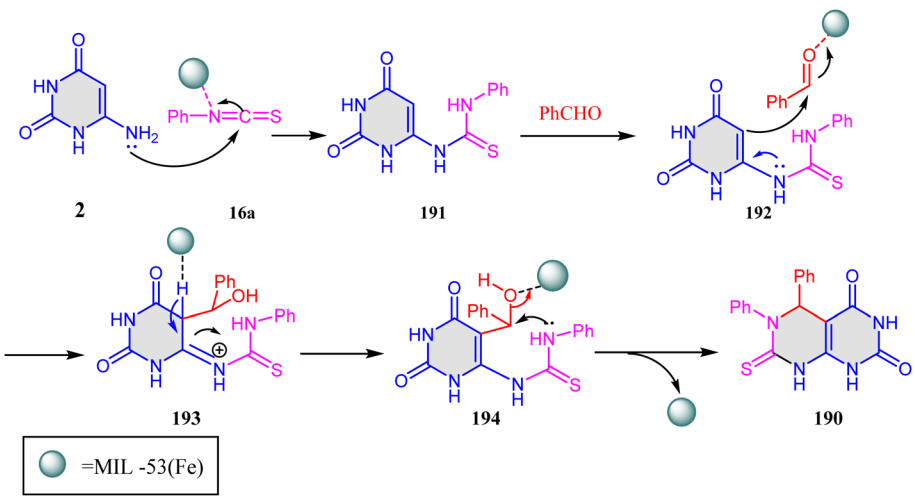

Scheme 71 Proposed mechanism for the synthesis of compounds **190a–i** catalyzed by MIL-53(Fe).

room temperature under ultrasound irradiation and catalyzed by TEDA-BAIL@UiO-66 (Scheme 73).[151]

The suggested mechanism for the formation of pyrimido[4,5-*d*]pyrimidine **196a–o** is shown in Scheme 74. The catalyst TEDA-BAIL@UiO-66 promoted the reaction as it acts as a Brønsted acid and enhances the aldehyde's carbonyl group's electrophilicity by releasing a proton. Next, Knoevenagel condensation between 6-aminouracil **2** and aromatic aldehydes afforded intermediate **197**, which was converted into alkene **198**. Following that, Michael's addition of urea or thiourea **195a,b** to alkene **198** led to the formation of intermediate **199**. A proton shift occurred to produce intermediate **200**. Finally, intermolecular cyclization of **200**, followed by the elimination of a molecule of NH_3, gave the final products **196a–o** (Scheme 74).[151]

2.2.7. Synthesis of pyrano-pyrimidine derivatives. Recently, in 2024, Das *et al.*[33] designed substituted chromeno[2,3-*d*]pyrimidine derivatives **202a–p** through the reaction between β-naphthol **201**, 6-amino-1,3-dimethyluracil (**2a**), and aromatic aldehydes in a deep eutectic solvent. The target compounds were produced in (75–94%) yields (Scheme 75). The suggested mechanism for the synthesis of compounds **202a–p** is depicted in Scheme 76. Initially, the reaction proceeded by activating an aldehyde in a three-component coupling reaction with DES,

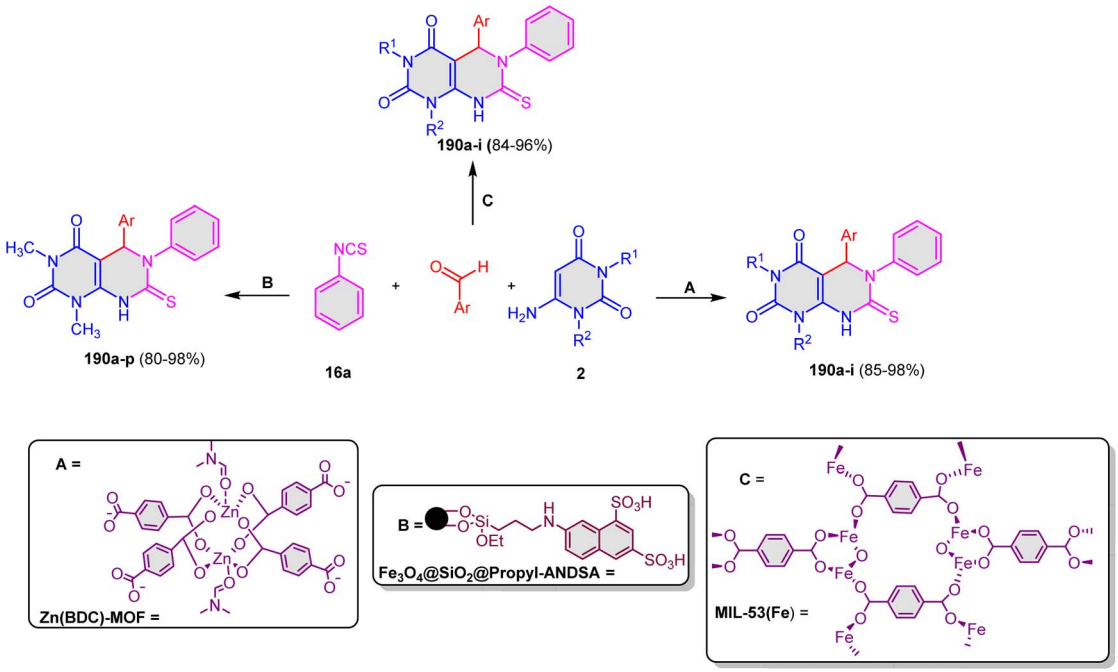

Scheme 72 Synthetic pathways for compound **190** under the conditions mentioned in Schemes 28–32, 34, 36, and 39.

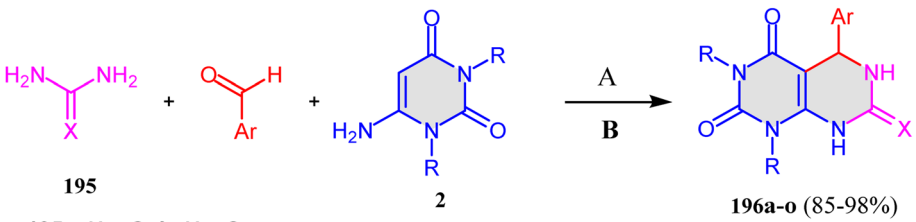

195a: X = O; **b**: X = S

196a: Ar = Ph, R = H, X = O; **b**: Ar = 4-BrC_6H_4, R = H, X = O; **c**: Ar = 4-ClC_6H_4, R = H, X = O; **d:** Ar = 4-$MeOC_6H_4$, R = H, X = O; **e**: Ar = 4-MeC_6H_4, R = H, X = O; **f**: Ar = 4-CNC_6H_4, R = H, X = O; **g**: Ar = 2,4-$Cl_2C_6H_4$, R = H, X = O; h: Ar = 2-OHC_6H_4, R = H, X = O; **i**: Ar = Ph, R = Me, X = O; **j**: Ar = 4-BrC_6H_4, R = Me, X = O; **k**: Ar = 4-ClC_6H_4, R = Me, X = O; **l**: Ar = 4-$MeOC_6H_4$, R = Me, X = O; **m**: Ar = 4-MeC_6H_4, R = Me, X = O; **n**: Ar = 4-FC_6H_4, R = Me, X = O; **o**: Ar = 4-$NO_2C_6H_4$, R = Me, X = S

Scheme 73 Ultrasound irradiation synthesis of pyrimidopyrimidines **196a–o**. Reagents and conditions: **A**; BAIL@UiO-66, EtOH/r.t, US irradiation.

which increased the aldehydic functional group's electrophilicity. After that, a regioselective nucleophilic interaction between the pi bond of β-naphthol **201** and the activated aldehyde resulted in the creation of a conjectured intermediate **203**. The highly reactive *o*-quinone methide intermediate (**B′**) was subsequently formed as a result of further dehydration of this intermediate (Scheme 76). **B′** is a good hetero-diene for [4 + 2] because of its prolonged conjugation and electron-deficient exocyclic olefinic activity reactions of cycloaddition. After that, intermediate **B′** was effectively captured by 6-amino-1,3-dimethyl uracil **2b** by a formal [4 + 2] process of hetero-cycloannulation, causing the production of intermediate **204**. Finally, the final products **202a–p** were obtained *via* DES-mediated deamination of intermediate **204**, releasing the active DES for the next catalytic cycle.[33]

The formed products **202a–p** exhibit a promising anti-proliferative activity against cancer cell lines. Therefore, with moderate to good IC_{50} values, it shows promise as a possible anticancer treatment candidate for hepatocellular and breast cancer. Compound **202m** (4-OH-3-MeO-Ph) and **202l** (3-OH-4-MeO-Ph) displayed significant inhibitory effects, with IC_{50} values of 31.38 and 28.21 mM against MCF7 cells, respectively. However, other derivatives such as phenyl, tolyl, and trifluoromethylphenyl exhibited approximately 5-fold less efficacy compared to compound **202m** and compound **202l**. Compounds **202a–n** were also screened against HepG2; compound **202m** also showcased commendable cytotoxic activity against HepG2, with an IC_{50} value of 46.39 mM. Compound **202f** (X = H, Y = 4-OH) displayed moderate cytotoxicity with an IC_{50} value of 64.79 mM against MCF7. Moreover,

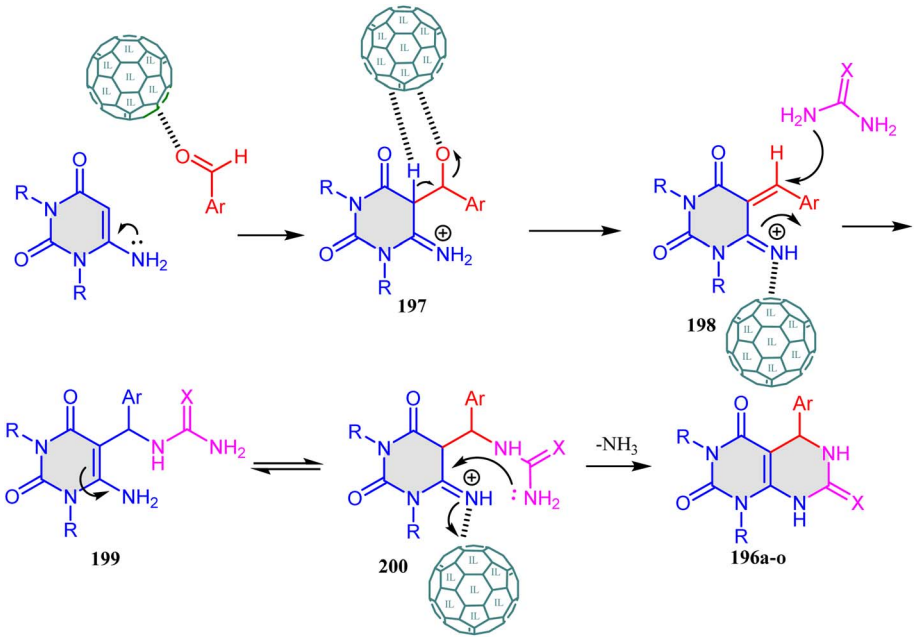

Scheme 74 Suggested mechanism for the synthesis of **196a–o**.

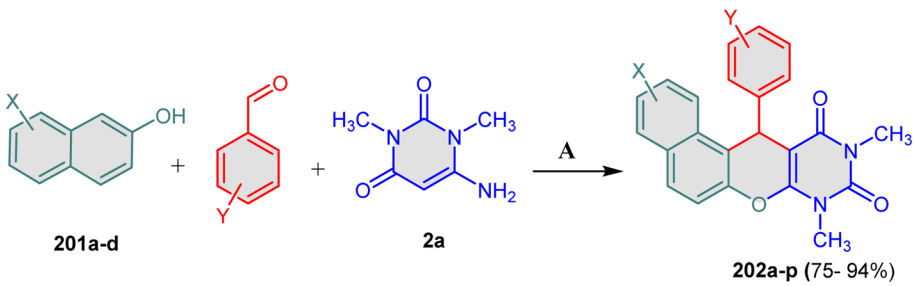

202a-p: **a:** X= H, Y= 2-Cl; **b:** X= H, Y= 4-F; **c:** X = H, Y= 4-CH_3O; **d:** X=H, Y= 4-CH_3; **e:** X = H, Y = 4-OH; **f:** X = H, Y= 2-OH; **g:** X = H, Y = 4-NO_2 ; **h:** X = H, Y= 3-NO_2 ; **i:** X = H, Y= 2-NO_2; **j:** X = H, Y = 4-F_3C, **k:** X = H, Y= 4-OH-3-CH_3O; **l:** X = H, Y= 4-OH-3-CH_3O; **m:** X = H, Y = 3-OH-4-CH_3O; **n:** X = 6-Br, Y= 4-Cl; **o:** X=6-CN, Y= 4-Cl; **p:** X=7-OCH_3, Y= 4-Cl

Scheme 75 Formation of chromeno[2,3-*d*]pyrimidines **202a–p**. Reagents and conditions: A = ChCl : α-CAA (1 : 1), 90 °C, 2 h.

compounds **202n** (X = Y = H), **202l**, and **202e** (X = H, Y = 4-Me) displayed relatively low toxicity, presenting IC_{50} values of 91.06, 88.53, and 91.05 mM against HepG2 cell lines, respectively.[33]

2.2.8. Synthesis of phenazines and pteridine derivatives. Jamaledini *et al.*[34] synthesized phenazine compounds containing 6-aminouracil moieties through a multi step reaction. At the beginning, 6-aminouracils **2** reacted with naphthalene-1,2-dione **205** in DMSO at 70 °C to form compounds **206a,b** in 85–92% yields. Following that, a condensation reaction between compound **206a,b** and *o*-phenylenediamine **207a–d** derivatives in $CHCl_3$ for 1 h afforded the target compounds of phenazine **208** in excellent yields (95–98%) (Scheme 77).

The reaction of 5,6-diamnouracils **49a–e** with 2,7-dibromo-9*H*-fluoren-9-one (**209**) in DMF for 20 min gave spiro compounds **211a–e** in 59–68% yields (Scheme 78).[152] On the other hand, **49** reacted with an acenaphthoquinone (**210**) in AcOH for 6 h to afford acenaphtho[1,2-*g*]pteridines **212a–f** in yields 60–71% (Scheme 78).[152] Most of the compounds displayed significant antiproliferative activity on the tested cell lines (Tables 26 and 27). Compounds **211a**, **211e**, and **212e** of scaffolds based on pteridine and purines were identified as the most potent hits in anti-proliferative screening, with GI50 values of 38 nM, 46 nM, and 44 nM, respectively. Compounds **211a**, **211e**, and **212e** showed promising EGFR inhibitory activity, with IC_{50} values of 87 nM, 98 nM, and 92 nM, respectively, when compared to erlotinib's IC_{50} value of 80 nM. According to the results, compound **211a** (R = Me, X = O) has the most potent anti-proliferative activity and is determined to be the most effective EGFR suppressor, with an IC_{50} value of 87 ± 07 nM, which is equal to erlotinib (IC_{50} = 80 nM).

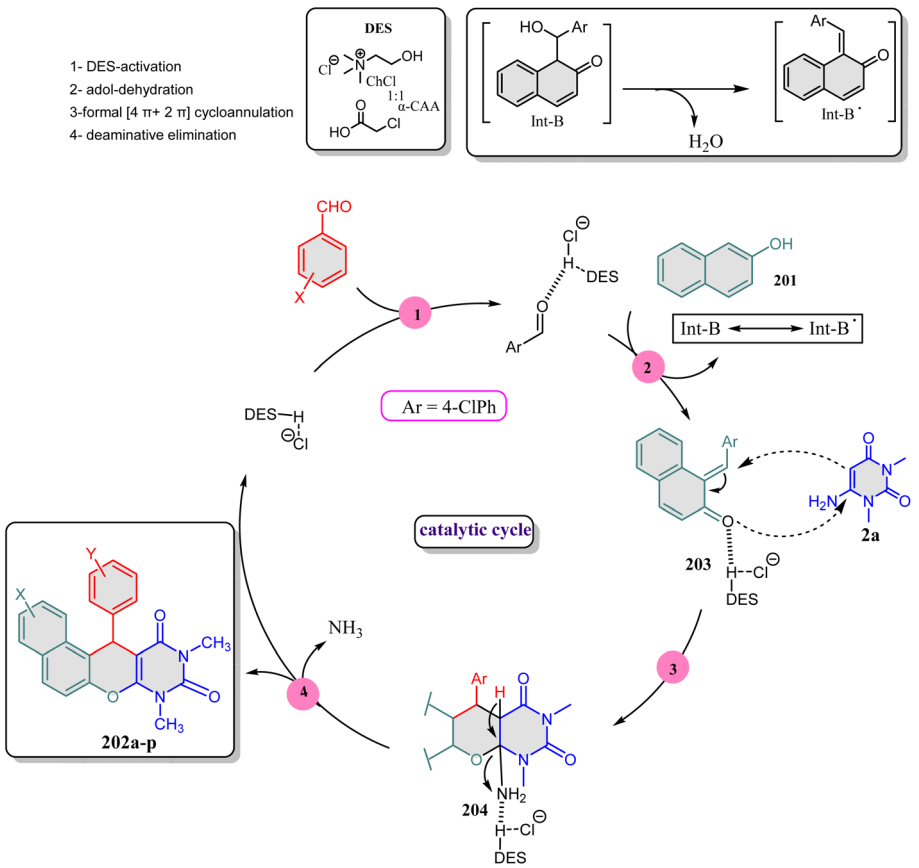

Scheme 76 Reaction mechanism for the synthesis of chromeno[2,3-*d*]pyrimidines **202a–p**.

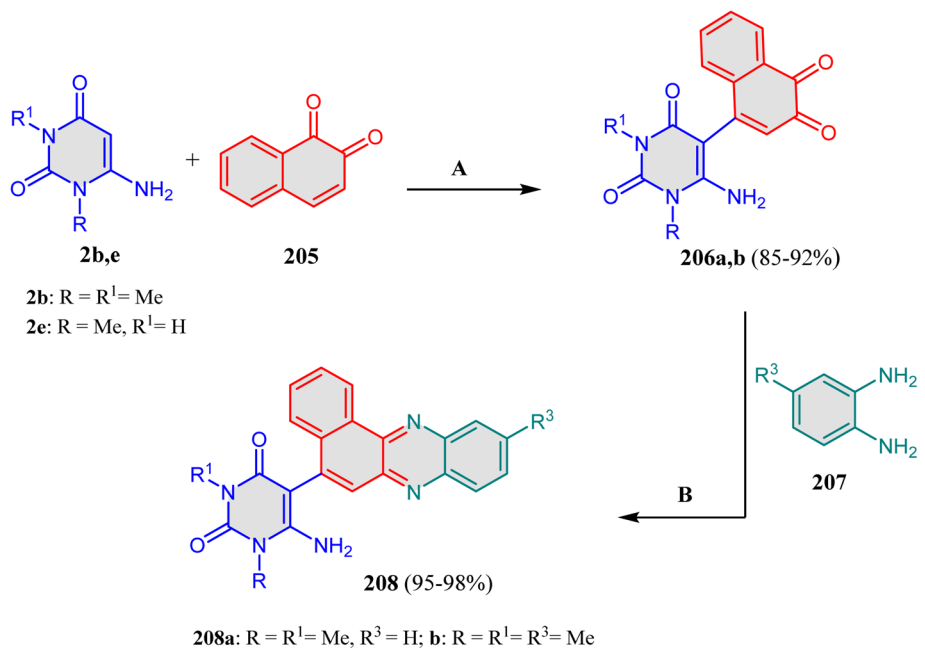

Scheme 77 Synthesis of phenazine scaffold **208**. Reagents and conditions: **A**; DMSO, 70 °C. **B**; $CHCl_3$, reflux, 1 h.

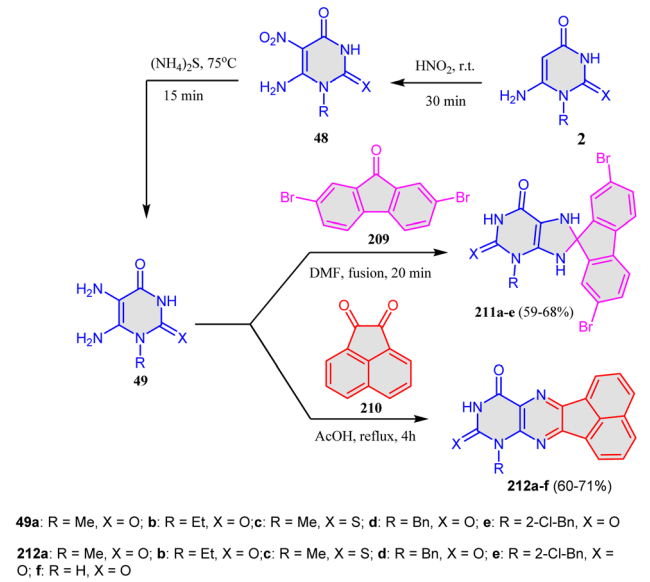

Scheme 78 Reaction of 5,6-diaminouracils **49** with 2,7-dibromo-9*H*-fluoren-9-one (**209**) and acenaphthoquinone **210**.

The mechanism describes the reaction of **49** with **209**, as shown in Scheme 79.[151] The reaction started with the nucleophilic attack of the amino group of diaminouracil **49** to the carbonyl group of 2,7-dibromo-9*H*-fluoren-9-one (**209**), adduct **213** was then produced, which lost a molecule of water to give adduct **214**. An intermediate **214** then underwent intramolecular aza-Michael addition, leading to the production of compounds **211a–e.**[152]

2.2.8.1 Structure activity relationship. According to the data presented in Tables 26 and 27, it was concluded that in the case of a replacement of the oxygen atom with a sulfur atom in compound **211c** (R = Me, X = S), the antiproliferative activity decreased compared to compound **211a**, indicating that the oxygen atom at position 2 is important owing to its antiproliferative properties. The results also imply that the antiproliferative activity of compound **211** is significantly influenced by the kind of third-position substitution, with activity rising in the following order: methyl > 2-chlorobenzyl > benzyl > ethyl. Correspondingly, pteridine derivatives **212a–f** demonstrated a moderate antiproliferative effect. Compound **212e** (R = 2-chlorobenzyl, X = O) was the most effective compound in this series against the screened cell lines, but it was 1.3 times less effective than the standard "erlotinib".

Table 27 IC_{50} values of compounds **211a**, **211d**, **211e**, **212a**, and **212e** against EGFR and $BRAF^{V600E}$

Compd	EGFR inhibition $IC_{50} \pm$ SEM (nM)	$BRAF^{V600E}$ inhibition $IC_{50} \pm$ SEM (nM)
211a	87 ± 07	92 ± 07
211d	105 ± 09	164 ± 15
211e	98 ± 08	137 ± 12
212a	112 ± 10	183 ± 17
212e	92 ± 07	109 ± 09
Erlotinib	80 ± 05	60 ± 05

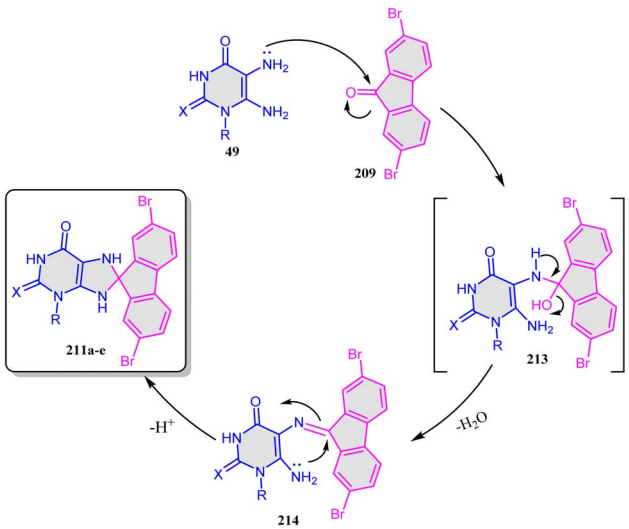

Scheme 79 Proposed mechanism for the synthesis of **211a–e**.

Table 26 IC_{50} values of compounds **211a–e** and **212a–f**

Compd	R	X	Cell viability%	Anti-proliferative activity $IC_{50} \pm$ SEM (nM)				
				A-549	MCF-7	Panc-1	HT-29	Average (GI_{50})
211a	Me	O	89	36 ± 3	40 ± 3	38 ± 3	38 ± 3	38
211b	Et	O	91	85 ± 8	88 ± 8	86 ± 8	86 ± 8	86
211c	Me	S	90	98 ± 9	103 ± 10	100 ± 9	102 ± 10	101
211d	Bn	O	91	52 ± 5	55 ± 5	54 ± 5	52 ± 5	53
211e	2-Cl-Bn	O	89	44 ± 4	48 ± 4	46 ± 4	46 ± 4	46
212a	Me	O	92	56 ± 5	60 ± 6	58 ± 5	58 ± 5	58
212b	Et	O	90	64 ± 6	69 ± 6	66 ± 6	68 ± 6	67
212c	Me	S	89	80 ± 8	83 ± 8	80 ± 8	80 ± 8	81
212d	Bn	O	91	90 ± 9	96 ± 9	90 ± 9	92 ± 9	92
212e	2-Cl-Bn	O	88	41 ± 4	46 ± 4	44 ± 4	44 ± 4	44
212f	H	O	90	76 ± 7	79 ± 7	75 ± 7	75 ± 7	76
Erlotinib	—	—	ND	30 ± 3	40 ± 3	30 ± 3	30 ± 3	33

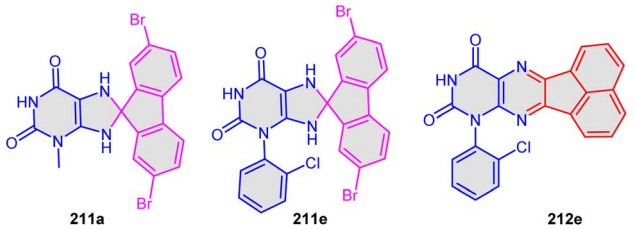

Fig. 14 Structures of the most anti-proliferative pteridine and purine molecules.

However, compound **212e** was similar to its analog **211e**, and compound **212a** (R = Me, X = O) was 1.5 times less effective than its analog **211a** (R = Me, X = O) and showed mild anti-proliferative effects. Moreover, antiproliferative activity decreased when a sulfur atom was substituted for the oxygen atom, as in compound **212c** (R = Me, X = S). Compounds **212d** (R = benzyl, X = O) and **212e** (R = 2-chlorobenzyl, X = O), in which the methyl group in **212a** was replaced by a benzyl and 2-chlorobenzyl moiety, respectively, demonstrated a significant difference in anti-proliferative activity. Compound **212d** demonstrated a marked decrease in anti-proliferative activity, being 1.5-fold less effective than **212a**, whereas **212e** outperformed **212a** in activity. Fig. 14 shows the structure of the most anti-proliferative pteridine and purine molecules.

2.2.8.2 Synthesis of pyridotriazolothiazolopyridopyrimidine. The reaction of 3-amino-2-formyl-8-(4-methoxyphenyl)-6-oxo-9,9*a*-dihydro-6*H*-thiazolo-[3′,2′:2,3][1,2,4]triazolo[1,5-*a*] pyridine-7,9-dicarbonitrile (**215**) with 6-aminouracil (**2a**) in DMF containing DBU at reflux temperature for 30 min yielded compound **216** in 76% yield (Scheme 80). The obtained compound pyridotriazolothiazolopyridopyrimidine **216** was screened for antimicrobial activity and revealed high efficiency against yeast fungus and Gram-negative bacteria.[153]

2.2.9. Synthesis of pyrimidine/isoindoline-1,3-diones. Very recently, in 2025, Shehta *et al.*[154] developed a multi-step reaction for the synthesis of pyrimidine/isoindoline hybrids. First, they prepared 2,6-dichloropyrimidin-4-amine **217** by treating 6-aminouracil **2a** with $POCl_3$. Next, they reacted isoindoline-1,3-dione with **218** in EtOH to give compound **219**, which reacted with different aromatic aldehydes to obtain the corresponding Schiff bases **220a–f**. However, when compound **219** was treated with hydrazine hydrate, the reaction proceeded to give 2-(6-amino-2-hydrazineylpyrimidin-4-yl)isoindoline-1,3-dione (**221**), which

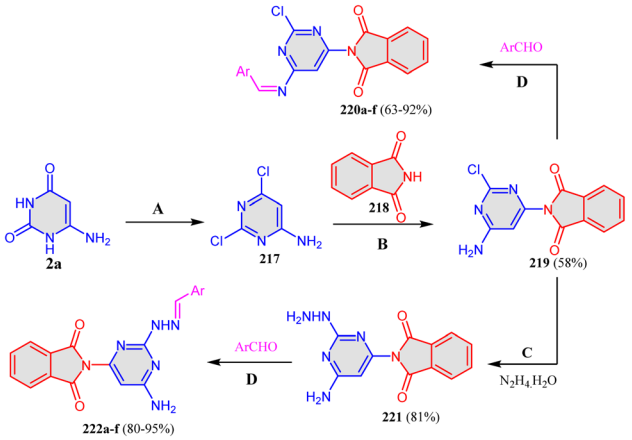

220a: Ar = 3-$NO_2C_6H_4$; **b**: Ar = 4-$NO_2C_6H_4$; **c**: Ar = 4-ClC_6H_4; **d**: Ar = 3,4-$(OMe)_2C_6H_3$; **e**: Ar = 2-OHC_6H_4; **f**: Ar = 3-OHC_6H_4
222a: Ar = 3-$NO_2C_6H_4$; **b**: Ar = 4-$NO_2C_6H_4$; **c**: Ar = 4-ClC_6H_4; **d**: Ar = 3,4-$(OMe)_2C_6H_3$; **e**: Ar = 2-OHC_6H_4; **f**: Ar = 4-$N(Me)_2C_6H_4$

Scheme 81 Synthesis of Schiff bases **220a–f** and **222a–f**. Reagents and conditions: **A**; $POCl_3$. **B**; EtOH, pip. **C**; EtOH, Et_3N, 9 h, rt. **D**; EtOH, Et_3N, 6 h, rt.

Table 28 Antitubercular activity of **220a–f** and **222a–f**

		M. tuberculosis MIC (μg mL^{-1})		
Compd	R	Sensitive	MDR	XDR
220a	3-NO_2	0.98	7.81	15.63
220b	NO	7.81	31.25	NA
220c	Cl	31.25	NA	NA
220d	3,4-$(OMe)_2$	31.25	125	NA
220e	OH	3.9	7.81	31.25
220f	OH	3.9	7.81	31.25
222a	NO_2	7.81	31.25	NA
222b	NO_2	15.63	62.5	31.25
222c	Cl	62.5	NA	NA
222d	OH	125	NA	NA
222e	OH	125	NA	NA
222f	4-NMe_2	0.48	1.95	7.81
Isoniazid		0.12	IA	NA

was allowed to react with different aromatic aldehydes to obtain 2-(6-amino-2-(2-(arylmethylene)hydrazineyl)pyrimidin-4-yl) isoindoline-1,3-dione **222a–f** (Scheme 81). The authors screened the synthesized compounds **222a–f** and **222a–f** as potential

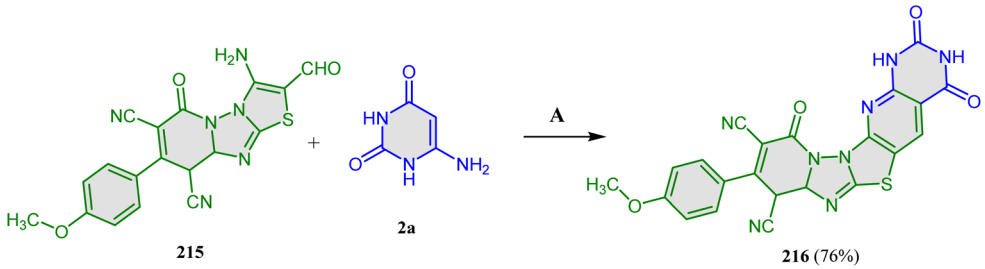

Scheme 80 Synthesis of pyridotriazolothiazolopyridopyrimidine **216**. Reagents and conditions: **A**; DMF/DBU, reflux, 30 min.

Table 29 *In vitro M. tuberculosis* enoyl-acyl carrier protein reductase inhibitory activity of **222f**, **220a**, and isoniazid

Compd	InhA IC_{50} (mean ± SD) (μM)
220a	1.646 ± 0.069
222f	0.717 ± 0.033
Isoniazid	0.323 ± 0.014

antitubercular agents against multi-drug-resistant (MDR) and extra-drug-resistant (XDR). Compounds **220b–d**, **222a**, and **222c–e** were inactive against *M. tuberculosis*. Moreover, compounds **220a** (Ar = 3-NO_2Ph), **220e** (Ar = 2-OH-Ph), **220f** (Ar = 3-OH-Ph), and **222b** (Ar = 4-NO_2-Ph) showed moderate activity (MIC 15.63–31.25 μg mL^{-1}) compared to the reference drug. Compounds **220a** and **222f** (Ar = 4-$N(Me)_2$Ph) displayed inhibition of MDR strain with MIC values equal 7.81 and 1.95 μg mL^{-1} and for XRD 15.63 and 7.81 μg mL^{-1}, respectively. However, compounds **220a** and **222f** inhibited the mycobacterial InhA enzyme with $IC_{50} = 1.64 \pm 0.069$ and 0.717 ± 0.033 μM (Tables 28 and 29), respectively, in comparison with isoniazid (INH) with $IC_{50} = 0.323 \pm 0.014$ μM, as a standard drug.

3 Conclusion

Due to the biological activity of 5-amino uracil, 6-aminouracil and their derived heterocycles, their synthesis has attracted a great interest in the field of medicinal chemistry. This study includes different methods reported for synthesizing the target molecules in the past 10 years, especially from 2014 to 2024. We also reported on the advantages of catalysis in synthesizing the target compounds using a multi-component reaction (MCR) sequence. Accordingly, we here shed light on the utility of catalysis in MCRs, which would provide the target molecules with excellent yields in addition to short reaction time, cost efficiency, and a simple workup procedure without extra purification techniques. This review also focused on the biological applications of the target molecules since they covered many biological activities, such as anti-cancer, anti-microbial, anti-inflammatory, anti-Alzheimer, and/or anti-tubercular agents.

Due to the therapeutic importance of heterocycles from 5-amino and 6-aminouracils, their synthesis has become valuable in the synthesis of numerous drugs. The synthesis of the former compounds has become more facile due to the utility of various eco-friendly catalysts in multicomponent reactions. Moreover, mild reaction conditions, good to excellent yields, and the absence of tedious separation procedures are the key advantages of their synthesis. The latter would encourage researchers to synthesize former heterocycles, which would lead to interesting biological applications.

Author contributions

A. A. A. (supervision, conceptualization, writing, editing, and submitting), E. M. O. (writing, editing), S. M. M. (supervision, editing), T. M. B. (supervision, editing), M. A. (editing), K. U. S. (editing), A. H. M. (supervision, editing), all authors have read and agreed to the published version of the manuscript.

Conflicts of interest

The authors declare no conflict of interest.

Data availability

There are no data generated.

Acknowledgements

This paper is based upon work supported by the Science, Technology & Innovation Funding Authority (STDF) under research project number 48275.

References

1 G. L. Patrick, *An Introduction to Medicinal Chemistry*, Oxford university press, 2023.
2 O. Michalak, M. Cybulski, M. Kubiszewski, N. Finiuk, Y. Kozak, D. Milenkovic, S. Żurawicka, P. Roszczenko, A. Bielawska and B. Trzaskowski, *Sci. Rep.*, 2025, **15**, 28803.
3 D. J. Brown, R. F. Evans, W. B. Cowden, M. D. Fenn, *Chemistry of Heterocyclic Compounds: The Pyrimidines*, 1994, vol. 52, DOI: **10.1002/9780470187395**.
4 W. B. Parker, *Chem. Rev.*, 2009, **109**, 2880–2893.
5 A. Pałasz and D. Cież, *Eur. J. Med. Chem.*, 2015, **97**, 582–611.
6 M. N. Khurshid, F. H. Jumaa and S. S. Jassim, *Mater. Today: Proc.*, 2022, **49**, 3630–3639.
7 S. A. El-Kalyoubi, E. S. Taher, T. S. Ibrahim, M. F. El-Behairy and A. M. M. Al-Mahmoudy, *Pharmaceuticals*, 2022, **15**, 494.
8 G. M. Ziarani and N. H. Nasab, *RSC Adv.*, 2016, **6**, 38827–38848.
9 N. H. Metwally, G. H. Elgemeie and F. G. Fahmy, *ACS Omega*, 2023, **8**, 36636–36654.
10 A. Arkan Majhool, M. Yakdhan Saleh, A. K. Obaid Aldulaimi, S. Mahmood Saeed, S. M. Hassan, M. F. El-Shehry, S. Mohamed Awad and S. S. Syed Abdul Azziz, *Chem. Rev. Lett.*, 2023, **6**, 442–448.
11 M. Sanduja, J. Gupta and T. Virmani, *J. Appl. Pharm. Sci.*, 2020, **10**, 129–146.
12 S. El-Kalyoubi, F. Agili, W. A. Zordok and A. S. A. El-Sayed, *Int. J. Mol. Sci.*, 2021, **22**, 10979.
13 V. A. Kezin, E. S. Matyugina, M. S. Novikov, A. O. Chizhov, R. Snoeck, G. Andrei, S. N. Kochetkov and A. L. Khandazhinskaya, *Molecules*, 2022, **27**, 2866.
14 O. Nesterova, D. Babaskin, Y. Tikhonova, N. Molodozhnikova and S. Kondrashev, *Res. J. Pharm. Technol.*, 2021, **14**, 2723–2728.
15 L. R. Yakupova and R. L. Safiullin, *Kinet. Catal.*, 2021, **62**, 49–55.
16 M. Alhilal, Y. A. M. Sulaiman, S. Alhilal, S. M. Gomha and S. A. Ouf, *Polycyclic Aromat. Compd.*, 2022, **42**, 6463–6474.
17 S. Mal and S. Das, *ChemistrySelect*, 2023, **8**, e202302146.

18 M. T. M. Sarg and S. S. El-Shaer, *Open J. Med. Chem.*, 2014, **4**, 39–60.
19 A. H. Poslu, Ş. E. Aslan, G. Koz, E. Senturk, Ö. Koz, M. Senturk, A. Nalbantsoy, A. Öztekin and D. Ekinci, *Arch. Pharm.*, 2024, **357**, 2300374.
20 H.-H. Guan, Y.-H. Huang, E.-S. Lin, C.-J. Chen and C.-Y. Huang, *Biochem. Biophys. Res. Commun.*, 2021, **551**, 33–37.
21 Z. Bulut, N. Abul, A. H. Poslu, İ. Gülçin, A. Ece, E. Erçağ, Ö. Koz and G. Koz, *J. Mol. Struct.*, 2023, **1280**, 135047.
22 M. S. Novikov, R. W. Buckheit Jr, K. Temburnikar, A. L. Khandazhinskaya, A. V Ivanov and K. L. Seley-Radtke, *Bioorg. Med. Chem.*, 2010, **18**, 8310–8314.
23 M. Friedland and D. W. Visser, *Biochim. Biophys. Acta*, 1961, **51**, 148–152.
24 M. Gütschow, T. Hecker, A. Thiele, S. Hauschildt and K. Eger, *Bioorg. Med. Chem.*, 2001, **9**, 1059–1065.
25 S. Zomorodbakhsh, B. Mirza, S. Yazdizadeh and E. Tavahodi, *Orient. J. chem*, 2014, **30**, 1379–1383.
26 R. Sariri and G. Khalili, *Russ. J. Org. Chem.*, 2002, **38**, 1053–1055.
27 I. Devi and P. J. Bhuyan, *Tetrahedron Lett.*, 2005, **46**, 5727–5729.
28 J. Jiang, L. H. Sigua, A. Chan, P. Kalra, W. C. K. Pomerantz, E. Schönbrunn, J. Qi and G. I. Georg, *ChemMedChem*, 2022, **17**, e202100407.
29 M. S. Alphey, L. Pirrie, L. S. Torrie, W. A. Boulkeroua, M. Gardiner, A. Sarkar, M. Maringer, W. Oehlmann, R. Brenk and M. S. Scherman, *ACS Chem. Biol.*, 2013, **8**, 387–396.
30 X. Cui, J.-J. Lin, S. Wang, J.-P. Li, X.-S. Xia and C. Huang, *Tetrahedron Lett.*, 2022, **89**, 153603.
31 M. Hisham, B. G. M. Youssif, E. E. A. Osman, A. M. Hayallah and M. Abdel-Aziz, *Eur. J. Med. Chem.*, 2019, **176**, 117–128.
32 X. Yang, J. P. D. van Veldhoven, J. Offringa, B. J. Kuiper, E. B. Lenselink, L. H. Heitman, D. van der Es and A. P. IJzerman, *J. Med. Chem.*, 2019, **62**, 3539–3552.
33 A. Das, S. Dey, R. N. Yadav, P. Dutta, S. Dhiman, P. J. Boruah, K. Sarkar, A. Sahu, A. Jana, A. K. Paul and M. F. Hossain, *New J. Chem.*, 2024, **48**, 7566–7578.
34 A. Jamaledini, M. R. Mohammadizadeh and S. H. Mousavi, *Monatsh. Chem.*, 2018, **149**, 1421–1428.
35 M. H. Abdollahi-Basir, F. Shirini, H. Tajik and M. A. Ghasemzadeh, *J. Mol. Struct.*, 2019, **1197**, 318–325.
36 A. Y. Aksinenko, T. V Goreva, T. A. Epishina, S. V Trepalin and V. B. Sokolov, *J. Fluor. Chem.*, 2016, **188**, 191–195.
37 A. B. Mahardhika, M. Załuski, C. T. Schoeder, N. M. Boshta, J. Schabikowski, F. Perri, D. Łażewska, A. Neumann, S. Kremers, A. Oneto, A. Ressemann, G. Latacz, V. Namasivayam, K. Kieć-Kononowicz and C. E. Müller, *J. Med. Chem.*, 2024, **67**, 9896–9926.
38 J. Yoon, W.-I. Choi, S. Parameswaran, G. Bin Lee, B. W. Choi, P. Kim, D.-S. Shin, H. N. Jeong, S. M. Lee, C. J. Oh, J.-H. Jeon, I.-K. Lee, M. A. Bae, H. Kim and J. H. Ahn, *Bioorg. Med. Chem. Lett.*, 2023, **94**, 129461.
39 H. S. Awes, A. L. El-Ansary, S. A. Abdel-Latif, S. Abdel-Khalik and S. M. Abbas, *J. Mol. Struct.*, 2025, **1325**, 140993.
40 N. B. Nandi, S. Roy, S. Ghanta, M. Mahanta, P. Dutta, J. Kłak, L. Sieroń, W. Maniukiewicz and T. K. Misra, *J. Mol. Struct.*, 2024, **1309**, 138215.
41 N. B. Nandi, A. Purkayastha, S. Roy, J. Kłak, R. Ganguly, I. Alkorta and T. K. Misra, *New J. Chem.*, 2021, **45**, 2742–2753.
42 Y. I. Murinov, V. Y. Mishinkin, O. V Akchurina, S. A. Grabovskii and N. N. Kabal'nova, *Russ. J. Gen. Chem.*, 2017, **87**, 1667–1674.
43 S. Singh, R. Singh, A. K. Singh, M. Yadav, S. K. Mishra, J. Dixit, P. Verma, K. N. Tiwari and K. K. Upadhyay, *Inorg. Chim. Acta*, 2024, **560**, 121812.
44 P. Rani, S. Chahal, R. Kumar, Mayank, P. Kumar, A. Negi, R. Singh, S. Kumar, R. Kataria, G. Joshi and J. Sindhu, *Bioorg. Chem.*, 2023, **138**, 106660.
45 B. S. Saikia, P. J. Borpatra, I. Rahman, M. L. Deb and P. K. Baruah, *New J. Chem.*, 2022, **46**, 16523–16529.
46 A. Arman, N. Nowrouzi and M. Abbasi, *Tetrahedron Lett.*, 2024, **151**, 155320.
47 D. Ali, A. K. Panday and L. H. Choudhury, *J. Org. Chem.*, 2020, **85**, 13610–13620.
48 B. Kumar, M. Sugunakara Rao, P. Kumar, S. Hussain and S. Das, *J. Mol. Struct.*, 2020, **1221**, 128827.
49 Z. M. Nofal, H. H. Fahmy, E. S. Zarea and W. El-Eraky, *Acta Pol. Pharm.*, 2011, **68**, 507–517.
50 Z. Hussain, M. A. Ibrahim, N. M. El-Gohary and A.-S. Badran, *J. Mol. Struct.*, 2022, **1269**, 133870.
51 S. Momeni and R. Ghorbani-Vaghei, *Heliyon*, 2025, **11**, e41149.
52 M. Verma, A. Thakur, S. Kapil, R. Sharma, A. Sharma and R. Bharti, *Mol. Diversity*, 2023, **27**, 889–900.
53 N. Lotfifar, A. Zare and G. Rezanejade Bardajee, *Org. Prep. Proced. Int.*, 2021, **53**, 379–386.
54 A. Zare, N. Lotfifar and M. Dianat, *J. Mol. Struct.*, 2020, **1211**, 128030.
55 A. H. Mohamed and R. M. Shaker, *J. Heterocycl. Chem.*, 2019, **56**, 2099–2104.
56 S. Pandey, A. Kamal, A. Kumar Kushwaha and S. Singh, *Asian J. Org. Chem.*, 2024, e202400409.
57 T. B. Johnson and D. A. Hahn, *Chem. Rev.*, 1933, **13**, 193–303.
58 T. B. Johnson and I. Matsuo, *J. Am. Chem. Soc.*, 1919, **41**, 782–789.
59 M. T. Bogert and D. Davidson, *J. Am. Chem. Soc.*, 1933, **55**, 1667–1668.
60 M. Roberts and D. W. Visser, *J. Am. Chem. Soc.*, 1952, **74**, 668–669.
61 V. A. Kezin, E. S. Matyugina, M. S. Novikov, A. O. Chizhov, R. Snoeck, G. Andrei, S. N. Kochetkov and A. L. Khandazhinskaya, *Molecules*, 2022, **27**(9), 2866.
62 J. W. Chern, D. S. Wise, W. Butler and L. B. Townsend, *J. Org. Chem.*, 1988, **53**, 5622–5628.
63 I. Wempen, I. L. Doerr, L. Kaplan and J. J. Fox, *J. Am. Chem. Soc.*, 1960, **82**, 1624–1629.
64 M. B. Alshammari, A. A. Aly, B. G. M. Youssif, S. Bräse, A. Ahmad, A. B. Brown, M. A. A. Ibrahim and A. H. Mohamed, *Front. Chem.*, 2022, **10**, 1076383.

65 E.-S. Lin, R.-H. Luo, Y.-C. Yang and C.-Y. Huang, *Bioinorg. Chem. Appl.*, 2022, **2022**, 1817745.
66 A. M. Fahim, E. H. I. Ismael, G. H. Elsayed and A. M. Farag, *J. Biomol. Struct. Dyn.*, 2022, **40**, 9177–9193.
67 S. Philip, D. R. Sherin, T. K. M. Kumar, T. C. Badisha Banu and R. M. Roy, *Mol. Diversity*, 2024, **28**, 1459–1469.
68 R. M. Shaker, M. A. Elrady and K. U. Sadek, *Mol. Diversity*, 2016, **20**, 153–183.
69 A. M. Fahim, M. A. Shalaby and M. A. Ibrahim, *J. Mol. Struct.*, 2019, **1194**, 211–226.
70 A. A. Aly, M. B. Alshammari, A. Ahmad, H. A. M. Gomaa, B. G. M. Youssif, S. Bräse, M. A. A. Ibrahim and A. H. Mohamed, *Arab. J. Chem.*, 2023, **16**, 104612.
71 J. Nowdehi, E. Mosaddegh, S. Khaksar, M. Torkzadeh-Mahani, M. Beihaghi and M. Yazdani, *J. Biomol. Struct. Dyn.*, 2024, 1–19.
72 J. Quiroga, P. E. Romo, A. Ortiz, J. H. Isaza, B. Insuasty, R. Abonia, M. Nogueras and J. Cobo, *J. Mol. Struct.*, 2016, **1120**, 294–301.
73 N. Tolstoluzhsky, P. Nikolaienko, N. Gorobets, E. V Van der Eycken and N. Kolos, *Eur. J. Org. Chem.*, 2013, **2013**, 5364–5369.
74 P. Sharma, N. Rane and V. K. Gurram, *Bioorg. Med. Chem. Lett.*, 2004, **14**, 4185–4190.
75 S. R. Kanth, G. V. Reddy, K. H. Kishore, P. S. Rao, B. Narsaiah and U. S. N. Murthy, *Eur. J. Med. Chem.*, 2006, **41**, 1011–1016.
76 V. S. V Satyanarayana, P. Sreevani, A. Sivakumar and V. Vijayakumar, *Arkivoc*, 2008, **17**, 221–233.
77 A. K. Srivastava, R. Sharma, R. Mishra, A. K. Balapure, P. S. R. Murthy and G. Panda, *Bioorg. Med. Chem.*, 2006, **14**, 1497–1505.
78 J. A. Valderrama, P. Colonelli, D. Vásquez, M. F. González, J. A. Rodríguez and C. Theoduloz, *Bioorg. Med. Chem.*, 2008, **16**, 10172–10181.
79 S. El-Kalyoubi, F. Agili, I. Adel and M. A. Tantawy, *Arab. J. Chem.*, 2022, **15**(4), 103669.
80 J. G. Tangmouo, A. L. Meli, J. Komguem, V. Kuete, F. N. Ngounou, D. Lontsi, V. P. Beng, M. I. Choudhary and B. L. Sondengam, *Tetrahedron Lett.*, 2006, **47**, 3067–3070.
81 K. M. Abu-Zied, T. K. Mohamed, O. K. Al-Duiaj and M. E. A. Zaki, *Heterocycl. Commun.*, 2014, **20**, 93–102.
82 J. Quiroga, C. Cisneros, B. Insuasty, R. Abonía, S. Cruz, M. Nogueras, J. M. de la Torre, M. Sortino and S. Zacchino, *J. Heterocycl. Chem.*, 2006, **43**, 299–306.
83 A. Drabczyńska, C. E. Müller, A. Schiedel, B. Schumacher, J. Karolak-Wojciechowska, A. Fruziński, W. Zobnina, O. Yuzlenko and K. Kieć-Kononowicz, *Bioorg. Med. Chem.*, 2007, **15**, 6956–6974.
84 A. N. Geisman, V. T. Valuev-Elliston, A. A. Ozerov, A. L. Khandazhinskaya, A. O. Chizhov, S. N. Kochetkov, C. Pannecouque, L. Naesens, K. L. Seley-Radtke and M. S. Novikov, *Bioorg. Med. Chem.*, 2016, **24**, 2476–2485.
85 J.-H. Chern, K.-S. Shia, T.-A. Hsu, C.-L. Tai, C.-C. Lee, Y.-C. Lee, C.-S. Chang, S.-N. Tseng and S.-R. Shih, *Bioorg. Med. Chem. Lett.*, 2004, **14**, 2519–2525.
86 A. Kumar, I. Ahmad, B. S. Chhikara, R. Tiwari, D. Mandal and K. Parang, *Bioorg. Med. Chem. Lett.*, 2011, **21**, 1342–1346.
87 S. I. Alqasoumi, A. M. Al-Taweel, A. M. Alafeefy, E. Noaman and M. M. Ghorab, *Eur. J. Med. Chem.*, 2010, **45**, 738–744.
88 I. Tomassoli, L. Ismaili, M. Pudlo, C. de los Ríos, E. Soriano, I. Colmena, L. Gandía, L. Rivas, A. Samadi, J. Marco-Contelles and B. Refouvelet, *Eur. J. Med. Chem.*, 2011, **46**, 1–10.
89 A.-R. B. A. El-Gazzar and H. N. Hafez, *Bioorg. Med. Chem. Lett.*, 2009, **19**, 3392–3397.
90 B. Huang, X. Liu, W. Li, Z. Chen, D. Kang, P. Zhan and X. Liu, *Arkivoc*, 2016, **6**, 45–51.
91 D. Yu, M. Suzuki, L. Xie, S. L. Morris-Natschke and K. Lee, *Med. Res. Rev.*, 2003, **23**, 322–345.
92 J. T. Desai, C. K. Desai and K. R. Desai, *J. Iran. Chem. Soc.*, 2008, **5**, 67–73.
93 A. C. Humphries, E. Gancia, M. T. Gilligan, S. Goodacre, D. Hallett, K. J. Merchant and S. R. Thomas, *Bioorg. Med. Chem. Lett.*, 2006, **16**, 1518–1522.
94 A. W.-H. Cheung, B. Banner, J. Bose, K. Kim, S. Li, N. Marcopulos, L. Orzechowski, J. A. Sergi, K. C. Thakkar and B.-B. Wang, *Bioorg. Med. Chem. Lett.*, 2012, **22**, 7518–7522.
95 G. Brahmachari, S. Begam and K. Nurjamal, *ChemistrySelect*, 2018, **3**, 3400–3405.
96 N. M. Evdokimov, S. Van Slambrouck, P. Heffeter, L. Tu, B. Le Calve, D. Lamoral-Theys, C. J. Hooten, P. Y. Uglinskii, S. Rogelj, R. Kiss, W. F. A. Steelant, W. Berger, C. J. Bologa, J. J. Yang, A. Kornienko and I. V Magedov, *J. Med. Chem.*, 2011, **54**, 2012–2021.
97 R. Gupta, G. Kumar and R. S. Kumar, *Methods Find. Exp. Clin. Pharmacol.*, 2005, **27**, 101–118.
98 C. E. Mueller, D. Shi, M. Manning Jr and J. W. Daly, *J. Med. Chem.*, 1993, **36**, 3341–3349.
99 G. Ahmad, M. Sohail, M. Bilal, N. Rasool, M. U. Qamar, C. Ciurea, L. G. Marceanu and C. Misarca, *Molecules*, 2024, **29**(10), 2232.
100 S. A. El-Kalyoubi, A. Ragab, O. A. Abu Ali, Y. A. Ammar, M. G. Seadawy, A. Ahmed and E. A. Fayed, *Pharmaceuticals*, 2022, **15**, 376.
101 E. A. Tanifum, A. Y. Kots, B.-K. Choi, F. Murad and S. R. Gilbertson, *Bioorg. Med. Chem. Lett.*, 2009, **19**, 3067–3071.
102 N. R. Emmadi, K. Atmakur, C. Bingi, N. R. Godumagadda, G. K. Chityal and J. B. Nanubolu, *Bioorg. Med. Chem. Lett.*, 2014, **24**, 485–489.
103 K. Sirisha, G. Achaiah and A. R. R. Rao, *Indian J. Pharm. Sci.*, 2014, **76**, 519–528.
104 V. E. Semenov, A. D. Voloshina, E. M. Toroptzova, N. V Kulik, V. V Zobov, R. K. Giniyatullin, A. S. Mikhailov, A. E. Nikolaev, V. D. Akamsin and V. S. Reznik, *Eur. J. Med. Chem.*, 2006, **41**, 1093–1101.
105 K. Yagi, K. Akimoto, N. Mimori, T. Miyake, M. Kudo, K. Arai and S. Ishii, *Pest Manag. Sci.*, 2000, **56**, 65–73.
106 G. Lu, X. Li, D. Wang and F. Meng, *Eur. J. Med. Chem.*, 2019, **171**, 282–296.
107 H. Wang, C. Wang and T. D. Bannister, *Tetrahedron Lett.*, 2015, **56**, 1949–1952.

108 D. Fuentes-Rios, M. DoSNM and R. Rico, *Lett. Org. Chem.*, 2024, **21**, 213–215.
109 H. R. Dehghanpour, M. H. Mosslemin and R. Mohebat, *J. Chem. Res.*, 2018, **42**, 35–39.
110 A. Zare, A. Ghobadpoor and T. Safdari, *Res. Chem. Intermed.*, 2020, **46**, 1319–1327.
111 S. El-Kalyoubi, S. S. Elbaramawi, W. A. Zordok, A. M. Malebari, M. K. Safo, T. S. Ibrahim and E. S. Taher, *Bioorg. Chem.*, 2023, **136**, 106560.
112 M. Ahmadi Sabegh, J. Khalafy and N. Etivand, *J. Heterocycl. Chem.*, 2018, **55**, 2610–2618.
113 P. S. Naidu and P. J. Bhuyan, *RSC Adv.*, 2014, **4**, 9942–9945.
114 H. Han, C. Li, M. Li, L. Yang, S. Zhao, Z. Wang, H. Liu and D. Liu, *Molecules*, 2020, **25**, 2755.
115 P. K. Maji and A. Mahalanobish, *Heterocycles*, 2017, **94**, 1847–1855.
116 L. Xia, W. A. C. Burger, J. P. D. van Veldhoven, B. J. Kuiper, T. T. van Duijl, E. B. Lenselink, E. Paasman, L. H. Heitman and A. P. IJzerman, *J. Med. Chem.*, 2017, **60**, 7555–7568.
117 J. Jiang, P. Zhao, L. H. Sigua, A. Chan, E. Schönbrunn, J. Qi and G. I. Georg, *Arch. Pharm.*, 2022, **355**, 2200288.
118 S. Yaragorla, D. Sneha Latha and R. Kumar, *Chem.–A Eur. J.*, 2024, **30**, e202401480.
119 K. Dzieszkowski, I. Barańska and Z. Rafiński, *J. Org. Chem.*, 2020, **85**, 6645–6662.
120 R. S. Dongre, J. S. Meshram, R. S. Selokar, F. A. Almalki and T. Ben Hadda, *New J. Chem.*, 2018, **42**, 15610–15617.
121 R. Javahershenas and J. Khalafy, *J. Heterocycl. Chem.*, 2017, **54**, 3163–3168.
122 D. K. Jamale, V. M. Gurame, N. J. Valekar, S. P. Hangirgekar, G. B. Kolekar and P. V Anbhule, in *Macromolecular Symposia*, Wiley Online Library, 2019, vol. 387, p. 1800202.
123 T. Farahmand, S. Hashemian and A. Sheibani, *J. Mol. Struct.*, 2020, **1206**, 127667.
124 P. Farokhian, M. Mamaghani, N. O. Mahmoodi, K. Tabatabaeian and A. F. Shojaie, *J. Chem. Res.*, 2019, **43**, 135–139.
125 A. M. Rad and M. Mokhtary, *Int. Nano Lett.*, 2015, **5**, 109–123.
126 G. M. Ziarani, N. H. Nasab, M. Rahimifard and A. A. Soorki, *J. Saudi Chem. Soc.*, 2015, **19**, 676–681.
127 S. Moradi, M. A. Zolfigol, M. Zarei, D. A. Alonso, A. Khoshnood and A. Tajally, *Appl. Organomet. Chem.*, 2018, **32**, e4043.
128 E. Saberikhah, M. Mamaghani, N. O. Mahmoodi and A. Fallah Shojaei, *Polycyclic Aromat. Compd.*, 2021, **42**, 297–315.
129 S. Esmaili, A. Khazaei and A. R. Moosavi-Zare, *Polycyclic Aromat. Compd.*, 2023, **43**, 6615–6626.
130 A. Morshedi and H. R. Shaterian, *J. Iran. Chem. Soc.*, 2019, **16**, 493–500.
131 E. Saberikhah, M. Mamaghani and N. O. Mahmoodi, *J. Chin. Chem. Soc.*, 2021, **68**, 902–916.
132 S. Dastmard, M. Mamaghani, L. Farahnak and M. Rassa, *Polycyclic Aromat. Compd.*, 2022, **42**, 1747–1760.
133 K. T. Patil, P. P. Warekar, P. T. Patil, S. S. Undare, G. B. Kolekar and P. V Anbhule, *J. Heterocycl. Chem.*, 2018, **55**, 154–160.
134 R. Bharti, P. Kumari, T. Parvin and L. H. Choudhury, *RSC Adv.*, 2017, **7**, 3928–3933.
135 F. A. Alatawi, K. Alatawi, H. Mattar, S. A. Alqarni, A. I. Alalawy, A. Fawzi Qarah, W. M. Alamoudi and N. M. El-Metwaly, *J. Photochem. Photobiol., A*, 2025, **459**, 116033.
136 M. Masoumi, M. Bayat and F. S. Hosseini, *Heliyon*, 2020, **6**, e05047.
137 A. Gholami, M. Mokhtary and M. Nikpassand, *Dyes Pigm.*, 2020, **180**, 108453.
138 H. Sepehrmansouri, M. Zarei, M. A. Zolfigol, A. R. Moosavi-Zare, S. Rostamnia and S. Moradi, *Mol. Catal.*, 2020, **481**, 110303.
139 B. B. F. Mirjalili, A. Bamoniri and N. Safajo, *Sci. Iran.*, 2022, **29**, 3142–3150.
140 A. P. Marjani, J. Khalafy, F. M. Arlan and E. Eynia, *Arkivoc*, 2019, (part v), 1–9.
141 S. El-Kalyoubi and F. Agili, *Molecules*, 2020, **25**, 5205.
142 M. Adib, F. Peytam, M. Rahmanian-Jazi, S. Mahernia, H. R. Bijanzadeh, M. Jahani, M. Mohammadi-Khanaposhtani, S. Imanparast, M. A. Faramarzi, M. Mahdavi and B. Larijani, *Eur. J. Med. Chem.*, 2018, **155**, 353–363.
143 N. Shaddel, F. Molaei Yielzoleh, K. Nikoofar and M. Zahedi-Tabrizi, *Inorg. Chem. Commun.*, 2024, **168**, 112929.
144 H. I. Abdelaal, A. R. Mohamed, M. F. Abo-Ashour, S. Giovannuzzi, S. H. Fahim, H. A. Abdel-Aziz, C. T. Supuran and S. M. Abou-Seri, *Bioorg. Chem.*, 2024, **152**, 107759.
145 K. D. Nance, E. L. Days, C. D. Weaver, A. Coldren, T. D. Farmer, H. P. Cho, C. M. Niswender, A. L. Blobaum, K. D. Niswender and C. W. Lindsley, *J. Med. Chem.*, 2017, **60**, 1611–1616.
146 R. Bakhshali-Dehkordi, M. A. Ghasemzadeh and J. Safaei-Ghomi, *J. Mol. Struct.*, 2020, **1206**, 127698.
147 P. J. Borpatra, G. K. Rastogi, M. B. Saikia, M. L. Deb and P. K. Baruah, *ChemistrySelect*, 2019, **4**, 3381–3386.
148 L. Suresh, P. Sagar Vijay Kumar, Y. Poornachandra, C. Ganesh Kumar and G. V. P. Chandramouli, *Bioorg. Med. Chem. Lett.*, 2017, **27**, 1451–1457.
149 M. H. Abdollahi-Basir, F. Shirini, H. Tajik and M. A. Ghasemzadeh, *Polycyclic Aromat. Compd.*, 2021, **41**, 1580–1589.
150 R. Ghorbani-Vaghei and N. Sarmast, *Appl. Organomet. Chem.*, 2018, **32**, e4003.
151 B. Mirhosseini-Eshkevari, M. A. Ghasemzadeh, M. Esnaashari and S. T. Ganjali, *ChemistrySelect*, 2019, **4**, 12920–12927.
152 S. A. El-Kalyoubi, H. A. M. Gomaa, E. M. N. Abdelhafez, M. Ramadan, F. Agili and B. G. M. Youssif, *Pharmaceuticals*, 2023, **16**, 716.
153 N. A. Alshaye and M. A. Ibrahim, *Polycyclic Aromat. Compd.*, 2024, **44**, 5899–5913.
154 W. Shehta, N. A. Alsaiari, B. Farag, M. M. Abdel-Aziz, S. Youssif, S. M. Elfeky, S. El-Kalyoubi and N. A. Osman, *SynOpen*, 2025, **9**, 73–83.